University of Zurich[UZH]

The Fate of Pyrogenic Carbon in Boreal Forest Soils

GEO 511 Master's Thesis

Author
Cristina Haldemann
13-927-199

Supervised by
Marcus Schiedung

Faculty representative
Dr. Samuel Abiven

29.01.2022
Department of Geography, University of Zurich

University of Zurich[UZH]

The Fate of Pyrogenic Carbon in Boreal Forest Soils

GEO511 Master Thesis

Edited By Cristina Haldemann

13-927-199

Supervised by
Marcus Schiedung

Faculty Representative
Dr. Samuel Abiven

Date of Submission: 29 January 2022
Department of Geography, University of Zurich

Acknowledgment

Foremost, I would like to express my gratitude to Samuel Abiven for proposing to me to participate in its research project by writing this master's thesis. As my faculty representative, I am glad Samuel recognized my motivation and considered me to be the right person for this work.

My deepest sense of gratitude goes to my supervisor, Marcus Schiedung, who was determinant in every aspect of my work. His patience and availability were greater than I could imagine, and his precious advice gently guided me toward the realization of this project.

Furthermore, I feel glad to have had Lisa Maria Pirisinu by my side in the laboratory K84 for the six months we worked together. Sharing our working days made me feel more confident and lightened my days.

I finally express my gratitude to Leonardo Rodoni, for continuously supporting and motivating me, to my brother Andrea, my closest friends Alice and Diego, and my parents for their great support and encouragement every time needed.

Abstract

Wildfires are common in the circumpolar region and are expected to become more frequent with climate change. These fires lead to the formation of pyrogenic carbon (PyC) as a by-product of incomplete combustion of vegetation biomass. After PyC enters the soil, its more labile fractions get decomposed and mineralized on a relatively short timescale, but a relevant fraction of PyC is highly aromatic and condensed, thus more resistant to biotic and abiotic decomposition. These components can remain in the soil for millennia, finally compensating the wildfire carbon emissions and acting as an atmospheric carbon sink.

Further, translocation, physical-chemical altering, and content of PyC in soils can be driven by soil texture, permafrost, and translocation due to steepness. The aim of this master's thesis is to provide a detailed investigation of the main drivers controlling the translocation and physical-chemical altering of PyC stored in soil organic carbon fractions along two Canadian landscape gradients, one in the South Slave Lake Region, (AB and NWT) and one in the Inuvik Region (NWT). The applied methods comprehend soil organic carbon fractionation by size and density, diffuse reflectance infra-red Fourier transformation spectroscopy (DRIFT), chemothermal oxidation at 375 °C (CTO-375) and benzene polycarboxylic acids (BPCA) analysis.

Results highlighted that soils from the Inuvik Region, which are affected by continuous permafrost conditions, lower pH, and greater clay content, store more SOC and PyC than soils from the South Slave Lake Region, which are affected by sporadic permafrost conditions and a pH > 6 due to carbonates.

The higher SOC and PyC stocks and concentrations in the soils of the Inuvik Region were attributable to the continuous permafrost conditions and higher soil moisture content, which likely reduce the decomposition rate and bury soil organic matter at greatest depths through cryoturbation, protecting trapped soil organic carbon from physical and chemical alteration. Further, also DRIFT analysis suggests a higher potential SOC cycling in the South Slave Lake Region, for both the bulk samples and SOC fractions, because of the lower aliphatic/aromatic and cellulose/lignin ratios, despite no difference for the organic layer and the particulate organic matter fraction were found.

Differences in SOC and PyC quantities along the landscape gradients only partially correlate with differences in steepness. Indeed, the homogeneous distribution of SOC and PyC in the South Slave Lake Region correlates with smooth differences in height between top and bottom of the catena and with the sporadic permafrost conditions, while the 50 m difference in height between top and bottom of the catena in the Inuvik Region, together with continuous permafrost conditions, likely cause a transport of SOC and PyC along the catena and in greater soil depths. The analysis of PyC quality at each landscape position and depth revealed that more physical-chemical altered PyC is not necessarily found at the bottom of the catenae, which is attributable to the protection of also more labile structures by permafrost.

The proportion of SOC and PyC in soil fractions revealed a higher stability and resistance against decomposition in case of association with silt and clay, and sand and aggregates, whereas protection against decomposition was lower if SOC and PyC were found in association with particulate organic matter. Further, the association of soil carbon with specific fractions is attributable also to the soil texture, and thus to the extent to which each fraction contributes to the bulk soil.

Thus, permafrost can be considered as the most relevant driver of both translocation and physical-chemical altering of PyC in boreal forest soils, while soil texture drives its association with specific soil fractions (all of which exhibit a different ability to stabilize carbon in soils), and differences in steepness only partially explain the translocation of PyC along landscape gradients.

Table of Contents

List of Figures

List of Tables

Abbreviations

Study Area and Landscape Positions

EUP Ecosystem Unit Plot

ST, SS, SB Landscape Positions: South Top, South Slope, South Bottom

NT, NS, NB Landscape Positions: North Top, North Slope, North Bottom

Carbon Related Abbreviations

SOC Soil Organic Carbon

TC, TOC, TIC Total Carbon, Total Organic Carbon, Total Inorganic Carbon

PyC Pyrogenic Carbon

SOC Fractions and Sample Type

DOC Dissolved Organic Carbon

POM Particulate Organic Matter

S+A Sand and Aggregates

s+c Silt and Clay

rSOC Resistant Soil Organic Carbon

OL Organic Layer

Methods Abbreviations

DRIFT Diffuse Reflectance Infra-Red Fourier Transformation Spectroscopy

CTO-375 Chemothermal Oxidation at 375°C

BPCA Benzene Polycarboxylic Acids

Chapter 1

Introduction

1.1 Origin of PyC during Vegetation Biomass Burning

Combustion is a chemical reaction involving a carbon-rich material as a reactant (e.g., wood) and oxygen as a limiting reagent (e.g., air). The products of this reaction generally comprise light, warmth and gaseous carbonaceous compounds which get released into the atmosphere, primarily in the form of carbon dioxide (CO_2) but also as carbon monoxide (CO) and methane (CH_4), whereas the remains of it depend on the carbon-rich precursor material (primarily vegetation biomass and fossil fuel) but mainly include ash and soot (Conard and Solomon, 2008). Combustion is a natural process when started by lightning (Conard and Solomon, 2008) and leads to bigger-scale phenomena such as wildfires. These natural disasters cause the release of carbon dioxide into the atmosphere, which contributes to global warming and, ultimately, climate change.

On the other hand, the limitation of oxygen supply during fire events reduces the efficiency of combustion, producing partially burned carbon-rich remains of vegetation biomass. These products of incomplete combustion go under the names black carbon (BC, in soil and sediment sciences) and elemental carbon (EC, in atmospheric sciences), comprehending a wide range of fire-derived organic matter such as aromatic residues (char), condensates (soot), charcoal, and biochar (as char intentionally produced for agricultural purposes) (Abiven and Santín, 2019; Hammes et al., 2007; Santín et al., 2015). Thus, a major part of the carbon involved in vegetation fires is emitted as CO_2 into the atmosphere, yet up to 15-25 % of vegetation C is subject to incomplete combustion.

Specifically, in a complete combustion process, vegetation biomass or fossil fuel is converted into CO_2, H_2O and inorganic residues (ash). However, under local or temporal oxygen limitations, combustion becomes incomplete, and pyrolysis takes place, producing various solid organic residues (Wiedemeier et al., 2016). Used in this thesis is the term pyrogenic carbon (hereafter PyC) to imply the whole spectrum of fire-derived carbonaceous solid residues produced through the incomplete combustion of vegetation biomass during natural fire events.

As presented in Figure 1 below, PyC is thus not one chemical compound with well-defined characteristics, but rather a continuum of thermochemically altered organic matter, which ranges from lightly charred to highly condensed polycyclic aromatic materials, and from macroscopic char fragments to micrometer-sized soot particles to individual compounds of pyrogenic origin (Bird et al., 2015; Wiedemeier et al., 2016). On one end of the combustion continuum are large charcoal particles, whose concentration in sediments reflects the burning history of local ecosystems due to their very short-range transport (Masiello, 2004). Further, the black carbon combustion continuum comprises labile, semi-labile, and stable components, depending on the combustion sources and processes (primarily on the temperature of formation and the nature of the precursor material

(Braadbaart et al., 2009)), with only the stable component likely to survive thermal, physical, and chemical degradation for centuries to millennia (Bird et al., 2015; Hammes et al., 2007).

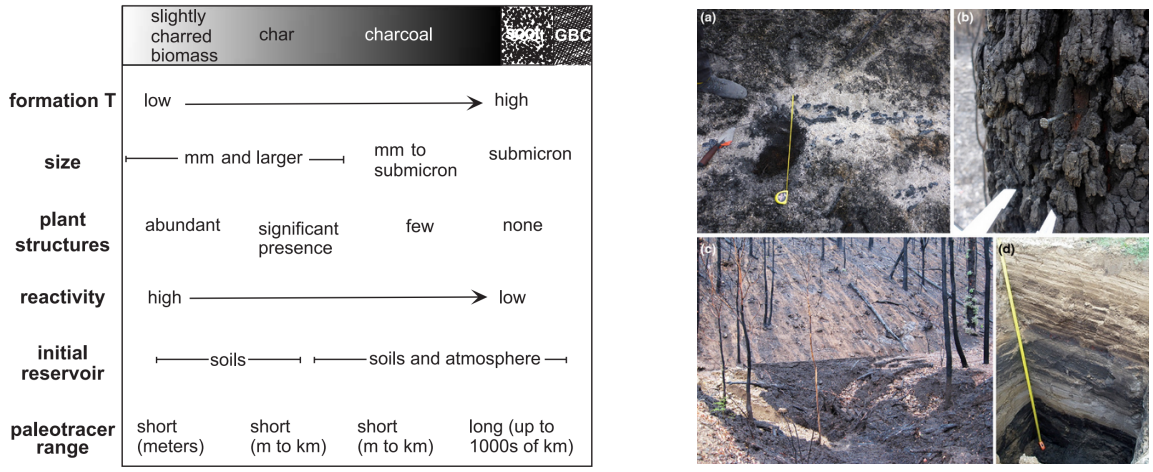

Figure 1: Left: The black carbon combustion continuum (Masiello, 2004), right: PyC formation after wildfires (Santín et al., 2015).

Indeed, a component of PyC is highly recalcitrant and persists in the environment for millennia, thus being considered chemically and biologically inert. However, it is now clear that a proportion of PyC can indeed degrade by undergoing transformations, translocation, and remineralization by a range of biotic and abiotic processes over a time period depending on several factors, ranging from a relatively short timescale (Bird et al., 2015), to a turnover of PyC in soils on a centennial timescale (Singh et al., 2012), to a millennial timescale (Wiedemeier et al., 2016).

PyC is ubiquitous in the environment, found in the atmosphere, soils, sediments, and water in both the marine and terrestrial environments (Hammes et al., 2007). The physicochemical characteristics of PyC are complex and highly variable, dependent on the organic precursor and the conditions of formation (Bird et al., 2015). PyC thus has particular features, among others, a high relative carbon content and high chemical aromaticity, and a comparably long mean residence time in the soil ranging from decades to millennia (Singh et al., 2012). Under certain circumstances, it may have a variety of positive effects on soil properties, e.g., increasing pH, water retention capacity, or nutrient availability and the retention of pollutants (Reisser et al., 2016).

Depending on the source, fires are estimated to globally generate between 114-379 Tg PyC per year, corresponding to ca. 0.2–0.6 % of the annual terrestrial net primary production (Santín et al., 2016); or between 40-215 Tg BC year^{-1} (Jones et al., 2020), in both cases forming a major component of residual charcoal and ash deposits.

The major sources of PyC are biomass burning and fossil fuel combustion, which deliver 7.5–17 Tg yr^{-1} to the atmosphere as fine aerosols and 56–123 Tg yr^{-1} to the soil surface as char. PyC can undergo a range of physical and chemical, biotic, and abiotic interactions and transformations after formation, leading to remineralization and/or to the physical disintegration and translocation of PyC in both particulate and dissolved form. Further, PyC is transported from the land to the ocean in particulate (19–80 Tg yr^{-1}) and dissolved (25–28 Tg yr^{-1}) form; the remineralization flux from PyC on land is estimated at 103–207 Tg yr^{-1}. As depicted by Figure 2 below, the major pools of PyC are ocean sediments (480–1440 Pg), marine dissolved organic carbon (26–145 Pg), and soils (54–109 Pg), plus an additional pool in terrestrial sediments for which no estimate of size is

available (Santín et al., 2016).

More than 80 % of PyC produced ends up in the soil, nevertheless PyC is ubiquitously present in all environmental compartments such as the atmosphere, water, soils and sediments (Hammes et al., 2007) and its abundance might even increase with the projected increase in global wildfire activity and the continued burning of fossil fuel. PyC is also increasingly produced from the industrial pyrolysis of organic wastes, which yields charred soil amendments (biochar) (Wiedemeier et al., 2016), it plays an important role in carbon sequestration in soils and sediments and may represent a significant sink in the global carbon cycle.

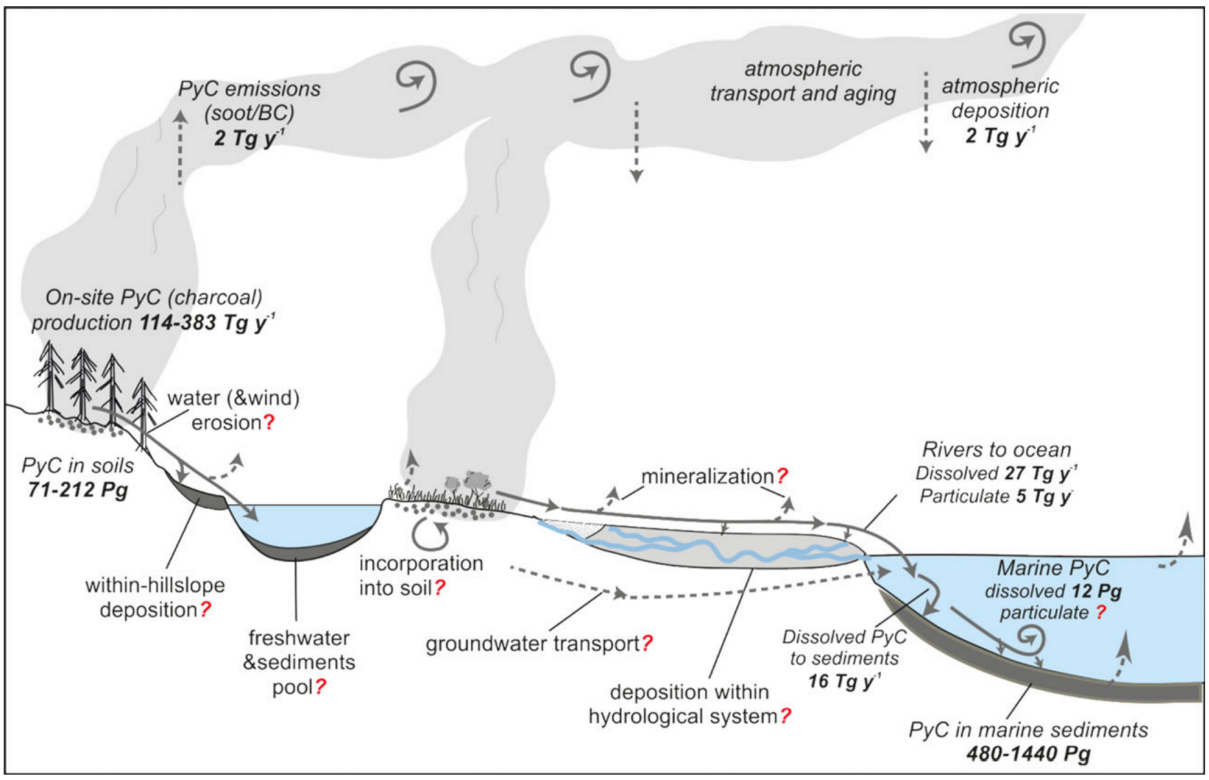

Figure 2: Global pyrogenic carbon cycle from vegetation fires, with fluxes between biosphere, atmosphere and pedosphere in Tg C yr^{-1} (Santín et al., 2016). Uncertainties and unknowns (represented here with red question marks) mainly comprehend the soil system (e.g. within-hillslope deposition) and the marine system; whereas production of atmospheric PyC (soot/BC) seems to be better quantified.

This thesis focuses on PyC in soils as a by-product of incomplete combustion during wildfires and investigates its fate after entering the soil system.

1.2 Entrance of PyC in Atmospheric and Marine Environments

For what concerns the atmosphere, PyC can enter it as an emission from both the biosphere and the pedosphere. During burning, a vast amount of organic carbon is rapidly oxidized and emitted as gases and aerosols in a much more intense and faster process than during respiration. Depending on the magnitude of the fire, the released CO_2 can be relevant in terms of net ecosystem CO_2 exchange with the atmosphere (Abiven and Santín, 2019). Further, part of the PyC produced during a fire is emitted into the atmosphere within smoke. This atmospheric PyC is situated at the smallest size end of the PyC spectrum ($<$ 1-2 µm) and is chemically the most recalcitrant (Abiven and Santín, 2019). Dry and wet deposition of PyC from the atmosphere to the soil is a global process that transports 2–10 Tg PyC per year to both land and ocean depositional settings spanning thousands of km (Abney and Berhe, 2018).

In soils, changes in organic carbon are associated with CO_2 exchange between terrestrial ecosystems and the atmosphere, which can impact regional carbon budgets. Indeed, a net carbon loss from soils to the atmosphere increases atmospheric CO_2 concentration, probably leading to higher global temperatures, which could ultimately accelerate the decomposition of SOM. On the other hand, net soil CO_2 sequestration from the atmosphere could help to mitigate the greenhouse effect and improve soil quality (Zimmermann et al., 2007).

Further, during wildfires, a wide range of pyrogenic carbon compounds form, and their size is essential in the determination of the transport distance, as smaller particles remain airborne for longer periods of time. Millimeter-size particles, for example, settle out of the atmosphere within 100 m of the fire source, while submicron soot particles can remain suspended in the atmosphere for months, if not subjected to oxidation and wash-out (Masiello, 2004). Thus, the ability of particles to remain suspended and transported in the air (and thus avoid soil storage) increases as particle size decreases. For PyC particles smaller than approximately 2 µm, the initial reservoir is predominantly the atmosphere. Finally, the transport of small particles can deliver PyC to remote environments such as the open ocean. (Masiello, 2004).

Concerning the entrance of PyC into the marine environment, PyC can reach the water system through deposition and transport from the atmosphere due to fluvial transfer from the terrestrial pool. A part of that is then buried in marine sediments (Lasslop et al., 2019).

Indeed, PyC in soils is part of the soil organic carbon and, as such, it can dissolve with water flowing through the organic horizon, thus leaching out of the soil system (Abramoff et al., 2018). According to Jones et al. (2020), dissolved pyrogenic carbon can constitute up to 5-10 % of dissolved organic carbon (DOC) in global rivers. The dissolved PyC content of DOC in boreal forests is estimated at around 5 % (Jones et al., 2020).

The residence time of oceanic PyC stocks is on the order of millennia to tens of millennia, likely an order of magnitude longer than soil PyC stocks (centuries to millennia) and multiple orders of magnitude longer than terrestrial organic carbon (decades to centuries). Hence, the production of PyC and its subsequent export to the global oceans significantly extends the residence time of terrigenous carbon in the Earth's system (Jones et al., 2020).

1.3 Terrestrial Pyrogenic Carbon Pool

After PyC enters the soil, its fate becomes unclear since labile fractions get decomposed and mineralized on a relatively short timescale, but a relevant fraction of PyC is highly aromatic and condensed, thus more resistant to biotic and abiotic decomposition. These components can remain in the soil for millennia, eventually compensating for wildfire carbon emissions and acting as atmospheric carbon sink (Bird et al., 2015; Jones et al., 2020). Furthermore, PyC content in soils is affected not only by soil properties such as texture and alkalinity (Reisser et al., 2016) but also by permafrost thawing and translocation due to cryoturbation (Aaltonen et al., 2019; Flannigan et al., 2009).

Generally, soils were recognized as a major PyC pool, ranging between 54-109 Pg (Bird et al., 2015). PyC is a ubiquitous component of soils, comprising up to 50 % of the soil organic carbon (SOC), particularly prevalent in systems highly prone to fires (Hammes et al., 2007). From the soil, PyC can be transported and effectively stored in an intermediate sediment pool before being delivered through rivers to the marine environment, where the largest and longest-term storage pool for PyC exists (Bird et al., 2015).

The global rate of PyC entering soil, mostly from biomass burning, is approximately 0.056–0.137 Pg C year^{-1} (Bird et al., 2015), a small amount compared with annual soil carbon inputs from net primary production (NPP) of approximately 60 Pg C (Leifeld et al., 2018). About 550 Pg of the global SOC stock is located in organic soils, most of it in northern peatlands (Leifeld et al., 2018). According to Reisser et al. (2016), PyC content in soils is affected by soil properties and found that soils with clay content greater than 50 % contain much more PyC ($>$ 30 % of the SOC) than soils with clay content lower than 5 % ($<$ 6 % of the SOC). Further, alkaline soils were showed to contain at least 50 % more PyC than acidic soils (Reisser et al., 2016).

Moreover, groups of parameters likely to influence the PyC content in soils include fire and land use (due to the inputs to the soil, which may vary based on the amount, type, and frequency of burning biomass); climate (since temperature and moisture influence decomposition of PyC); and physical and chemical soil parameters such as clay content and pH (which also play a role in decomposition and the stabilization processes of PyC) as well as topography, which has an impact on erosion rates or accumulation of PyC (Reisser et al., 2016).

Further, decomposition is an important pathway for the loss of PyC from soil (Abney and Berhe, 2018). However, PyC can also exit the soil system by leaching into groundwater. Indeed, PyC degradation does not always imply PyC mineralization and thus net loss. Indeed, during the process of PyC leaching, some of the solid PyC retains its pyrogenic nature but becomes soluble in water. In many cases, the quantities of PyC and total organic carbon in water and soils are directly correlated (Abiven and Santín, 2019). Changes to inputs or outputs of soil organic carbon (SOC) can affect land carbon storage and can alter the function of terrestrial ecosystems and their ability to serve as a source or sink of C (Abramoff et al., 2018).

Finally, estimations of PyC content as a mass percentage of total SOC and of PyC stocks in tonnes per hectare in the first 2 m soil depth were acquired for almost the whole globe. For what concerns the Canadian region, which will come to the fore in this thesis, PyC content is estimated between 4.4-10.5 % of total SOC (Fig. 3), which is lower than the content estimated in other regions, such as Brazil and India, but the stocks of PyC in Canada are among the highest ones. Indeed, Figure 4 highlights an estimated PyC stock between 8.6-32.0 tha^{-1} in the first 2 meters of soil depth.

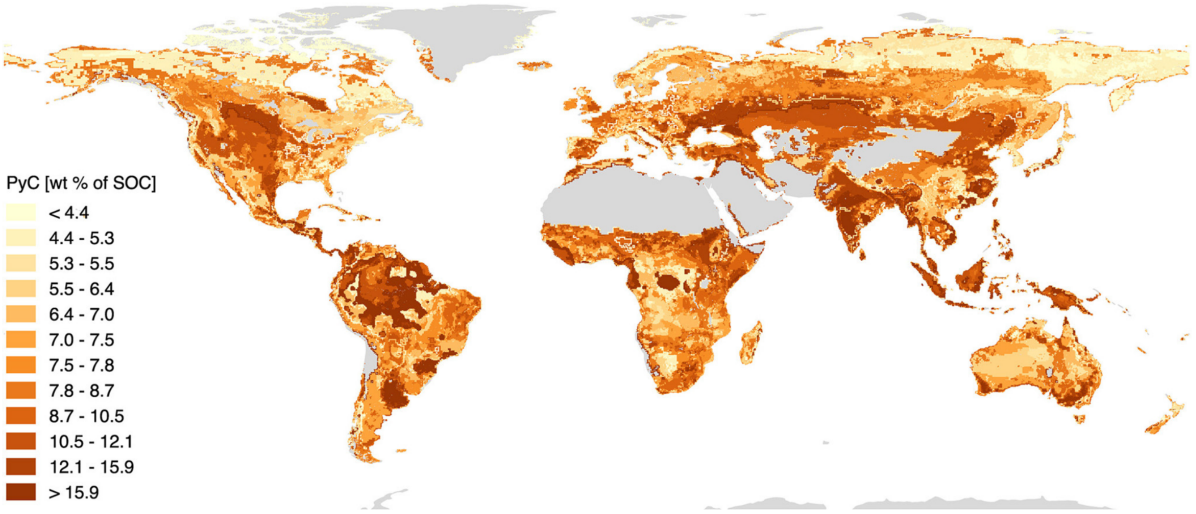

Figure 3: Global predicted PyC content as a mass percentage of the total SOC (Reisser et al., 2016).

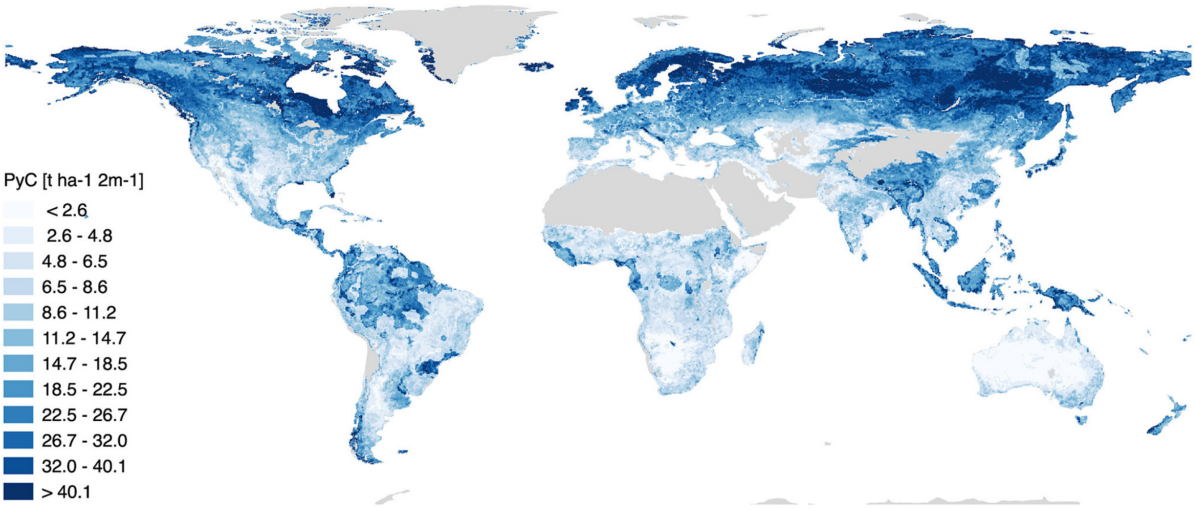

Figure 4: Global predicted PyC stocks as tha^{-1} in the first 2 m soil depth (Reisser et al., 2016).

1.4 Erosion and Transport of Pyrogenic Carbon along Landscape Gradients

PyC can be lost from soils not only due to decomposition but also due to soil erosion (Abney and Berhe, 2018). After a wildfire, some physical properties of the soil, such as nutrient availability, water infiltration, and soil pH, can change. These changes in physical properties of soil have implications for the lateral movement of water and PyC (Fig. 5). Indeed, fires can lead to the destabilization of topsoil, reducing aggregation and aggregate protected carbon and increasing soil hydrophobicity, which can lead to increased erodibility of soil post-fires through both water and wind-driven erosion processes. PyC erosion rates are thus driven by fire, geomorphology and climate (Abney and Berhe, 2018).

According to Abney and Berhe (2018), about 70–90 % of the eroded topsoil material is redistributed downhill or downstream, and this material is not exported out of the source watersheds but instead is deposited in toe slope and foot slope landform positions. Over time, the PyC that is not transported by erosion is mobilized downward into the profile via dissolution, leaching, and biological processes that render it more susceptible to in-solution transport with flowing water. However, the PyC that remains on the soil surface is exposed to wetting- and drying-cycles that are likely to render it more susceptible to leaching losses, although some research has indicated that the material left after leaching may be less easily decomposed (Abney and Berhe, 2018).

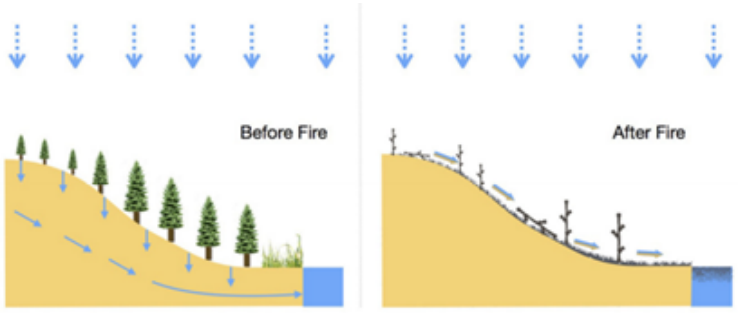

Figure 5: On the hillslope scale, fires alter dominant hydrologic flow regimes in soil, reducing infiltration and subsurface flow of water and increasing surface runoff (Abney and Berhe, 2018).

Erosion is thus a particularly important flux for PyC in soil when it stays in surface layers because this leaves PyC vulnerable to weathering forces of wind and water. Further, in burned watershed selective transport of PyC during interrill erosion (soil movement that occurs when raindrops strike exposed soil) can be double than in unburned watershed (Abney and Berhe, 2018). In other words, there might be a preferential way of PyC erosion, so PyC is likely to be redistributed throughout the landscape differently than non-pyrogenic carbon (Abney and Berhe, 2018).

The amount and content of PyC that is laterally spread across the soil surface by erosion is influenced by PyC concentration, location, chemical composition, and physical size. These characteristics are all the result of complicated interactions between the type and density of combustible vegetation (i.e., fuel load), combustion conditions (e.g., temperature, duration, oxygen availability), and the frequency of fire episodes (Abney and Berhe, 2018).

Further, the geomorphology of a landscape can significantly impact the erosion of PyC. In particular, the steepness of a hillslope has a direct effect on the amount of sediment transported by soil erosion, where an increased gradient increases the mass of transported sediment (Abney and Berhe, 2018).

Furthermore, the location within a landscape where PyC is formed or deposited can be critical for the long-term fate of the PyC. If PyC is produced on eroding landform positions (e.g., convex or linear positions such as summits and shoulders or foot slope positions), then it is more likely to be transported laterally by wind or water erosion processes, or gravity driven diffusive mass transport, compared to PyC produced in depositional landform positions (concave or flat positions such as toeslopes, or alluvial plains) (Abney and Berhe, 2018).

However, if the PyC is either formed or deposited on depositional landform positions, then it is more likely to persist in the catchment longer and be stabilized in the depositional landform positions by forming physical and/or chemical associations with soil minerals, or to get buried by subsequent erosion/deposition events that bring sediment to the depositional position, as has been found for non-pyrogenic carbon (Abney and Berhe, 2018).

1.5 SOC in Permafrost Affected Soils

As previously announced, the focus of this thesis is set on PyC in soils of the Canadian boreal region, which is, among others, affected by huge wildfires. However, a further driver of PyC stocks and transport in soils of particular interest in boreal ecosystems is permafrost.

One quarter of the Northern Hemisphere and 17 % of the Earth's exposed land surface is underlain by permafrost (from permanent and frost), which is defined as soil with a temperature remaining at or below 0 °C for at least two consecutive years (Biskaborn et al., 2019). A common process going on in permafrost-affected soil is cryoturbation. Cryoturbation is a dominant soil forming process in arctic permafrost regions and refers collectively to all soil movements due to frost action that lead to the mixing of soil layers due to repeated freeze-thaw processes (Bockheim, 2007; Kaiser et al., 2007). Although some cryoturbation may occur in areas of seasonal frost, it most commonly occurs in permafrost areas and is often accompanied by patterned ground. Further, cryoturbation occurs most strongly under conditions of poor drainage, where the parent materials are enriched in silt, and where frost boils are present. Importantly, cryoturbation can redistribute and incorporate SOC into the active layer and near-surface permafrost (Bockheim, 2007). The magnitude of this process is dependent on local factors such as the occurrence of frost boils, the presence of ice-wedge polygons, silt content, and imperfect drainage (Bockheim, 2007).

After cryoturbation has moved SOC to the cold, deeper soil layers, little to no biological decomposition will take place, making soil temperature a key driver of SOC decomposition and cryoturbation a process which may significantly reduces soil organic matter decomposition rates, thus ultimately impeding physical-chemical alteration of PyC and release of CO_2 to the atmosphere (Bockheim, 2007; Kuhry et al., 2010). Alltogether, these conditions of low temperatures and water logging in permafrost terrain have led to the accumulation of large stocks of SOC in permafrost soils (Hugelius et al., 2013). According to Kuhry et al. (2010), belowground organic carbon in the northern circumpolar permafrost region is estimated around 1672 Pg C, with disproportionately large amounts in cryoturbated soils, loess-like deposits of the yedoma complex, and peat deposits, which often exhibit a low degree of decomposition (Kuhry et al., 2010).

However, arctic warming in the past decades led to an increase in the thickness of the seasonal thaw layer (active layer), and warming of the near-surface permafrost, which will likely release previously protected soil organic matter, making it available for microbial decomposition and end in the release of carbon dioxide to the atmosphere (Bockheim et al., 2003; Diochon et al., 2013). Indeed, deeper soil carbon in permafrost terrain was observed to be released in Alaska, northern Sweden and Siberia (Kuhry et al., 2010). Thus, there is concern that the release of CO_2 from arctic soils may have caused the arctic regions to change from a sink for atmospheric CO_2 to a source

(Bockheim et al., 2003). Thawing permafrost could result in remobilization of the previously frozen SOC pools and the release of large amounts of greenhouse gases (Kuhry et al., 2010).

On the other hand, cryoturbation is also expected to increase due to arctic warming, leading to an increase in the incorporation of SOC (and PyC, as part of it) at depth, thereby enabling the soil to store more SOC and reducing the loss of CO_2 to the atmosphere from soil respiration (Bockheim, 2007). Thus, generally, climate change impacts the thawing permafrost carbon feedback (Kuhry et al., 2010). The feedback from permafrost C to climate change depends on the amount of carbon stored in permafrost soils and on the rate of release of CH_4 and CO_2 to the atmosphere via microbial decomposition of thawed organic matter (Kuhry et al., 2010).

In arctic Canada, Turbic Cryosols cover 79 % of the soil area with considerable amounts of carbon stored in the cryoturbated horizons (Kaiser et al., 2007). The importance of cryoturbation for the arctic carbon cycle may change in the future, since frost heave strongly depends on soil temperature and soil water content, while cryoturbation is sensitive to changes in climate. Understanding the fate of cyroturbated organic carbon therefore becomes a potentially important factor for predicting arctic carbon fluxes under changing climatic conditions (Kaiser et al., 2007). Finally, permafrost warming is happening globally and has the potential to amplify global climate change due to the unlocking of soil organic carbon in frozen sediments (Biskaborn et al., 2019).

1.6 Wildfires and PyC in Boreal Systems

PyC stocks and residence time in soils of the Canadian boreal region are affected by permafrost, but its production mainly depends on wildfires. Indeed, wild-land fire is a prevalent natural disturbance across the boreal forest region (De Groot et al., 2013), and this area stores about 800 Pg C, or one-third of all terrestrial carbon due to its vast size and extensive peatlands. Boreal wild-land fire emits an annual average of 182 Tg C, about 9.1 % of global fire emissions (De Groot et al., 2013).

Boreal forest dynamics are largely driven by disturbances such as fire, a prevalent force of change across the boreal circumpolar region, which can even be the dominant driver of Canadian boreal forest carbon balance (Bond-Lamberty et al., 2007; De Groot et al., 2013). These wildfires are common in the circumpolar region and are expected to become more frequent with climate change, with warmer temperatures associated with increased area burned in Canada and Alaska (Aaltonen et al., 2019; Flannigan et al., 2009).

In Canada, most fires occur as high-intensity crown fires due to lightning during the summer months, which are responsible for 80 % of the area burned by large fires (greater than 200ha) (De Groot et al., 2013; Flannigan et al., 2009). Over the past three to four decades, Canadian fires have burned over an annual average of 2 million hectares, and large fire frequency between 2001-2007 was determined to be higher than in the 1970-2009 period, although the average large fire size was smaller, and most fires occurred in mid-summer (Conard and Solomon, 2008; De Groot et al., 2013; Flannigan et al., 2009).

Fire activity is driven by the local and regional climate. Changes in climate, such as increased temperatures lead to increased fire frequency, transforming areas burned from carbon sinks to carbon sources for decades before turning again to carbon sinks. Thus, climate is indirectly but ultimately responsible for determining the boreal forest carbon dynamics (Bond-Lamberty et al., 2007).

The fire regime is a historical summary of the timing and extent of fire behaviour accumulated on a landscape over many years by many fires. A fire regime thus encompasses characteristics such as fire intensity and severity, type and size of fire, season of burn and fire frequency. On the other hand, fire behaviour encompasses fire intensity and type, fuel consumption, and rate of fire spread. The connection between fire behaviour (small scale) and fire regimes (large scale) is important

because it can be used to scale-up stand-level fire behaviour models to serve as fire regime models. In this way, the history of fire events and associated fire behaviour are used to assess the fire regime (De Groot et al., 2013).

Large fires occur most frequently in northern Canada, where fires in these remote areas are usually started by lightning, and direct suppression action is limited (or not taken) because there are few values at risk. There are many human-caused fires in southern areas of Canada in the spring and autumn, but few of these fires become large because they are usually easily accessible for rapid initial attack (De Groot et al., 2013).

Crown fire is not possible in deciduous forests or grasslands and can only occur in mixedwood stands if the coniferous component is $> 50\,\%$ and the conifer component is capable of crowning. Therefore, even though the North American boreal forest is dominated by a high-intensity crown fire regime, there are many areas within the fire perimeter that are burned as surface fire, or remain unburned, depending on forest composition and weather conditions during the fire (De Groot et al., 2013).

Figure 6: Canadian landscape two years after a wildfire (picture by Marcus Schiedung, 2019).

This picture, taken by Marcus Schiedung in 2019 shows what a boreal landscape looks like two years after a wildfire. Wildfires can get so dense that a local lack of oxygen occurs, leading to an inefficient combustion of wood and thus to the formation of pyrogenic carbon. The PyC dynamic in the Northern Circumpolar Region is so far not well understood, enhancing the relevance of sampling soils from this remote landscape.

For what concerns the permafrost conditions in boreal soils, Aaltonen et al. (2019) investigated the effect of wildfires on the continuous permafrost zone in the Canadian permafrost region and showed that fire had a significant effect on the active layer depth. Indeed, fire increased the active layer depth and decreased the organic layer thickness. Further, fire can influence carbon stocks and also the quality of organic matter changes after the fire, leading to combusted organic carbon that is more resistant to decomposition. (Aaltonen et al., 2019). For these reasons, investigating PyC in boreal landscapes is of essential importance for the understanding of atmospheric carbon sequestration on a long timescale.

1.7 The Role of PyC for Boreal Climate

The Northern Circumpolar Region is considered the most prone to increased energy emissions from climate change (Batjes, 2016). Climate change mitigation strategies rely heavily on carbon storage in forests and therefore require an understanding of the interactions between fire, vegetation and the carbon cycle (Lasslop et al., 2019).

Wildfire events interact with the global carbon cycle and thus affect the climate and potential climate change. The combustion of vegetation biomass leads to a reduction of terrestrial biomass, leading to a reduction in the amounts of carbon stored on land but an increase in the emissions of various trace gases and aerosols. However, pyrogenic carbon production during these fire events partly offsets the carbon source effect of fire emissions as PyC accumulates in soils and sediments over decadal to centennial timescales and even to millennial timescales in ocean sediments. Thus, fire emissions substantially influence the atmospheric budgets of greenhouse gases, other trace gases, and aerosols (Lasslop et al., 2019). For example, fire emissions influence atmospheric chemistry and trigger reactions that influence the lifetime of methane and increase ozone concentration, air pollution levels, and acid deposition with side effects on vegetation (Lasslop et al., 2019).

The net effect on carbon storage of a fire is determined by the ecosystem's ability to recover the combusted carbon stocks and the fate of the combusted carbon. The combusted carbon can either be lost to the atmosphere or accumulate in terrestrial or oceanic systems through the production of highly stable solid pyrogenic carbon (Lasslop et al., 2019).

Post-fire boreal forest soils are typically a long-term CO_2 source because of decomposition of organic matter and root respiration and a CH_4 sink because of microbial oxidation. The warming effect from the CO_2 source is much stronger than the CH_4 sink cooling effect.

Since the industrial revolution, human manipulation of the PyC cycle has increased substantially through activities that either enhance (fossil fuel combustion, land clearing) or suppress (active fire management, overgrazing, landscape segmentation) PyC production (Bird et al., 2015). Indeed, the use of fossil fuels for energy production in industry and transportation is a significant anthropogenic source of PyC today (Wiedemeier et al., 2016).

Concerning the permafrost, the latter is another carbon reservoir responding to climate change. Indeed, thawing of permafrost due to global warming causes the release of carbon into the atmosphere (Zimov et al., 2006) and cryoturbation redistributes organic carbon into soils (Diochon et al., 2013).

Further, climate, land use, and other anthropogenic and natural drivers have the potential to influence fire dynamics in many regions (Van Der Werf et al., 2017). Nonetheless, anthropogenic fossil fuel–derived PyC contributes only a minor amount (0.2 % of global atmospheric emissions) (Lasslop et al., 2019).

Thus, the anthropogenic influence on the global pyrogenic carbon cycle is not considered in this thesis, nor is the atmospheric and marine pyrogenic carbon pool. The focus is set on PyC in permafrost affected soil systems along landscape gradients in the Canadian boreal region.

1.8 Related Work

This master's thesis can be considered an insight into the ongoing PhD project of Marcus Schiedung, which focuses on the dynamics of PyC in an arctic system and considers the transport and mobility of PyC in soils. Together with Severin Luca-Bellè's PhD project, which focuses on the pathways of pyrogenic carbon in the soil environment of a tropical ecosystem, these two PhD projects are part of a larger project to determine where on Earth fire-derived carbon is stored.

1.9 Objectives

The potential main drivers contributing to PyC's physical and chemical alteration and translocation along landscape gradients are soil texture, pH, permafrost, and translocation due to steepness. PyC can further be deposited within hillslopes, can enter in intermediate pools such as water reservoirs or finally escape the soil system either due to water flux or due to surface runoff; ultimately entering the marine system as dissolved and particulate PyC (Bird et al., 2015; Cotrufo et al., 2016; Santín et al., 2016).

However, the extent to which these drivers contribute to PyC's translocation or fate in the landscape is still unclear, as is its age and stocks at different landscape positions. The aim of this master's thesis is to enable a better understanding of the drivers contributing to PyC's physical and chemical alteration in soils as well as its transport along two landscape gradients in the Canadian boreal forest soils. It is of particular interest to understand the role of individual SOC fractions, such as the particulate organic matter (POM), the sand and aggregates (S+A), the silt and clay (s+c) and the residual soil organic carbon fraction (rSOC) in the stability of PyC and its resistance against degradation. Overall, the main research question this thesis aims to answer is:

"Which are the main drivers controlling the translocation and physical-chemical altering of PyC stored in soils of the Canadian boreal forests at different landscape positions (e.g. elevated, slope and depressions)?"

The main hypotheses are:

1. There is a preferential way of PyC translocation in respect to translocation of SOC along landscape gradients and soil depths.
2. Translocation of PyC to depositional landscape position due to soil erosion causes greater contributions of PyC stocks at the bottom of landscape gradients.
3. More altered PyC is located in depositional landscape positions.
4. Quality and quantity of PyC depend on the association with specific SOC fractions (e.g., silt and clay, sand and aggregates, or particulate organic matter).
5. Permafrost affects vertical translocation of PyC by cryoturbation and reduces decomposition of SOC.
6. The soil characteristics and permafrost conditions are determinant for the cycling of SOC.

To test the hypotheses, the quantity and quality of both SOC and PyC will be investigated at six landscape positions along two Canadian landscape gradients (three positions each), and at several soil depths.

Chapter 2

Materials and Methods

2.1 Study Area: Locations of Landscape Gradients

The northern circumpolar region (delimited by the July 13 °C isotherm in the north and the July 18 °C isotherm in the south) is home to the boreal forest, which covers about 1.3 billion ha of land, representing the largest forest biome and one third of global forest cover. This forest is characterized by relatively few tree genera commonly found across the entire region, primarily Fir *(Abies)*, Birch *(Betula)*, Larch *(Larix)*, Spruce *(Picea)*, Pine *(Pinus)*, and poplar *(Populus)*, although tree species are different between Eurasia and North America. This distinct continental separation in forest species composition is matched by the marked difference in continental fire regimes. Indeed, the connection between plant species and fire regime is well-known: vegetation is fuel, which affects flammability and fire behaviour through fuel consumption (De Groot et al., 2013).

The study area encompasses two separated landscape gradients in two regions of Canada, as visible in Fig. 7 below: soils from the South Slave Lake Region (Alberta and Northwest Territories), under discontinuous permafrost conditions, and soils from the Inuvik Region (Northwest Territories), under continuous permafrost conditions.

Figure 7: Study area with the northern landscape gradient in the Inuvik Region and the southern one in the South Slave Lake Region (Figure made with Google Earth Pro).

2.1.1 South Slave Lake Region

According to the Ecological Stratification Working Group (1995), the sampling location in the South Slave Lake Region is located in the Canadian ecozone of the Boreal Plains, precisely in the ecoregion of the Slave River Lowland.

The Boreal Plains ecozone is part of the flat Interior Plains of Canada, a northern extension of the Great Plains of North America, and extends from British Columbia in the northwest to the southeastern corner of Manitoba, covering 650'000 km^2. The subdued relief consists of low-lying valleys with few bedrock outcrops and plains stretching through almost two-thirds of Alberta. Timber covers 84 % of the Boreal Plains, with agriculture accounting for less than 20 % of the land area. (Ecological Stratification Working Group, 1995).

The climate of the Boreal Plains ecozone is determined by its location in the heart of North America, resulting in continental climatic conditions, and is typified by long cold winters and short moderately warm summers. The mean annual temperature ranges between -2 °C to 2 °C whereas the annual precipitation is approximately 450 mm, hence greater than the evaporation rate, resulting in surplus moisture of up to 100 mm near the southern edge of the ecozone and up to 300 mm in the northern and foothills regions (Ecological Stratification Working Group, 1995).

Further, fire is the most powerful influence on the forest, determining distribution and growth rates. In a typical year, more than one million hectares burn, despite increasingly effective fire suppression and prevention efforts (Ecological Stratification Working Group, 1995). Between 1980 and 1999, 13.36 % of the Boreal Plaines' forested area burned, corresponding to 7.921 million hectares (Flannigan et al., 2009).

Figure 8: Landscape on the slope along the catena in the South Slave Lake Region. Vegetation consists mainly of Jack Pine and Poplar, with a scarcer presence of Spruce. The stand is more than 80 years old and the trees are $>$ 25 m high (picture by Marcus Schiedung, 2019).

Moreover, in the terrestrial ecoregion of the Slave Reaver Lowland in northeastern Alberta, the mean annual temperature is approximately -2 °C, with a mean summer temperature of 13 °C and a mean winter temeprature of -17.5 °C. The ecoregion is classified as having a subhumid mid-boreal ecoclimate. Its boreal vegetation was captured in Figure 8 and is typically medium to tall, comprising closed stands of trembling aspen, balsam poplar, and jack pine, with white and black spruce, and balsam fir occurring in late successional stages. Cold and poorly drained fens and bogs are covered with tamarack, black spruce, ericaceous shrubs, and mosses. Underlain by relatively flat, low-relief Palaeozoic carbonates, and except for the delta, the region is mainly an undulating sandy plain with some eolian features. Peatland covers up to 50 % of the land area. As part of the Northwest Territories (NWT) and northern Alberta (AB), the South Slave Lake Region is affected by sporadic to discontinuous permafrost conditions with low ice content (Ecological Stratification Working Group, 1995).

2.1.2 Inuvik Region

Soils from the Inuvik Region, Northwest Territories, affected by continuous permafrost conditions, are located in the Canadian ecoregion of the Great Bear Lake Plain, which is part of the terrestrial ecoprovince of the Great Bear Lowlands in the ecozone of the Taiga Plains (Ecological Stratification Working Group, 1995).

The Taiga Plains are an area of low-lying plains centred on Canada's largest river, the Mackenzie, and its many tributaries. It is Canada's sixth largest ecozone, with an area of approximately 550'000 km^2. Approximately 90 % of the Taiga Plains are located in the western Northwest Territories, with small extensions into northeastern British Columbia and northern Alberta. It is bounded to the east by Great Bear and Great Slave lakes, to the west by the rolling foothills of the Mackenzie Mountains, to the north by the Mackenzie Delta, and to the south by the spruce forest of the Boreal Plains.

The Taiga Plains feature typically subdued relief, consisting of broad lowlands and plateaus. The nearly level to gently rolling plains are occasionally interrupted by some of the larger river valleys, which can be hundreds of metres deep. Other signs of the dynamic power of large rivers include steep, fast-eroding riverbanks and ice-scoured shores.

The subarctic climate is characterized by short, cool summers and long, cold winters, with cold arctic air ingluencing the area for most of the year. Precipitation is low to moderate, averaging 250-500 mm a year across much of the ecozone. Snow and freshwater ice-cover persist for six to eight months annually (Ecological Stratification Working Group, 1995). Permafrost, where present, detracts from the soil's productivity by chilling it and creating waterlogged conditions in the thawed active layer near the surface.

The vegetation communities of the Taiga Plains are depicted in figure 9 and are dominated by a few species well-adapted to poor soil conditions and the harsh subarctic climate. Tree species of the northern taiga forest include Black Spruce, White Spruce, Jack Pine, Tamarack, Paper Birch, Trembling Aspen, and Balsam Poplar. Willow and alder shrubs also flourish in this habitat.

Low shrubs are abundant throughout this ecozone and include many species of heathers, such as Labrador Tea and Leatherleaf, plus a wide array of berry-producing species, including cranberries, currants, and blueberries. Forest fires that destroy several thousand hectares of trees are not uncommon in this ecozone. On average, 1 % of the Northwest Territories' forests burn every year (Ecological Stratification Working Group, 1995).

Between 1980 and 1999, 11.237 million hectares of forested area burned, corresponding to 21.64 % of the whole forested area in the Taiga Plains, making this Canadian ecozone the second for percentage of forested area burned, after the West Boreal Shield (Flannigan et al., 2009).

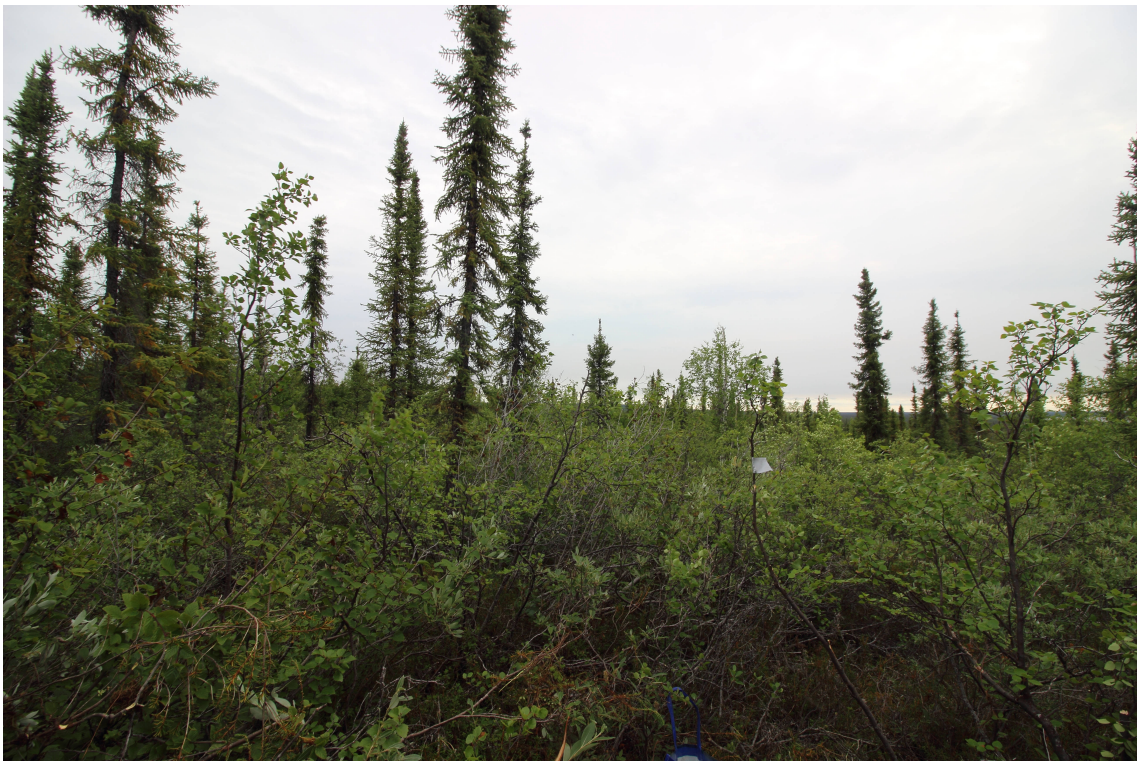

Figure 9: Landscape along the slope of the chosen catena in the Inuvik Region. Vegetation comprises mainly Spruce, followed by Poplar and some bushes, such as Red Willow and Labrador (picture by Marcus Schiedung, 2019).

Many taiga plant species benefit from the regular cycle of fires, which can purge old, stagnant forests of insects and disease. The distinctive mosaic of forest types created by fires usually results in a boost to the overall productivity and diversity of habitats available to wildlife.

Moreover, the Great Bear Lake Plain extends southward from the Mackenzie River delta to Great Bear Lake, including some of the terrain surrounding the southern shore of the lake. The mean annual temperature is around -9 °C. The mean summer temperature is 8°C and the mean winter temperature is -25.5 °C. Mean annual precipitation ranges 200-300 mm. The ecoregion is classified as having a high subarctic ecoclimate. The latitudinal limits of tree growth are reached along its northern boundary (Ecological Stratification Working Group, 1995).

The predominant vegetation consists of open, very stunted stands of black spruce and tamarack with secondary quantities of white spruce and a ground cover of dwarf birch, willow, ericaceous shrubs, cottongrass, lichen, and moss. Poorly drained sites usually support tussocks of sedge, cottongrass, and sphagnum moss. Low shrub tundra, consisting of dwarf birch and willow, is also common. Composed of flat-lying Cretaceous shale and Devonian limestone strata, the surface of this ecoregion is generally below 310 m.a.s.l. The ecoregion is generally covered by undulating glacial drift and outwash deposits. Turbic Cryosols with Static and Organic Cryosols developed on organic deposits with deep permafrost are the dominant soils. Unfrozen Organic and Brunisolic soils also occur. Permafrost is extensive and discontinuous, with low to medium ground ice content, and is characterized by sparse ice wedges (Ecological Stratification Working Group, 1995).

2.2 Characterization of Soil Sampling Sites

Soil samples were collected by Marcus Schiedung and Severin-Luca Bellé in 2019 along both landscape gradients (i.e., South Slave Lake Region and Inuvik Region) at three landscape positions (i.e., top, slope, and bottom), inside of defined "Ecosystem Unit Plots" (EUP), from which soil material was extracted at several depths. Soil profiles of each EUP are exhibited in Figure 11 and further information about pH-values and cation exchange capacity (CEC) can be found in Table 10 in the appendix.

As visible in figure 10, on each location a sample plot of 900 m^2 divided into 9 pits (named 1-9) was realized, and sampling material was then grouped into composites with soil from three pits each, leading to three replicates (a, b, and c) per EUP and depth. Furthermore, sampling was acquired at 0-15 cm, 15-30 cm, 30-45 cm, and 45-60 cm depths at all pits.

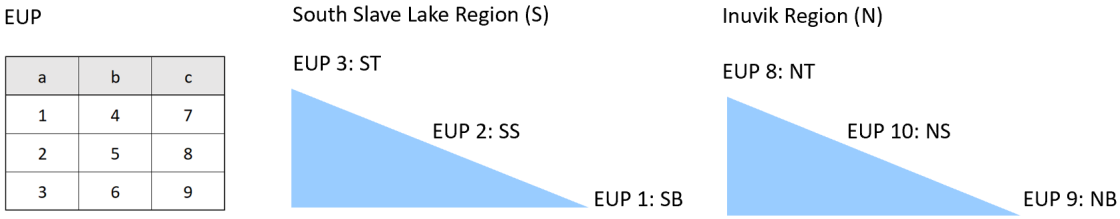

Figure 10: Ecosystem Unit Plot (EUP, left) with 9 pits in 3 composited replicates (a, b, and c) for 3 field replicates along each catena (top, slope, and bottom) and 2-3 soil depths.

The chosen landscape gradient (hereafter also called catena) at the South Slave Lake Region covers a distance of 200 m, with 100 m distance between the sampling locations. The bottom of the catena (hereafter SB for South Bottom), which faces the Pine Lake, is located at 270 m.a.s.l., the sampling location on the slope (hereafter SS for South Slope) at 275 m and the top of the catena (hereafter ST for South Top) at 280 m, with a difference in elevation of 10 m. According to the WRB soil classification, the soil profiles were classified as Regosols to Cambisols. The soil texture is mainly affected by sand, followed by silt and finally by clay particles. The pH was always greater than 6, so soils in this area are affected by the carbonate buffer system.

The selected catena in the Inuvik Region covers a distance of 600 m, with 200 m between the top, slope, and bottom location. The bottom of the catena (hereafter NB for North Bottom), which faces the sea, is located at 50 m above sea level, the sampling location on the slope (hereafter NS for North Slope) at 65 m and the top of the catena (hereafter NT for North Top) at 90 m, with a difference in elevation of almost 50 m. Soil profiles led to the WRB classifications of Cryosols, despite some different characteristics along the catena. The texture differs from the south as it comprehends greater amounts of silt, followed by minor amounts of clay, and finally sand compounds. Since the pH was always lower than 6, soils are no longer affected by the carbonate buffer system.

Further, in the South Slave Lake Region the time since fire consist of more than 54 years, whereas in the Inuvik Region in more than 40 years. Permafrost depth in the latter was $>$ 60 cm at top, $>$ 40 cm along the slope and 30 cm at the bottom of the catena, whereas in the second landscape gradient there was almost no permafrost.

Soil characteristics as presented in Table 1 were determined by Marcus Schiedung. Soil type was determined according to the FAO (2014), whereas moisture classes are based on Johnstone et al. (2008).

Table 1: Permafrost conditions, soil type, and moisture class for individual sampling locations along the catenae.

Catena	Landscape Position	EUP	Name	Permafrost Conditions	Soil Type	Moisture Class
North	Top	8	NT	Continuous	Folic Cambic Cryosol	Subxeric
	Slope	10	NS		Folic Cambic Cryosol	Mesic
	Bottom	9	NB		Glacic Dystric Cryosol	Mesic to Subhygrid
South	Top	3	ST	Sporadic	Folic Dystric Cambisol	Subxeric to Mesic
	Slope	2	SS		Folic Brunic Regosol	Subxeric to Mesic
	Bottom	1	SB		Folic Dystric Gleysol Colluvic	Mesic

In terms of soil moisture classes, the South Slave Lake Region was described as subxeric to mesic at the top and slope of the catena, and mesic at the bottom, whereas differences in soil moisture classes are more pronounced in the Inuvik Region, with subxeric conditions at the top, mesic conditions on the slope, and even mesic to subhygric conditions at the bottom.

Soil moisture increases in the bottom direction along both catenae, although the northern landscape gradient exhibits higher moisture than the southern one. Indeed, there was very noticeable surface moisture along the catena in the South Slave Lake Region, which evolved into moderate surface moisture, whereas there was some noticeable and well-drained surface moisture at the top of the landscape gradient in the Inuvik Region, which became more noticeable along the slope and considerable at the bottom. (Johnstone et al., 2008).

For what concerns the determination of the soil type, Cryosols, such as in the Inuvik Region (three lower profiles in Fig. 11), comprise mineral soils formed in a permafrost environment. The subsurface layer (cryic horizon) is permanently frozen, and if present, water occurs in the form of ice. Cryogenic processes are the dominant soil-forming processes in most Cryosols (FAO, 2014).

On the other hand, soils from the South Slave Lake Region comprise Cambisol at the top, Regosol at the slope, and Gleysol at the bottom of the catena. Cambisols, such as at the ST, combine soils with at least an incipient subsurface soil formation. Transformation of parent material is evident from structure formation and mostly brownish discoloration, increasing clay percentage, and/or carbonate removal. Regosols, such as those at the SS, are very weakly developed mineral soils in unconsolidated materials. Regosols are extensive in eroding lands and accumulation zones, particularly in arid and semiarid areas and in mountainous terrain. Finally, because Gleysols are high in organic matter and have low pH values, they provide a better habitat for micro- and mesoorganisms, accelerating the decomposition of soil organic matter (and thus the supply of plant nutrients) (FAO, 2014).

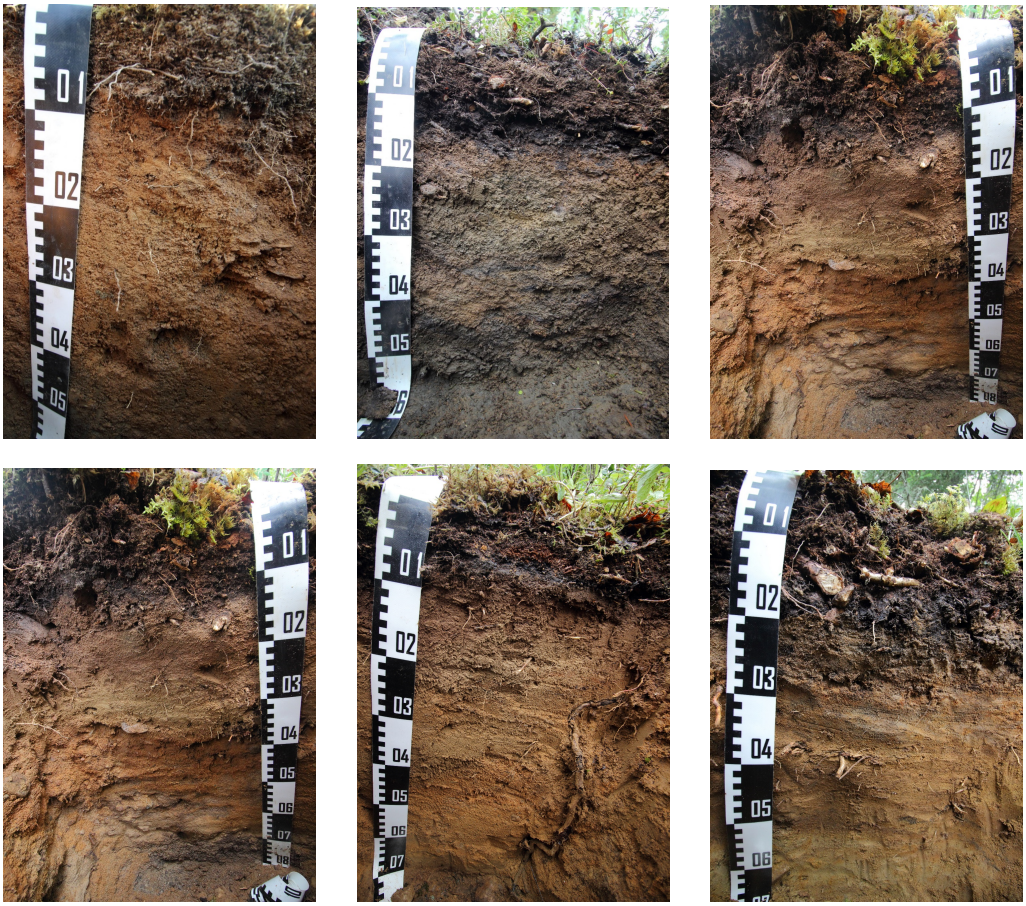

Figure 11: Soil profiles of each landscape position. Upper line from left: Profiles from the Inuvik Region with top (left), slope (centre) and bottom position (right). Lower line from left: profiles from the South Slave Lake Region with top (left), slope (centre), and bottom position (right).

2.3 Sample Composition and Measurement Setup

After measurement of the relative abundance of C in all soils, only depths with a SOC > 1 % were selected for this thesis, since lower carbon concentrations would not be sufficient for detection in the single SOC fractions. This led to 41 composited samples (hereafter composites) of ca. 40 g of mass each. Specifically, since in the South Slave Lake Region the C percentage was greater than 1 % till 30 cm depth, two soil depths were considered, i.e., 0-15 cm and 15-30 cm, for a total of 18 composite samples, despite the availability of material till 60 cm depth. On the other hand, in soils from the Inuvik Region, C > 1 % till 45 cm depth, leading to a third soil depth at 30-45 cm and a total of 23 composite samples. For details of each composite, please refer to table 9 in the appendix. Further, pH measurement revealed lower values in the Inuvik Region, and since the pH was always clearly lower than 6, no fumigation was applied to samples from this region, whereas in the South Slave Lake Region pH > 6, indicating that those soils are still affected by the carbonate buffer system.

Composites were used for the investigation of the drivers controlling PyC translocation and physical-chemical altering along landscape gradients and in soil depths. For this, soils were investigated with different methods represented in figure 12, which comprehend SOC fractionation by size and density, which was applied first, followed by fumigation with hydrochloric acid to the sample in the south with the sole purpose of erasing carbonates and thus measuring total organic carbon. Chemothermal oxidation at 375 °C was applied for the quantification of PyC in the bulk samples and SOC fractions. Diffusive infrared Fourier transformation spectroscopy (DRIFT) was conducted to investigate the SOC quality and benzene polycarbocyclic acids analysis (BPCA) to determine the quantity and quality of PyC in the composite samples. Prior to the determination of C % in the bulk samples through dry combustion with Picarro, homogenization of the sample was done by milling an aliquot of the composite samples in a horizontal mill at f = 30 /s for 3 min and 30 sec.

Figure 12: Some impressions from the lab. In the upper line from left: a composite sample, with the consequent sand and aggregate, silt and clay, and particulate organic matter fractions, originated after fractionation. In the second line: the dissolved organic fraction (left) and the extraction of the residual soil organic carbon fraction from the silt and clay fraction. In the lower line from left: DRIFT and chemothermal oxidation at 375 °C.

2.4 Soil Organic Carbon Fractionation

Soil organic carbon fractionation by size and density based on Zimmermann et al. (2007) and re-elaborated by Poeplau et al. (2013) was applied for the investigation of soil carbon stability and quantity. As depicted in figure 13, this process resulted in five fractions (represented in ovals), from which dissolved organic carbon (DOC) and particulate organic matter (POM) are considered labile and/or dynamic carbon pools (i.e., with a short turnover time of 6 months to 1 year), whereas sand and aggregate (S+A) and silt and clay (s+c) fractions are considered stable pools (thus having an intermediate turnover time of 10-50 years), because they are physically and chemically protected against fast decomposition (Zimmermann et al., 2007; Abramoff et al., 2018). Finally, a residual fraction (rSOC) was determined by chemical oxidation with 6 % NaOCl and regarded as a passive or even inert pool (Zimmermann et al., 2007). The latter is supposed to have the longest turnover time, of 100-1000 years, and is considered to be chemically or physically stabilized (Abramoff et al., 2018).

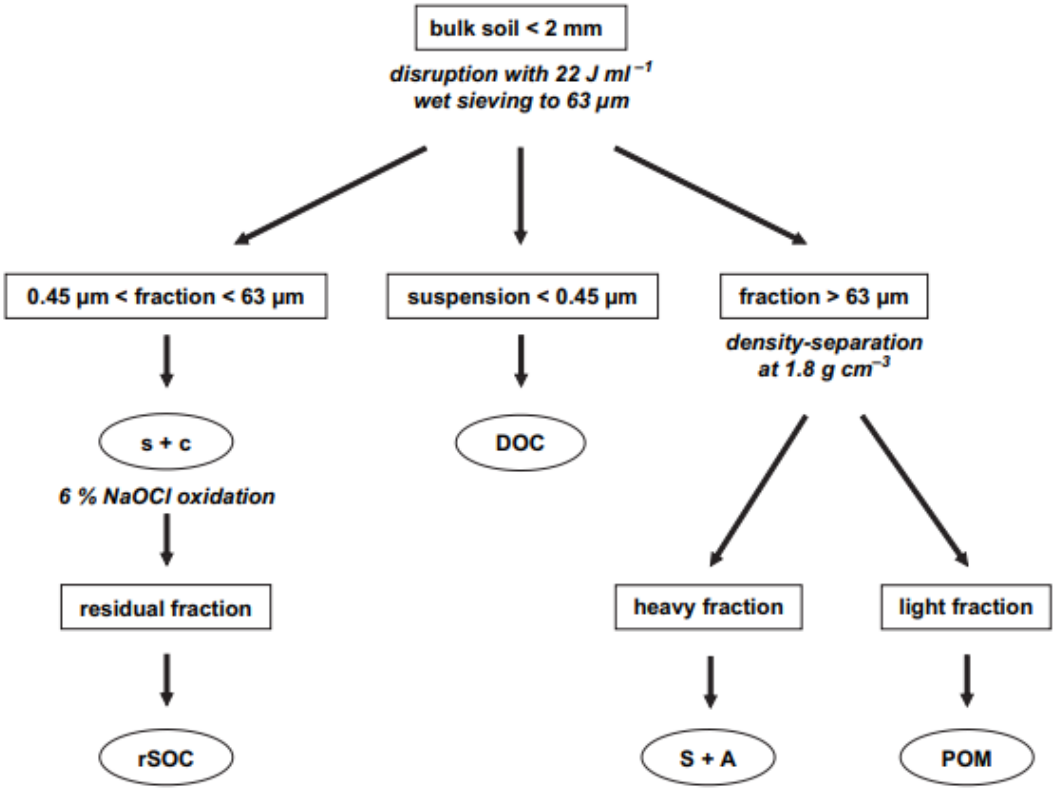

Figure 13: Soil organic carbon fractionation by density. Carbon content in DOC was not measured because assumed to be lower than 5 % (Jones et al., 2020; Zimmermann et al., 2007). Total carbon (TC) and total organic carbon (TOC) were investigated for POM, S+A, s+c, and rSOC, whereas PyC was measured only in the three fractions POM, S+A, and s+c.

For fractionation, 20 g of dried (40 °C) and sieved (< 2 mm) composited soil have been weighted in a 250 ml round flask and mixed with 150 ml of deionized water for dispersion with an ultrasonic probe. The latter was calibrated to a constant output energy of 22 J/ml, an amplitude of 70 %, a

pulse of 0.5 s and a duration of 92 s to disperse labile microaggregates. The suspension was immersed in the probe for 1-2 cm to ensure a maximal cavitation effect, and consequently set occluded C free (Poeplau et al., 2013).

Thereafter, samples have been wet sieved over a 63 µm sieve using an aerosol flush to apply pressure while avoiding physical breakdown of the aggregates. This step permitted the separation of the coarse (S+A), fine (s+c) and dissolved organic carbon fraction (DOC). The samples have been flushed until the rinsing water was clear (with 1'000-1'400 ml depending on the sample, with generally less water needed for the Southern composites). The > 63 µm fraction contains the POM (after dispersion) and S+A fractions. These were dried at 40 °C in a weighed aluminium evaporation dish and weighed. At this point, due to higher clay content in the composites from the Inuvik Region, the suspensions of DOC and s+c of the latter have been subject to sedimentation in the fridge before vacuum filtration. This intermediate step was not done for composites from the South Slave Lake Region.

The remaining suspension containing the < 63 µm fraction (i.e. s+c, rSOC and DOC) was filtered to 0.45 µm using a vacuum filtration aperture and glass-fiber filters. Then, the s+c and rSOC fraction (> 0.45 µm) was rinsed from the filter paper and dried in a weighted aluminium dish at 40 °C and weighted after drying. After that, the filtrated solution was weighted, and an aliquot of it (ca. 45 ml) was taken and frozen. No measurement of the carbon content in the dissolved organic carbon fraction occurred, since the latter is assumed to have less than 5 % of total carbon (Zimmermann et al., 2007).

Fractionation by density was applied to the dry > 63 µm fraction for the separation of the POM from the S+A fraction. The samples were placed in a 50 ml centrifuge tube and a sodium polytungstate (SPT) solution with an adjusted density of 1.8 g cm^{-3} was added to reach a total volume of 50 ml. The samples were slightly shaken and allowed to settle for 1 hour, then centrifuged for 15 min at 1000 g (2'8000/min), allowed to settle again for 30 min and finally separated. The floating POM was decanted in a weighed and labelled 60 µm sieve bag, and the heavier S+A fraction was flushed in a second labelled and weighed sieve bag. All bags have been washed under running water to remove SPT, dried at 40 °C and weighted (Zimmermann et al., 2007).

Finally, the rSOC fraction was separated from the dried < 63 µm fraction (s+c) by chemical oxidation with 6 % NaOCl. For this, 0.5 g of s+c were weighted in a 15 ml centrifuge tube and filled up to 13.5 ml with 6 % NaOCl. Oxidation was allowed for 18 hours at room temperature (25 °C) in a fume hood. After, samples were centrifugated for 15 min at 1000 g (2'8000/min), decanted, washed with deionized water, and centrifugated again. Oxidation and washing were then repeated twice. The remaining sample was dried at 40 °C for a week and used for the measurement of C % through dry combustion with Picarro.

An aliquot of all solid (POM, S+A, s+c) fractions was milled and used for the determination of carbon content and $\delta^{13}C$ value. A mass recovery of the solid fractions was determined as the total mass of fractions with respect to the initial sample mass and corresponds to 96.7-99.1 % for samples from the South Slave Lake Region and 90.0-97.7 % for samples from the Inuvik Region. Similarly, a carbon recovery based on the sum of total carbon content in each fraction with respect to the amount of total carbon in the bulk sample was computed according to the following formula:

$$Carbon\ recovery\ [\%] = \frac{m_{bulk} * C_{bulk}\ [mgC]}{m_{POM} * C_{POM} + m_{S+A} * C_{S+A} + m_{s+c} * C_{s+c}\ [mgC]} \tag{2.1}$$

With m_x as mass in grams of the fraction x and C_x as the carbon percentage of the same fraction. Samples whose carbon balance was lower than 80 % were subjected to a second fractionation. If the second attempt was better than the first one, only the second was considered; if there were no differences, the first one was taken. For three samples from the bottom of the catena in the South (1, 2 and 4) a second fractionation was done to increase the mass of the s+c fraction (otherwise lower than 1 g) and since both attempts show similar carbon recoveries, the replicates a and b (from fractionation 1 and 2, respectively) were physically mixed. After having made a second fractionation where needed, carbon recovery corresponds to 80.3-106.8 % for the samples in the South Slave Lake Region (except for sample 11b, with a recovery of 73.23 %) and to 78.3-109.5 % for the samples in the Inuvik Region, except for samples from NS (i.e., North Slope) with a depth of 15-30 cm and 30-45 cm, whose carbon recovery is in the range of 65.3-75.1 % also after having made a second fractionation for all of them.

2.5 Diffuse Reflectance Infra-Red Fourier Transformation Spectroscopy (DRIFT)

Diffuse Reflectance Infra-Red Fourier Transformation Spectroscopy, hereafter DRIFT, is a mid-infrared (MIR) spectroscopy method used to investigate the quality of SOC and PyC in the organic layer of each EUP, the bulk samples, and the five soil organic carbon fractions of each composite sample along landscape gradients and depth profiles. During measurement, infra-red electromagnetic radiation interacts with molecular bonds within the functional groups of SOM, giving origin to spectra of absorbance with individual peaks for specific chemical structures, allowing a qualitative determination of the relative concentration of soil organic matter functional groups (Stumpe et al., 2011; Yeasmin et al., 2017). For this, four absorption bands were selected along the IR-spectrum according to Chatterjee et al. (2012) and Laub et al. (2020) as visible in table 2:

Table 2: Chosen peaks of absorbance and corresponding wavelength region (Chatterjee et al., 2012; Laub et al., 2020).

Absorption Range	Chemical Structure
$2915 - 2940\ cm^{-1}$	C-H aliphatic stretch, decrease
$1590 - 1660\ cm^{-1}$	Aromatic-carboxylate absorption band
$1210 - 1260\ cm^{-1}$	Cellulose peak
$1500 - 1510\ cm^{-1}$	Lignin peak

A total of 211 spectra were obtained in the 4000-400 cm^{-1} wavenumber range, with a resolution of 4 cm^{-1} and 64 scans per sample. Potassium bromide (KBr) was measured as a background signature according to Yeasmin et al. (2017). The spectra comprise measurements of six organic layer samples (one for each EUP), 41 measurements of the bulk samples, S+A, s+c, POM, and rSOC fractions (i.e., one measurement for each of the five fractions of the composite sample plus the bulk measurement).

Since the quality of the spectral information depends on the level of sample grounding (Stumpe et al., 2011), different levels of milling were tested for bulk samples and individual fractions before proceeding with the acquisition of the 214 spectra. Generally, lightly milled soil samples were found to provide qualitatively better spectral information than more intensively milled soil samples (Stumpe et al., 2011).

Sample preparation for bulk and S+A fraction consisted of ball-milling of 1 spoon of material with a horizontal mill for 10 s at a frequency of f = 15/s, whereas the POM fraction was milled either by hand or for 30 s at a frequency of f = 20/s and the s+c and rSOC fractions did not require special treatment (no milling since fraction grain size < 45 µm). Due to a lack of volume to fulfil the standard holder, POM fractions of samples 11b, 12b, 18a, 25a, 27a, and rSOC fraction of composite sample 1mix were obtained by using a smaller sample holder. Prior to measurement, KBr was measured as a background signature with the smaller holder and a t-test was done to ensure there was no significant difference between measurements taken with the two different holders in the wavelength regions of interest for this thesis.

The t-test takes into account 20 measurements with *Miscanthus* (standard for plant-based material) and 20 with Chernozem (standard for soil samples) for both the standard and smaller holder, in the wavenumber range of 4000-400 cm^{-1}. In cases where the p-value of the t-test was lower than 0.05, the difference in the spectral signature made by using the standard and the smaller holder was considered to be significant. All areas along the spectra with significant differences are described in table 3 below:

Table 3: Wavelength region of influence of the smaller non-standard sample holder for Miscanthus and Chernozem, determined through t-test.

Sample Type	IR-range	Peak
Miscanthus	1843-1857 cm^{-1}	Quartz overtones
	858-773 cm^{-1}	Aromatic C-H out-of-lane bend
	950–680 cm^{-1}	O-H bending of phyllosilicates, Fe and Al oxides
	950–680 cm^{-1}	Si-O bending of quartz
Chernozem	2879-2819 cm^{-1}	Aliphatic C-H stretching of CH_3 and CH_2
	2850-2820 cm^{-1}	Aliphatic C-H (Difference between samples)

Consequently, the significant differences in the spectra are not acquiring in the wavelength region of interest for this study. The acquired spectra were used to compute the aliphatic/aromatic and cellulose/lignin ratios with the help of an R-script. An overview of the mean ratios for each landscape position and depth can be found in the appendix table 7.

The lignin peak at 1510 cm^{-1} is significantly correlated to the total C content and $C : N$-ratio, whereas distinct peaks in the region from 1510 to 1230 cm^{-1} may serve as a proxy for the evaluation of the decomposition of forest litter in soils (Stumpe et al., 2011).

2.6 Chemothermal Oxidation at 375°C (CTO-375)

Chemo-thermal oxidation at 375 °C (CTO-375) based on Agarwal and Bucheli (2011) and Gustafsson et al. (2001) with fumigation according to Walthert et al. (2010) was used for quantification of the most stable and condensed form of PyC in the 41 soil carbon fractions and bulk samples.

Approximately 40 mg of dried (40 °C) and milled soil sample (10 mg for POM material) was weighted in pre-tared Ag-capsules (5x9 mm, Hekatech, Germany). For bulk, POM and s+c material, each sample was weighted in four times and composited for the analysis into 2 replicates with 2 capsules each, whereas for S+A each sample was weighted 6 times, giving origin to 2 replicates with 3 capsules of 40 mg each. The samples were placed in a muffle oven for combustion at 375 °C with sufficient oxygen supply for 24 hours. The temperature was increased to 350 °C with 10 °C/min, and then to 375 °C with 1 °C/min. The first phase with a fast increase of the temperature is to avoid any charring in the samples and the second phase with a slow temperature increase is to avoid a temperature overshoot (Agarwal and Bucheli, 2011).

After removal from the muffle oven, remaining carbonates were removed by fumigation with HCl vapour based on Walthert et al. (2010) as described in the previous section to avoid PyC overestimation (Hammes et al., 2007). Thereafter, Ag-capsules were put into tin capsules to allow better heat transfer and combustion. The $\delta^{13}C$ values and PyC content were determined through dry combustion at high temperature (950 °C) with Picarro.

To ensure there is no production of PyC during high combustion in the oven, four samples of Chernozem of 40 mg each were added at the end of each tray, combined in two replicates of two times 40 mg, and the final C % after CTO-375 was measured. Considering that Chernozem has a fixed C % of 2.01, if after CTO-375 the measured PyC % with respect to TOC is in the range 1.8-2.5 % it was assumed no production of PyC occurred in the laboratories during sample preparation. The measured values were in the expected range for all Chernozem control samples, except for two samples whose PyC content was lower than 1 % of TOC and two samples with a PyC content of 2.7 % of TOC.

As well as after fumigation, the quantity of PyC in mg in each fraction was computed by multiplying the mass of the fraction with the percentage of C in the samples after CTO-375. Since the sum of mg PyC in the fractions exceeds the mg of PyC in the bulk sample, a correction was made for the determination of the relative and absolute distribution of organic carbon into the individual fractions, according to the same formula as for total carbon. Recovery of pyrogenic carbon after CTO-375 is in the range 21.96-90.43 % in soils from the South Slave Lake Region, except for composite samples number 1, 2, 4 and 5, with 439.07 %, 1294.49 %, 258.26 % and 180.55 %, respectively. In the Inuvik Region, PyC recovery is in the range 35.64-100.15 %, except for composite samples numbers 32 and 39, with a recovery of 147.99 % and 143.99 %, respectively.

Concerning the $\delta^{13}C$ values, all measurement performed with Picarro whose maximal peak was lower than 200 ppm was not taken and used because it is below the detection limit. Thus, all $\delta^{13}C$ values measured after CTO-375 (i.e. $\delta^{13}C$ for PyC in the soil fractions and bulk sample) are not considered here. A detailed summary of the average $\delta^{13}C$ values after fumigation and after CTO-375 can be found for each landscape position and depth in Table 8 in the appendix.

2.7 Benzene Polycarboxylic Acids (BPCA) Analysis

The benzene polycarboxylic acid (BPCA) method allows the simultaneous assessment of PyC's characteristics, quantity, and isotopic composition (^{13}C and ^{14}C) on a molecular level, providing information on the quantities and number of the PyC markers that can be related to the source and formation conditions of the PyC (Hammes et al., 2007). The method is applicable to a wide range of environmental sample materials and detects PyC over a broad range of the combustion continuum, i.e., it is sensitive to slightly charred biomass as well as high temperature chars and soot (Wiedemeier et al., 2016). This molecular marker method is broadly applicable within PyC research as it directly targets the "backbone" of PyC, i.e., its polycyclic condensed structures that form during the thermal treatment and that are therefore inherent to all the various forms of PyC.

Extraction and quantification of BPCAs were applied to the 41 bulk samples and six organic layers for estimations of the aromaticity and condensation level of the molecular cluster composing the PyC along the catena. The analytical procedure depicted in figure 22 includes acid digestion, oxidation, and liquid chromatography with the HPLC (Wiedemeier et al., 2016).

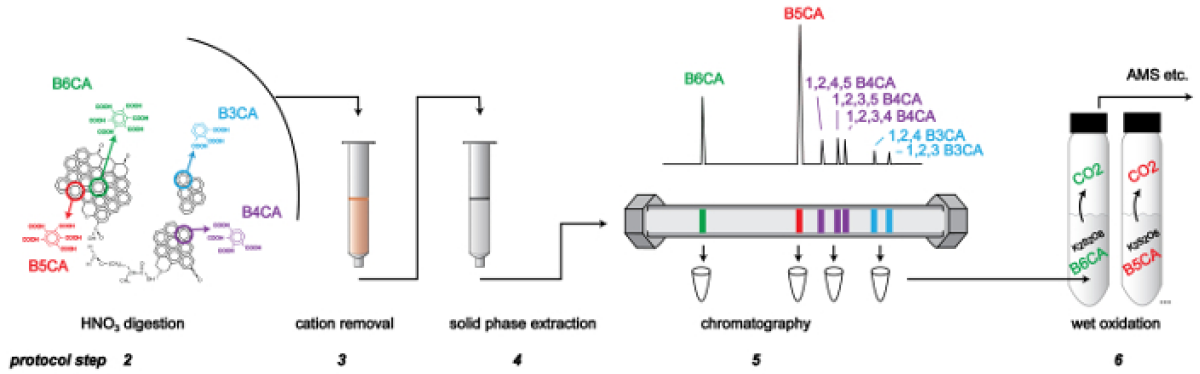

Figure 14: BPCA analysis procedure (Wiedemeier et al., 2016).

In order to chromatographically analyse such pyrogenic compounds, PyC is first digested with nitric acid (HNO_3) under high temperature and pressure, which leads to the breakdown of the large polycyclic structures into their building blocks, the individual BPCAs, and can thus be used to obtain a measure of the contribution of PyC to SOC (Glaser et al., 1998; Wiedemeier et al., 2016).

Digestion was made by adding 2 mL of nitric acid (HNO_3) 65 % in a tube with a sample containing 3-5 mg OC and then homogeneously shaken by using a vortex. Then, the tube was put into a pressure chamber with glass lids and covered with PTFE covers. Pressure bombs have been heated in a small oven at 170 °C for 8 h 10 min. Once the samples were digested, the pressure chambers were removed from the oven, opened, and the quartz digestion tube containing the sample was removed.

Samples were combined with ultra pure water and filtered with a glass fiber filter in a vacuum system until a volume of 25 ml was reached; the vacuum system was prepared by using a plastic bag to collect solvents. The 25 ml extract was placed into a resin filter to be purified with deionized water from charged non-target material (e.g. cations). Samples have been freeze-dried over night and apolar compounds were removed.

The BPCAs are then, after a few purification steps, amenable to high performance liquid chromatography (HPLC) analysis. Each BPCA compounds gives origin a specific peak, which can be identified and quantified. PyC is thus isolated and analyzed on a molecular level and can be used

to quantify PyC abundance in environmental compartments. The BPCA method additionally characterizes the investigated PyC when relative yields of B3-, B4-, B5- and B6CA are compared: The respective proportion of differently carboxylated BPCAs is linked to the size of the original polycyclic structures and is therefore indicative of PyC's quality and pyrolysis temperature (Wiedemeier et al., 2016).

2.8 Measurement of TC, TOC and PyC in Soil

2.8.1 Fumigation with Hydrochloric Acid

Determination of the pH value of all soil samples showed soils in the South Slave Lake Region to be rich in carbonates, which contribute to the total carbon content, ultimately impeding the direct measurement of the SOC content of these soils with Picarro. For this, fumigation with hydrochloric acid (HCl) vapour based on Walter et al. (2016) was applied for determination of organic C content only to the samples from the catena in the South Slave Lake Region (composites 1-18). Soils from the Inuvik Region showed pH values consistently lower than 6 and thus are no longer affected by the carbonate buffer system. In this case, the SOC content in soils corresponds to the total carbon content measured through dry combustion.

This method can be used for a reliable determination of organic C in carbonate-containing soils because it effectively separates organic and inorganic C without altering the organic matter, removes all carbonates prior to C and $\delta^{13}C$ analysis, and no losses of organic C and no alteration of its $\delta^{13}C$ signature occur (Walthert et al., 2010).

Fumigation of bulk (25-30 mg), S+A (40-160 mg), s+c (6-30 mg) and POM (2-3 mg) was done with duplicates, except for POM, for which only one measurement for each sample was taken. For all samples, the minimal amount of mass was determined according to the percentage of total carbon, leading to samples with C content between 0.2-1.0 mg. The latter have been placed into small silver capsules (9 mm by 5 mm), to which 50 µL of 1 % HCl was added. Samples were exposed for 8 hours to HCl vapour produced by 100 mL of 37 % HCl in a closed desiccator. After that, samples were transferred in a fresh titer plate and placed in a continuously vacuumized desiccator containing drying granules for 24 hours, and finally placed in a vacuum oven operating at 35 °C–40 °C with a vacuum of 200–300 hPa for 3 days.

After removal from the oven, capsules containing the dried samples were packed in larger tin capsules (10x10 mm) and dry combusted at 950 °C in a Picarro-analyzer for determination of $\delta^{13}C$ and carbon content in percent. Again, Chernozem and Miscanthus were used as standards for soil and plant-based material, respectively. Recovery of organic carbon stands around 69.26-95.83 % for soils from the South Slave Lake Region, whereas for soils from the Inuvik Region the same values as for total carbon are being considered (65.34-109.49 %), since no fumigation was applied. The quantity in mg of organic carbon in the individual fractions was computed by multiplying the mass of the fraction with the organic carbon percentage measured with Picarro after fumigation. A correction of the mass of OC into the fractions was made by considering the mass loss during fractionation according to the following formula:

$$Corrected\ mass\ of\ TOC\ [mgC] = \frac{m_{fraction_i} * C_{fraction_i}\ [mgC]}{\sum_{n=i}^{i} fraction_i\ [mgC]} * TOC_{bulk}\ [mgC] \tag{2.2}$$

2.8.2 Dry Combustion

Carbon content and ^{13}C signal were measured applying dry combustion through a Picarro device with a running temperature of 950 °C. Measurement time was set to 900 seconds and a limit for integration was set to 50 ppm for TC and TOC and to 20 ppm for PyC. Thus, the measurement stops either if the C concentration in ppm decreases below the threshold or after 15 minutes, in case there is a long tailing. Further, a maximum of six samples was measured between two standard samples of Chernozem (for bulk, S+A and s+c) or *Miscanthus* (for organic layers and POM fraction).

As highlighted by table 5 below, the sample mass was adapted to the estimated carbon content for each sample type. In case the maximal $^{12}CO_2$ peak was lower than 200 ppm the measurement was repeated, except for measurement of PyC, for which $\delta^{13}C$ values were not used.

Table 4: Overview of weighted mass for standards, bulks, and fractions for TC, TOC, and PyC measurements. Sample mass was adapted to reach 0.2-1.0 mg of C in each sample.

Sample Type	TC	TOC	PyC
Miscanthus	2-3 mg	2-3 mg	1 mg
Chernozem	12-15 mg	12-15 mg	5-7 mg
Bulk	12-15 mg	23-26 mg	2x40 mg
POM	2-3 mg	2-3 mg	2x10 mg
S+A	20-40 mg	30 or 2x40 mg	2x40 mg
s+c	5-10 mg	25-30 mg	2x40 mg
rSOC	-	13-16 mg	2x40 mg
OL	-	-	2x10 mg

The actual sample mass used exceeds the range listed in the table for a few cases with extremely low or high C content. Further, measurements of TOC and PyC were done with duplicates for all sample types, except for TOC measurement in the POM fraction.

Specifically, 12-15 mg of Chernozem soil (C = 2.01 %; $\delta^{13}C$ = -28.6 ‰; maximal $^{12}CO_2$ peak = 1'200 ppm) were used as standard measurement for soil material, whereas 2-3 mg of a C_4-plant of the genus Miscanthus (C = 47.5 %; $\delta^{13}C$ = -14.5 ‰; maximal $^{12}CO_2$ peak = 7'500 ppm) were used as standard measurement for the POM fraction, due to its plant-based origin.

2.9 Calculations

Stocks of SOC and PyC were estimated by using the carbon content, bulk density and depth of soil layers as described by Poeplau et al. (2017):

$$SOC\ Stock\ [tha^{-1}] = BD_{fine}\ [gcm^{-3}] * C_{content}\ [\%] * Depth\ [cm] * 100 \tag{2.3}$$

Stocks of PyC were estimated according to the same formula. The relative contents (%) of SOC and PyC in the 41 bulk samples and the related bulk density of fine soil were used to compute the cumulative stocks of SOC and PyC for the six landscape positions considered and related soil depths.

Calculations of standard deviation (SD), standard error (SE) and error propagation were done according to the following formulas:

$$Standard\ deviation\ SD = \sqrt{\frac{\sum_{i=1}^{N}(x_i - \mu)^2}{N}} \tag{2.4}$$

$$Standard\ Error\ SE = \frac{SD}{\sqrt{N}} \tag{2.5}$$

$$Standard\ Error\ propagation_{\ 0-30cm} = \sqrt{SE^2_{0-15cm} + SE^2_{15-30cm}} \tag{2.6}$$

with N as the total number of observations, μ as the population mean, and x_i as the value in the data distribution. However, for NB none of those were possible at 15-30 cm and 30-45 cm depth since only one composite sample was available, due to too high ice content in the soil during sampling.

Finally, estimations of the quantities of PyC in the bulk samples were determined by using both CTO and BPCA. For the latter, the total quantity of PyC was further corrected with a factor of 2.27 (Glaser et al., 1998). Quantities of PyC measured with the two methods were compared both for the corrected and not corrected quantities determined through BPCA analysis.

2.10 Statistical Analysis

Statistical analysis was conducted using the software R Studio (Version 4.1.0). Plots of the results were carried out using either R Studio or Excel (Version 2110). Statistics were applied to the stocks of SOC and PyC between the six locations for each soil depth, to both the relative and absolute distribution of SOC and PyC between soil fractions and between landscape positions at the same depth, and to the aliphatic/aromatic and cellulose/lignin ratios between the six locations and between the soil fractions. The level of significance was always kept to $\alpha = 0.05$.

Regarding the stocks, since they were calculated cumulatively among soil depths (for 0-15, 0-30, and 0-45 cm) the data used for the statistical analysis of the latter were computed by addition of the stocks of the first soil depth into the second, and those to the third, resulting in cumulative values (along soil depth) for the 41 bulk samples. Prior to statistical analysis, descriptive statistics of standard error and deviation were investigated for all six landscape positions at individual levels of soil depth. After, since the data were not normally distributed, a log_{10}-transformation of both SOC and PyC stocks was applied to conform the data to normality. The latter was tested by using a Shapiro-Wilk test of normality for both the transformed and not-transformed data. With $p = 0.1$ and $p = 0.5$ for stocks of PyC and SOC respectively, the H0 hypothesis of the transformed values originating from a normally distributed population could not be rejected.

The differences in stocks were tested between the six locations for all depths by using a one-way analysis of variance (ANOVA), for which a Bonferroni correction was performed to adjust the p-values (thus reducing the risk of an α-error), and to identify the groups with significantly different means. However, since in the Inuvik Region permafrost conditions were continuous, sampling at 15-30cm and 30-45cm depth at the bottom of the catena (NB) was only partially possible, leading to only one composite for each of the two lower depths, whereas three replicates are still available for the first soil depth. Consequently, no standard deviation, nor standard error was computed for the location NB at the two lower depths, and the location was erased for Bonferroni correction at those soil depths.

Statistical analysis of both the relative and absolute distribution of SOC and PyC between soil fractions and between different landscape positions was preceded by square-root and log_{10}-transformation of the data, but none of them was powerful enough, so the non-parametric Kruskal-Wallis test was applied, but no significant difference was found.

For what concerns DIRFT, neither the aliphatic/aromatic nor the cellulose/lignin ratio were normally distributed, neither in the landscape positions nor inside the soil fractions. Furthermore, neither the square root nor the log_{10}-transformation was enough powerful to normalize the distribution. Therefore, the non-parametric Kruskal-Wallis test by ranks was applied to test the significant difference in the ratios between the six landscape positions and between the bulks and fractions. Again, Bonferroni correction of the p-values was applied to avoid α-error.

Finally, both ratios were computed for each soil fraction and landscape gradient (Fig. 24 e and f), thus t-tests were made between the two catenae to test differences in the ratios of each fraction. Therefore, the following symbols were used:

Table 5: Significant codes (lower line) for each p-value range.

0 - 0.001	0.001 - 0.05	0.05 - 0.01	0.01 - 0.1	0.1 - 1
'***'	'**'	'*'	'.'	' '

Chapter 3

Results

3.1 Stocks and Concentrations of PyC and SOC

Stocks of SOC and PyC originate from their respective concentrations in the bulk samples, which in the case of PyC were measured through CTO-375, resulting in PyC_{CTO}. As visible in figure 15, the stocks of both SOC and PyC are almost constant along the catena in the South Slave Lake Region (S, left part of the figures), with a total stock (i.e., in the first 30 cm) of circa 40 tha^{-1} of SOC and 1 tha^{-1} of PyC at the top, slope, and bottom. However, there is an increase in the stock of SOC along the catena in the Inuvik Region (N), with a total of 60 tha^{-1} at the top, 120 tha^{-1} along the slope, and more than 180 tha^{-1} at the bottom of the catena. This increase in bottom direction is consistent along all soil depths, with the total stocks of SOC being 1.5, 3 and 4.5 times greater in the Inuvik Region (N, north) than in the South Slave Lake Region (S, south), at the three respective landscape positions.

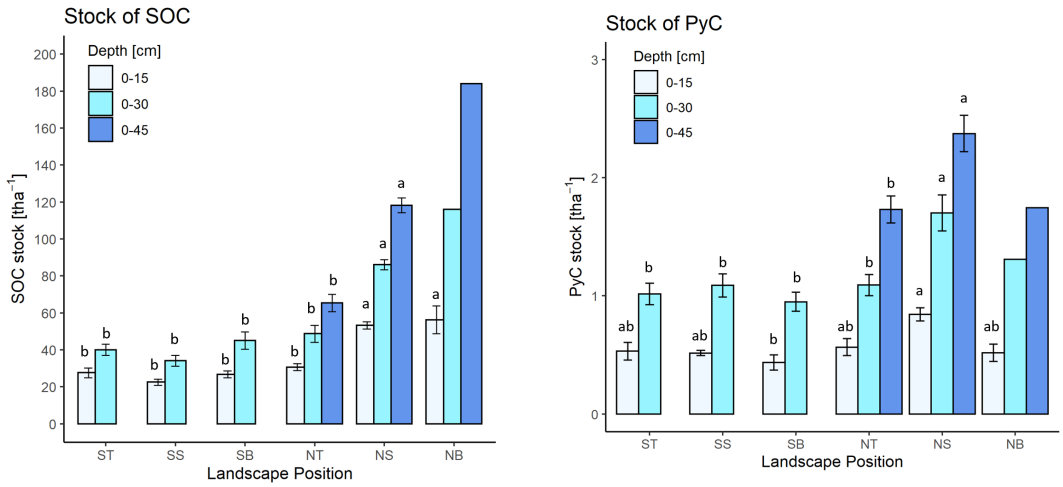

Figure 15: Stocks of SOC (left) and PyC (right) in tonnes per hectare along the catenae in the South Slave Lake Region (S) and Inuvik Region (N) with top (T), slope (S) and bottom (B) position. Standard error is not available in the 0-30 cm and 0-45 cm depth of NT because only one measurement per depth was taken. Significant differences between landscape positions (small letters) were calculated individually for each soil depth considered.

Statistically, there is no significant difference between the stocks of SOC along the southern catena, not for the initial 0-15 cm depth, nor for the total stock in the first 30 cm. In the Inuvik Region though, NT is significantly lower than NS and NB at all depths considered, but NS and NB showed no difference between each other. Furthermore, significant differences in SOC stocks in 0-15 cm depth between the two landscape gradients occur between NS, NB, and the three southern landscape positions, but not for NT, which shares the same mean as the southern locations. The same is valid for 0-30 cm depth, with no significant changes occurring at greater soil depths. Finally, the northern SOC stocks at 0-45 cm depth cannot be compared to other groups, but by considering their magnitude, there is an evident increase in stock of SOC along both slope and depth, with the stocks almost doubling at each new depth.

For what concerns the stock of PyC, the variation between the six landscape positions is smaller, covering a range of 1-3 tha^{-1}. Indeed, there is generally 0.5 tha^{-1} in the first 15 cm and 1 tha^{-1} in the first 30 cm depth in the South Slave Lake Region, with no trend along the landscape gradient. In the north, NT and NB show almost the same values, whereas greater stocks are found at NS at all soil depths. Specifically, in the first 15 cm there is always less than 1 tha^{-1}, in 0-30 cm there are almost 2 tha^{-1} at NS, and in the total 45 cm depth considered at NS there are 2.5 tha^{-1}.

Statistically, the only significant difference at 0-15 cm depth is given by the groups SB and NS, showing the lowest and highest stocks, respectively. At 0-30 cm depth, NS is significantly higher than all other groups. Finally, since at NB only one measurement was taken for the two lowest depths, no standard error is available and also no comparison between NB and the other groups is possible. Thus, the group NB was not considered in the ANOVA for the two lowest depths. A detailed overview of the stocks in tonnes per hectare of both SOC and PyC in the bulk soil and in the SOC fractions (including bulk densities of the fine soils and standard errors, SE) can be found in Table 11 (for stocks of SOC) and Table 12 (for stocks of PyC), respectively.

Quantities in SOC and PyC have been further investigated by depth profiles (Fig.16). TC and SOC differ only in the South Slave Lake Region (ST, SS, and SB, in black), since fumigation was applied only there, whereas in the Inuvik Region, soils were no longer affected by the carbonate buffer system, and thus TC is only made by SOC.

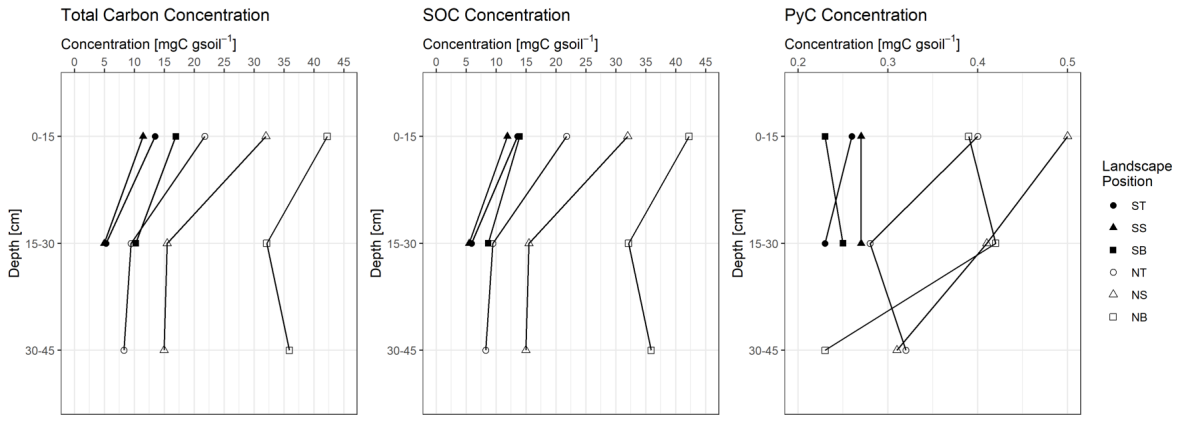

Figure 16: Concentration of total carbon (left), SOC (middle) and PyC (measured through CTO-375, right) in mgC per gram of bulk soil along landscape gradients and soil depths. The South Slave Lake Region is represented by black symbols, whereas white symbols indicate the Inuvik Region.

As visible in Fig. 16, concentrations of TC and SOC range from 5 to 45 mg per gram of soil, whereas the concentration of PyC is between 0.2-0.5 mg C g soil^{-1}. Further, by considering both SOC and PyC, it appears clear that the variation in concentration is much smaller in the south (ST, SS, and SB) than in the north (NT, NS, and NB).

Indeed, in the southern catena, SOC concentrations are in the range of 10-15 mgC g soil^{-1} in the first 15 cm depths and between 5-10 mgC g soil^{-1} at 15-30 cm depth, with no discernible change along the landscape gradient. On the other hand, SOC concentration in the Inuvik Region is in the range of 20-45 mgC g soil^{-1} and increases from NT to NS and then to NB at all soil depths, with clear differences between the landscape positions. Further, in the north, the concentration of SOC decreases from the first to the second soil depth, but it stays stable or even increases at 30-45 cm depth (in NB).

For what concerns the concentration of PyC, values in the north (with a range of 0.25-0.5 mgC gsoil^{-1}) are always higher than those in the south, which are in the range of 0.21-0.27 mgC gsoil^{-1}. However, the concentration of PyC has no clear trend along landscape gradients nor along soil depths, with both decreases and increases in the concentration along soil depths and the greatest concentrations along the northern slope. Indeed, in the Inuvik Region the SOC carbon concentration decreases with depth from 0-15 cm to 15-30 cm but then remains almost constant from 15-30 cm to 30-45 cm at top and slope and even increases at the bottom. Concerning the concentration of PyC, there is a reduction with depth from 0-15 cm to 15-30 cm at top and slope, but an increase at the bottom. However, the concentration of the last soil depth decreases at the slope and bottom but increases at the top.

3.2 Distribution of SOC in Soil Fractions

The relative and absolute distribution of SOC was measured in the solid SOC fractions POM, S+A, s+c and rSOC, with the latter being a subfraction of s+c (Fig.17 and Fig. 18). SOC in the POM fraction (hereafter SOC_{POM}) can make up to 50 % of the whole SOC in the south, and its magnitude always decreases with depth, usually down to 30 %. In the North, the contribution of SOC_{POM} to the total SOC is lower, with the highest relative content of 42.9 % being in the first 15cm depth at the top of the northern catena (NT) and the lowest being 9.9 % in 30-45 cm depth in the same landscape position. Overall, the SOC_{POM} in the north is close to 10 % at 30-45 cm depth, between 20-30 % at 15-30 cm depth and between 30-40 % at 0-15 cm depth.

Regarding S+A, this fraction accounts for the smallest relative abundance of SOC, which ranges between 3.2-18.8 % in the south and 8.9-34.7 % in the north. In the south, the SOC_{S+A} increases with depth and along the catena in the bottom direction, whereas in the north SOC_{S+A} decreases along the catena in the bottom direction, but regarding the trend in soil depth, both increase (NT) and stability (NS and NB) are present.

The silt and clay fraction also account for a high relative content of SOC. Indeed, in the south SOC_{s+c} is in the range 21.3-55.1 %, and the relative SOC content in this fraction increases with depth. Also in the north there is a trend of increase in SOC_{s+c} with depth, but there is also relatively more SOC in this fraction than in the south, with SOC_{s+c} between 42.0 % and 65.5 %.

Finally, SOC_{rSOC} accounts for the smallest contribution to SOC, with only 2.8-11.5 % in the south and 3.3-24.1 % in the north. Again, the relative content of SOC in this fraction increases with depth in all landscape positions, except at NS, where the greatest relative abundance is found at 15-30 cm depth. Generally, this plot highlights that only the relative content of SOC in the POM fraction decreases with depth, whereas overall considered, the relative abundance of SOC in the S+A, s+c, and rSOC fractions increases with depth.

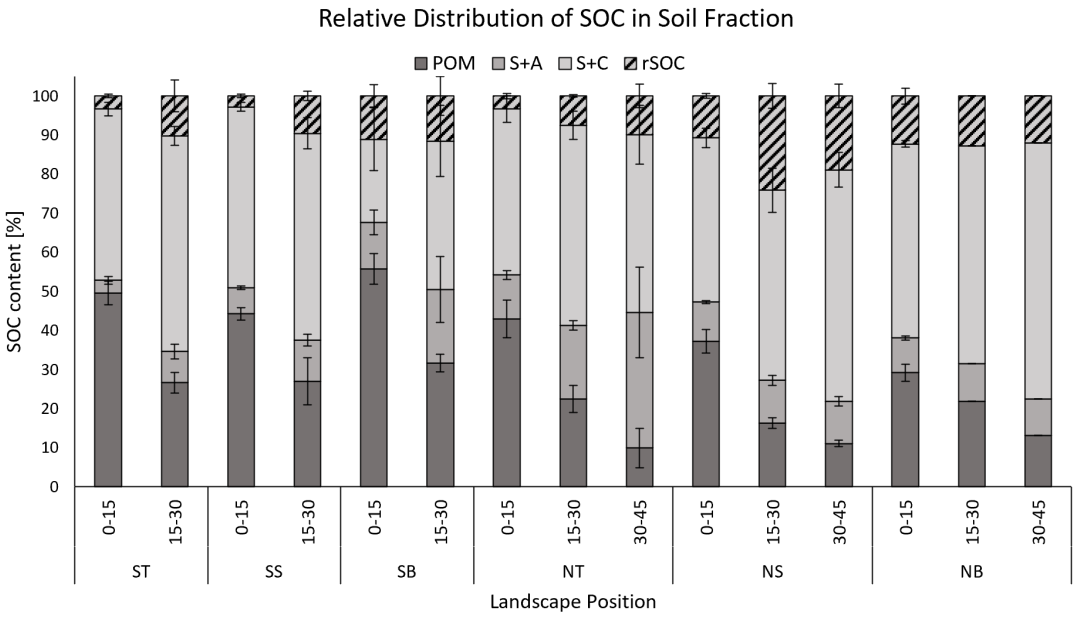

Figure 17: Relative distribution of SOC in the POM, S+A, s+c, and rSOC fractions, including standard error.

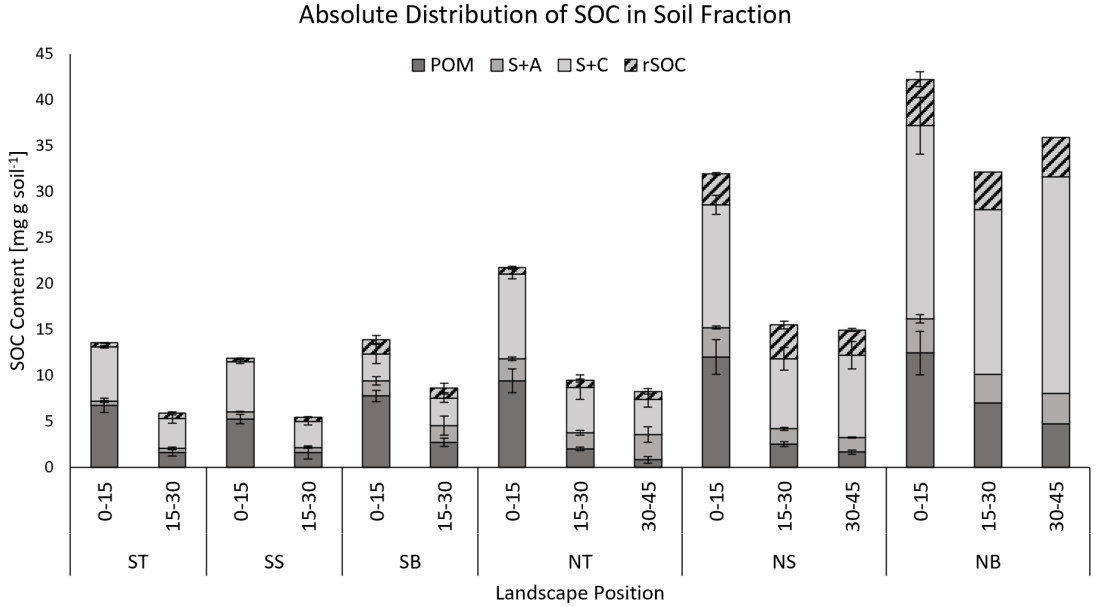

Figure 18: Absolute distribution of SOC in the POM, S+A, s+c, and rSOC fractions, including standard error.

Regarding the absolute SOC content in the soil fractions (Fig.18), clear differences between the two landscape gradients are visible. Indeed, in the South Slave Lake Region, the majority of SOC is found in the POM fraction, followed by a minor contribution from the s+c fraction, and minimal contributions from the S+A and rSOC fractions. On the other hand, in the Inuvik Region the s+c fraction accounts for the majority of SOC, followed by the POM and rSOC fractions, and finally by the S+A fraction. Furthermore, the SOC content in the rSOC fraction generally increases with depth in both catenae, but especially in the northern one. Decreases in the SOC content with depth are mainly due to lower contributions from the POM and s+c fractions with depth, whereas the SOC content in the S+A and rSOC fractions exhibits no clear variation with depth.

The exact relative and absolute distribution of SOC in the soil fractions can be found in Table 13 in the appendix.

3.3 Distribution of PyC in Soil Fractions

Regarding the PyC content in the SOC fractions, PyC in the rSOC fraction was measured but gave unrealistic results and thus was omitted. The relative abundance of PyC (Fig.19) is thus described as distributed into the POM, S+A, and s+c fractions.

The relative abundance of PyC is lowest in the POM fraction in all six landscape positions considered and in all soil depths. Indeed, PyC_{POM} is in the range of 3.3-15.2 % in the South Slave Lake Region and between 1.5-12.0 % in the Inuvik Region. Further, PyC_{POM} decreases with depth at ST, NT, NS, and NB between 0-15 cm and 15-30 cm, but increases at SS and SB from 0-15 cm to 15-30 cm and also at NS from 15-30 cm to 30-45 cm depth.

The PyC content in the S+A fraction is much greater, ranging between 25.4-79.3 % in the south and between 13.9-71.7 % in the north. The relative abundance of PyC_{S+A} increases with depth at ST, SS, NT, and NS, whereas it decreases at SB and NB. Finally, the PyC content in the s+c fraction ranges between 15.5-71.3 % in the south and 25.7-82.8 % in the north. Further, the relative abundance of PyC in this fraction always decreases with depth in all landscape positions, except at NB, where there is an increase from 15-30 cm to 30-45 cm depth.

Generally, the locations and depths are highly heterogeneous in their distribution of PyC. Interestingly, it seems that the majority of PyC in the South Slave Lake Region (ST, SS, and SB) is associated with the S+A fraction, whereas in the Inuvik Region (NT, NS, and NB) PyC is mainly associated with silt and clay (s+c). However, no significant difference in the PyC content between the two latter soil fractions was found. Exact values and standard errors for each landscape location and depth are found in Table 14 in the appendix.

The total PyC content (Fig.20) is almost constant in the South Slave Lake Region, and shows greater variability in the Inuvik Region. The absolute content of PyC_{POM} ranges between 0.01-0.05 mgC gsoil^{-1} in both catenae with decreases in depth at ST, NT, NS, and NB but increases with depth at SS and SB. Higher contents of PyC are found in the S+A fraction, with 0.07-0.22 mgC gsoil^{-1} in both landscape gradients. Generally, there is a decrease with depth at SB and NB, whereas there is an increase with depth at ST, SS, NT, and NS. Finally, the content of PyC_{s+c} is in the range of 0.04-0.19 mgC gsoil^{-1} in the south and 0.15-0.39 mgC gsoil^{-1} in the north, with an increase in the content with soil depth at SB and NB for 0-15 cm to 15-30 cm, whereas there is a decrease with depth at ST, SS, NT, NS, and at NB from 15-30 cm to 30-45 cm depth.

Statistical analysis was done for both the relative and absolute distribution of SOC and PyC between the six landscape positions at equal soil depths and between the soil fractions of each column (i.e., per each landscape position and depth). No significant difference between any groups was found.

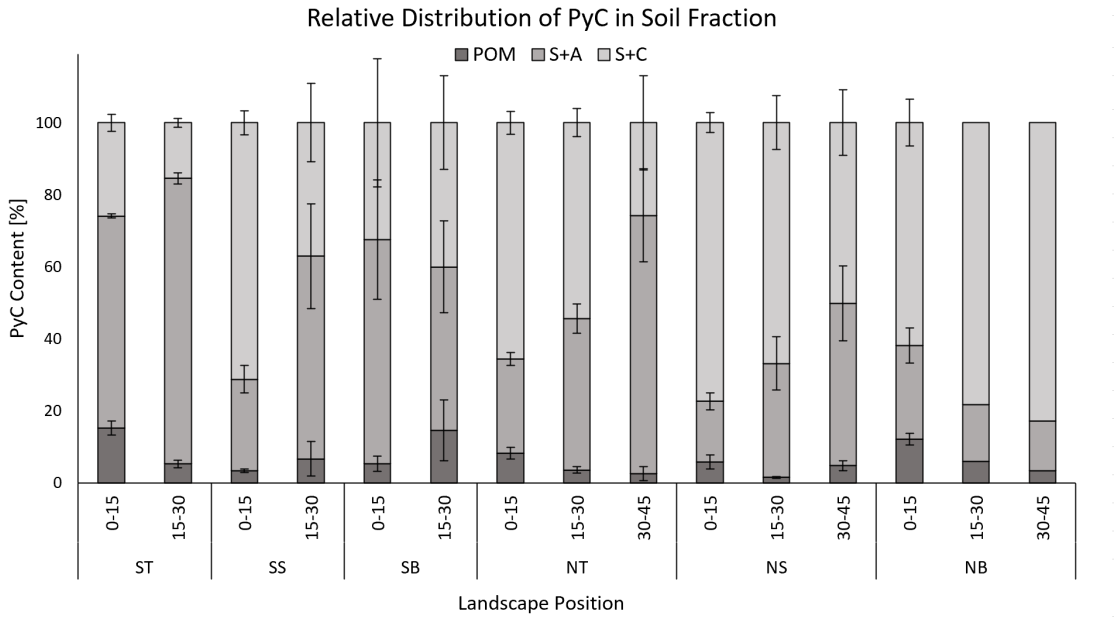

Figure 19: Relative distribution of PyC in the POM, S+A and s+c fractions with standard error.

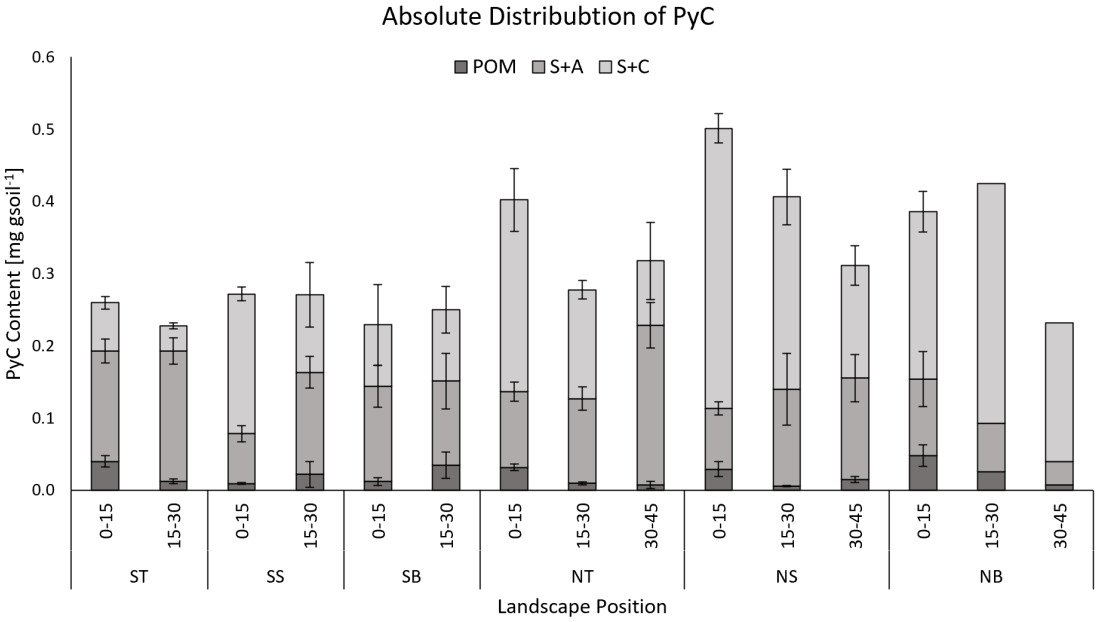

Figure 20: Absolute distribution of PyC in the POM, S+A and s+c fractions with standard error.

Lastly, SOC and PyC concentrations (measured through CTO-375) were investigated for the bulk soil and the individual soil fractions (Fig. 21). As part of SOC, PyC was expected to increase with increasing SOC concentration in soils (Soucémarianadin et al., 2014). As visible in the figure below, the highest coefficient of determination ($R^2 = 0.73$) is found in the POM fraction in the Inuvik Region (labelled as North), whereas the lowest relationship between SOC and PyC concentrations ($R^2 = 0.0016$) is found in the S+A fraction at the same site.

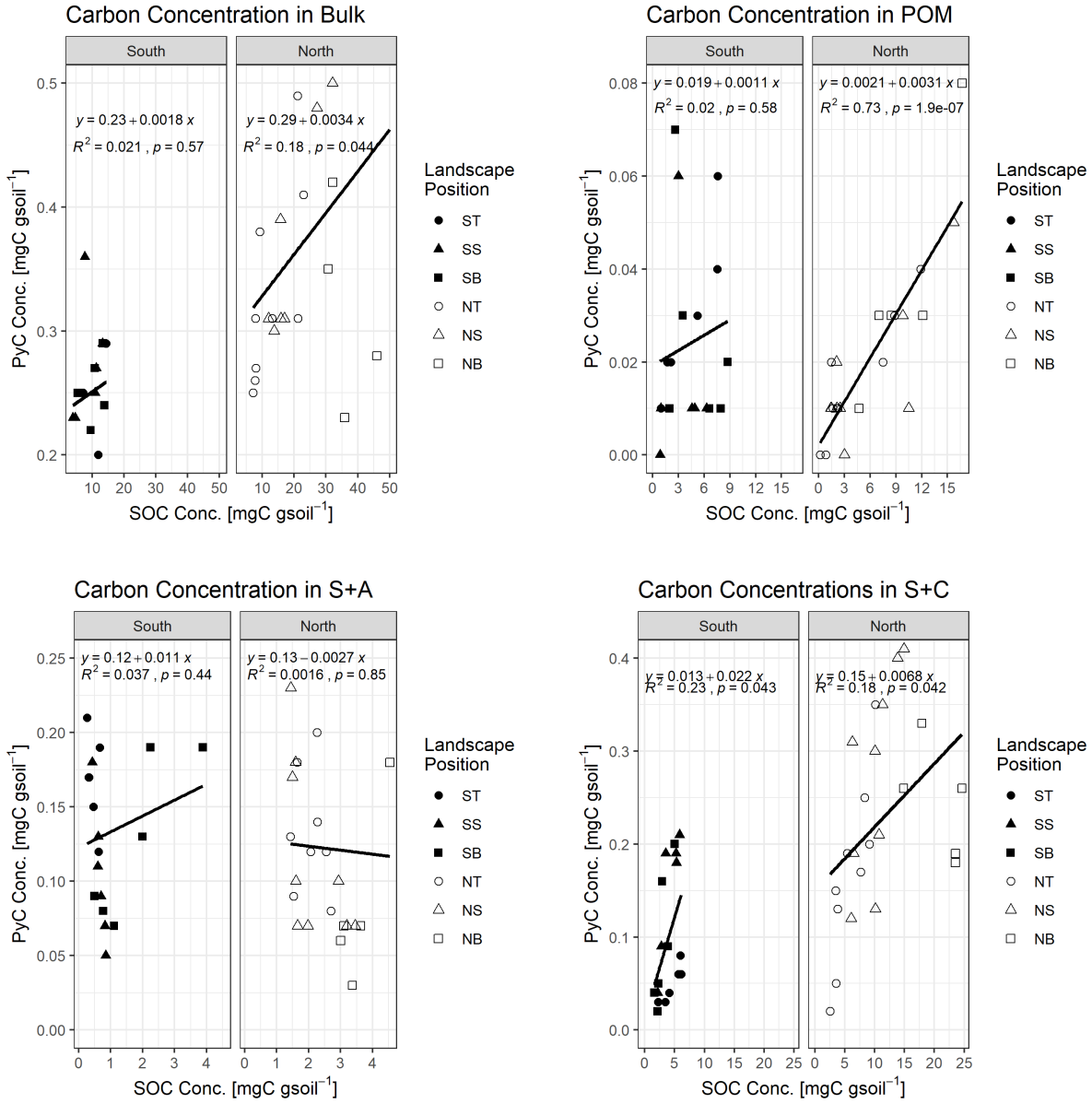

Figure 21: Relation between SOC and PyC concentration in the bulk samples and in the POM, S+A and s+c fractions at the two landscape gradients. The South Slave Lake Region is labelled as "South", while the Inuvik Region as "North". R-square and linear regression equations have been calculated individually for the two sites.

Generally, the linear regression model does not fit the measurements when the variation in PyC concentration is not explained by a variation in SOC. Specifically, the SOC concentration does not explain the concentration of PyC, especially in the S+A fraction at both landscape gradients, excluding a linear correlation between the two carbon concentrations. Further, also in the bulk samples and in the other fractions, only a poor linear correlation between SOC and PyC was detected, with R^2-values between 0.02-0.23 for the bulk, the S+A and the s+c fractions.

Finally, the relationship between SOC and PyC concentrations in soils is always weaker in the South Slave Lake Region, except in the s+c fraction. A more detailed representation of the SOC and PyC concentrations in bulk samples and fractions for individual soil depths can be found in Fig. 25 in the appendix.

3.4 Quantification of PyC through CTO-375 and BPCA Analysis

Quantification of PyC acquired both through CTO-375 (hereafter PyC_{CTO}) and BPCA analysis (PyC_{BPCA}). The first method was applied to bulk samples and SOC fractions, and was used to produce all the so-far presented PyC related results, whereas the second method was applied to the bulk samples only and is used to analyse the quality of PyC and compare its detected quantities through both methods.

As visible in the table below, PyC_{CTO} is between 0.65-5.05 % of TOC, whereas that of PyC_{BPCA} is between 0.53-10.63 % of TOC. Further, since PyC conversion to BPCAs is known to be incomplete, results were corrected with an empirically determined factor of 2.27 (Glaser et al., 1998). The corrected quantity of PyC (PyC_{BPCA}/TOC Glaser 1998) is 1.20-10.12 times higher than PyC_{CTO} in the South Slave Lake Region and 2.75-37.37 times higher than PyC_{CTO} in the Inuvik Region. Thus, quantities of PyC detected through BPCA are always greater than through CTO-375, except for the top of the southern catena (ST), with PyC_{BPCA} being half of PyC_{CTO} in 15-30 cm depth.

Table 6: Relative PyC (left) and BPCAs contents (right) in the bulk samples, determined through CTO-375 and BPCA analysis. Location NB shows no standard deviation (SD) for the two lowest depths because only one sample was collected. For all other locations and depths, the standard deviation considers 3 replicates.

Pyrogenic Carbon Content in Bulk Samples																			
EUP	Location	Depth	PyC_{CTO} / TOC	SD	PyC_{BPCA} / TOC	SD	PyC_{BPCA} / PyC_{CTO}	PyC_{BPCA} / TOC (Glaser 1998)	SD	PyC_{BPCA} / PyC_{CTO} (Glaser 1998)	mean B3CA	SD	mean B4CA	SD	mean B5CA	SD	mean B6CA	SD
		[cm]	[%]		[%]			[%]			[%]		[%]		[%]		[%]	
3	ST	0-15	1.91	0.18	3.62	1.46	1.90	8.22	3.32	4.32	7.8	0.4	30.9	4.4	36.9	2.8	24.4	6.9
		15-30	3.91	0.42	2.08	0.69	0.53	4.71	1.56	1.20	5.4	2.3	22.5	4.9	41.2	3.2	30.9	5.0
2	SS	0-15	2.30	0.12	7.72	5.29	3.35	17.53	12.01	7.61	5.3	2.2	28.2	0.7	36.5	3.2	30.0	5.5
		15-30	5.05	0.55	5.61	6.01	1.11	12.74	13.65	2.52	5.1	0.8	25.8	6.1	36.3	1.9	32.7	4.9
1	SB	0-15	1.66	0.55	7.41	2.06	4.46	16.82	4.68	10.12	4.8	1.3	23.6	6.8	38.4	0.3	33.2	7.7
		15-30	3.14	1.24	4.21	2.32	1.34	9.56	5.27	3.04	5.6	0.4	29.8	7.0	43.7	8.9	20.9	9.7
8	NT	0-15	1.85	0.42	6.05	3.70	3.27	13.73	8.40	7.42	6.2	2.2	28.6	1.7	37.2	2.4	28.0	4.9
		15-30	3.07	0.59	3.72	2.61	1.21	8.43	5.94	2.75	5.1	1.1	24.6	3.0	35.8	2.1	34.4	4.8
		30-45	3.83	0.35	5.06	3.63	1.32	11.49	8.23	3.00	6.5	1.5	32.9	1.1	29.1	2.4	31.5	1.7
10	NS	0-15	1.58	0.16	3.50	2.49	2.21	7.96	5.65	5.02	9.1	5.1	30.0	7.5	35.6	0.6	25.3	12.0
		15-30	2.59	0.50	3.43	2.70	1.32	7.78	6.13	3.01	6.9	1.0	29.9	3.0	34.7	2.4	28.6	1.2
		30-45	2.13	0.41	11.92	4.84	5.59	27.05	11.00	12.69	4.5	0.6	32.4	1.9	32.3	1.2	30.8	3.3
9	NB	0-15	0.94	0.29	5.00	3.67	5.34	11.36	8.34	12.11	9.1	5.1	30.0	7.5	35.6	0.6	25.3	12.0
		15-30	1.32	-	5.92	-	4.47	13.44	-	10.15	6.3	-	28.6	-	36.3	-	28.7	-
		30-45	0.65	-	10.63	-	16.46	24.12	-	37.37	5.8	-	34.0	-	29.5	-	30.7	-

Furthermore, the percentage of PyC_{CTO} with respect to TOC increases with depth at all six landscape positions, except at NS and NB from 15-30 cm to 30-45 cm depth, where the quantity of PyC_{CTO} decreases. On the other hand, the percentage of PyC_{BPCA} with respect to TOC decreases from 0-15 cm to 15-30 cm at ST, SS, SB, NT, and NS but increases at NT, NS, and NB from 15-30 cm to 30-45 cm depth. Interestingly, NB is the only location where the quantity of PyC_{BPCA} with respect to TOC increases with depth along the whole depth profile.

Moreover, Fig. 22 depicts that the content of PyC_{BPCA}/TOC (represented with black dots) decreases with depth at ST, SS, SB, and NT between 0-15 cm and 15-30 cm depth, but increases at NB for all depths and at NT and NS between 15-30 cm and 30-45 cm depth. The highest relative abundance of PyC_{BPCA}/TOC is found at 30-45 cm depth along the slope of the northern catena (NS), and than at the bottom of the same catena, at the same soil depth. On the other hand, the lowest content of PyC_{BPCA}/TOC is found at ST.

The mean BPCAs are represented as relative content (%) for all six landscape gradients at the individual soil depths. Generally, B3CA shows the lowest relative abundance, followed by B4CA and B6CA, whereas the highest relative abundance is given by B5CA. Figure 22 depicts a general increase in the mean B6CA content with depth in the six landscape positions (except SB and NT). Generally, the variations in abundance are greater in the South Slave Lake Region than in the Inuvik Region. In all cases, the mean B3CA% is between $4.5 - 9.1$ %, that of B4CA% is $22.5 - 34.0$ %, that of B5CA% is $29.1 - 43.7$ % and that of B6CA% is $20.9 - 34.4$ %.

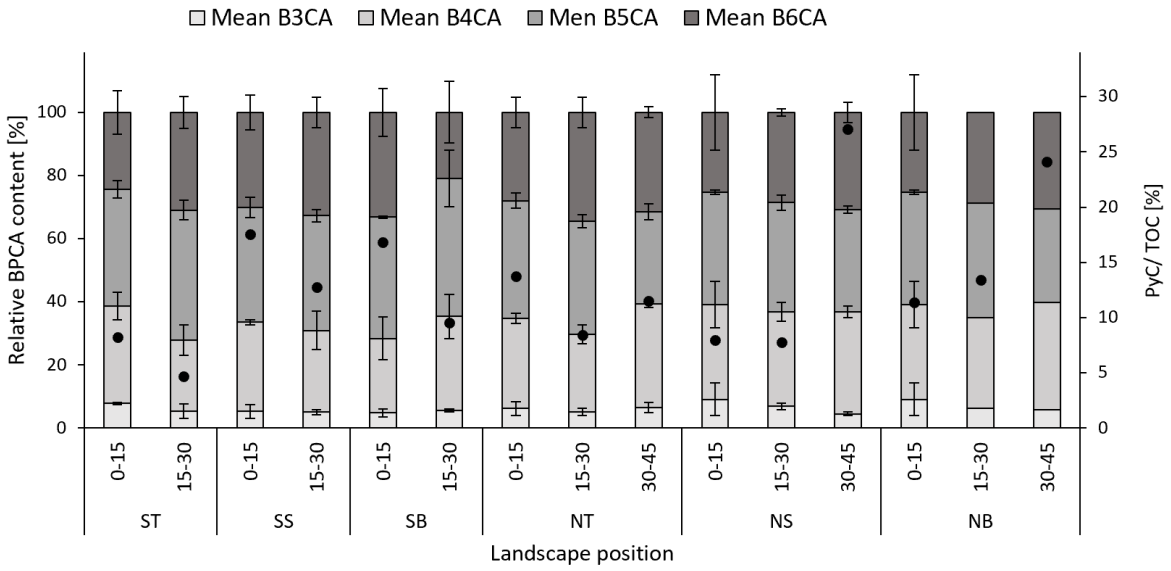

Figure 22: Relative content of BPCAs along landscape gradients for each soil depth, with error bars for each BPCA type. Black dots represent the relative content of PyC_{BPCA} (%) with respect to the total organic carbon content (right y-axis).

Finally, depth profiles of PyC/SOC % were made for both PyC_{CTO} and PyC_{BPCA} (Fig. 23), and show divergent trends. Indeed, the concentration of PyC_{CTO} with respect to SOC increases with depth till 30 cm and then decreases in the Inuvik Region till 45 cm depth, whereas the concentration of PyC_{BPCA} decreases with depth with respect to the total SOC and increases only in the Inuvik Region from 30 to 45 cm depth.

The PyC content is in the range of 1-5 % for PyC_{CTO}/SOC and 5-25 % for PyC_{BPCA}/SOC, hence close to five times higher.

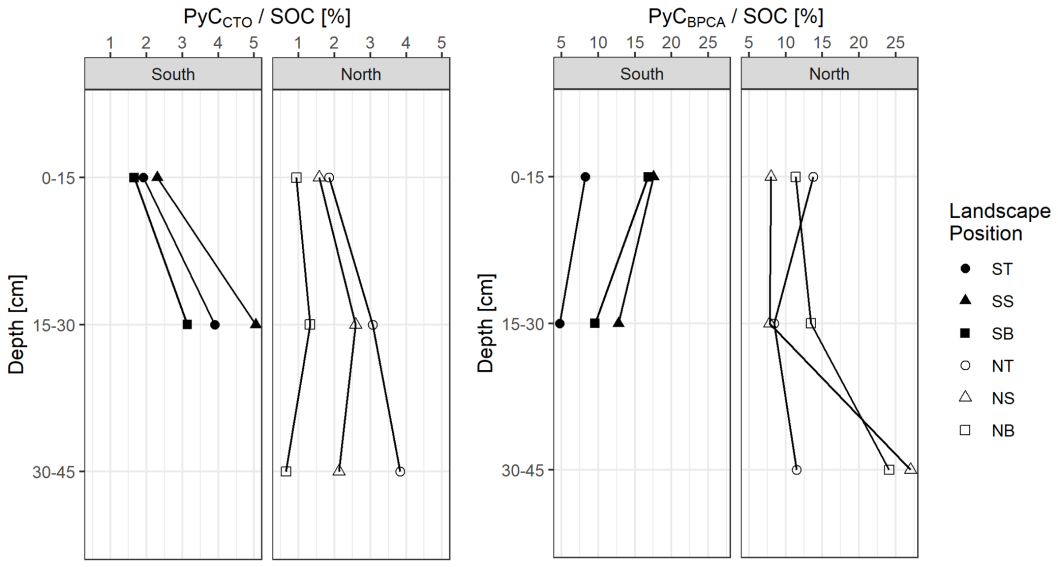

Figure 23: Depth profiles of PyC measured in the bulk samples through CTO-375 (left) and BPCA (right) as percentage of SOC.

3.5 DRIFT Analysis

Aliphatic/aromatic and cellulose/lignin ratios were investigated at the six landscape positions for all depths and also between the organic layer (OL), bulk samples and SOC fractions (Table 7).

Ratios for individual fractions (left table) originate as an average of all landscape positions and soil depths together (thus N = 41 because it is the total number of composites), enhancing only differences between SOC fractions, bulk samples, and organic layers, whereas ratios for landscape positions (right table) originate as an average of only the bulk measurements at all depths.

The left table highlights that higher aliphatic/aromatic rations can be found in the organic layers (OL) and in the POM fraction, whereas higher cellulose/lignin ratios belong to the bulk samples and to the s+c fraction, followed by OL and POM. On the other hand, the right table enlightens NT as the location with the highest values for both ratios, followed by Ns and Nb and finally by the three southern locations. A summary of the two ratios for each landscape position and depth (including organic layers) can be found in the appendix at Table 15.

Table 7: Mean and standard error (SE) of the aliphatic/aromatic and cellulose/lignin ratios for each soil fraction, bulk sample, and organic layer (left), and for the six landscape positions (right), with N corresponding to the number of counts.

N	Fraction	Mean Aliphatic/Aromatic Ratio	SE	Mean Cellulose/Lignin Ratio	SE
6	OL	0.72	0.05	0.95	0.08
41	Bulk	0.39	0.02	2.70	0.85
41	POM	0.69	0.02	0.83	0.02
41	S+A	0.23	0.03	0.42	0.10
41	S+C	0.33	0.02	1.21	0.44
41	rSOC	0.15	0.02	0.54	0.05

EUP	Location	N	Mean Aliphatic/Aromatic Ratio	SE	Mean Cellulose/Lignin Ratio	SE
3	ST	6	0.25	0.01	0.32	0.02
2	SS	6	0.27	0.05	0.41	0.14
1	SB	6	0.21	0.02	0.22	0.02
8	NT	9	0.59	0.01	10.27	2.67
10	NS	9	0.45	0.01	0.93	0.07
9	NB	5	0.47	0	0.88	0.11

Figure 24 highlights the differences in the ratios between the six landscape positions (Fig. 24 a and b, with each group containing only measurements of the bulk samples), between the SOC fractions, bulk samples, and organic layers (Fig. 24 c and d, with each fraction containing the measurements from all 41 composites), and lastly, Fig. 24 d and e take a closer look at the two middle figures 24 c and d, enhancing the differences between the two catenae.

As visible in the figure 24, the aliphatic/aromatic ratio is in the range of 0-1, whereas the cellulose/lignin ratio is in the range of 0-3. However, the highest cellulose/lignin ratio exceeds 20.01, with the majority of the outliers belonging to the bulk and s+c fraction of NT (top of the northern catena), but were not displaced for better visual representation of the trends along the catenae. Mean aliphatic/aromatic and cellulose/lignin ratios (as represented in Fig. 24 a and b) have been computed for each soil depth and can be found in Fig. 26 in the appendix.

Similarly, since the main differences between organic layers, bulk samples and SOC fractions depicted in Fig. 24 c and d remain the same in the six landscape positions, the ratios described in this section originate as an average of all the landscape positions, but the same plots for each individual landscape position can be found in the appendix in Fig. 27 for the aliphatic/aromatic ratio and Fig. 28 for the cellulose/lignin ratio.

Generally, the mean aliphatic/aromatic ratio (Fig. 24a) is higher in the three northern landscape positions, with ratios in the Inuvik Region almost twice as high as those in the South Slave Lake Region. The same trend is valid also for the cellulose/lignin ratio (Fig. 24 b), with especially high values at the top the northern landscape position (the median is close to ten and the maximum exceeds 20, thus not visible for better representation of the other groups). Cellulose/lignin ratios

are higher than aliphatic/aromatic ones due to the minimal lignin peak, which causes the high ratio. Further, the two ratios share the same trend along the landscape gradients, which relies on the fact that aliphatic compounds comprehend, among others, polysaccharides such as cellulose and hemicellulose (Chatterjee et al., 2012), while the lignin structure consists of aromatic rings with side chains (Thevenot et al., 2010); thus, in other words: cellulose is an aliphatic and lignin an aromatic compound.

Statistically, there is no significant difference in the aliphatic/aromatic ratios between the three landscape positions inside the same catena (except for NT), but between the two catenae. Indeed, the aliphatic/aromatic ratio at ST and SB is significantly lower than at NT and NS, whereas SS differs only from NT. Further, cellulose/lignin ratios at ST and SB are significantly lower than those in the three northern locations, whereas the average ratio at SS is not different that that at NS and NB. In both cases, the ratio at NT is significantly higher than that of all other groups. Same plots for each soil depth can be consulted at Fig. 26 in the appendix.

For what concerns differences between the ratios in the SOC fractions (Fig. 24 c and d), higher aliphatic/aromatic ratios are found in the organic layer (OL) and in the POM fraction, which correlates with their plant-based origin. Further, for both ratios there is no significant difference between the organic layer and the POM fraction, but their aliphatic/aromatic ratios are significantly higher than those of all other fractions. Further, the mean aliphatic/aromatic ratio of the bulks differ from all other groups except from the s+c fraction, rSOC differs from all other groups except from S+A, and S+A differs from all other groups except from s+c and rSOC.

The differences in the cellulose/lignin ratios among fractions are much less prominent: significant differences occur between POM and the three SOC fractions S+A, s+c, and rSOC, which are significantly lower. Further, the average ratio in the bulk is similar to that of all other groups, except from S+A, whose ratio is significantly lower. The latter is however not different from the ratio in the organic layer, probably due to the many outliers in the S+A fraction.

Finally, sub-figures 24 e and f highlight the differences in the ratios between the two catenae, with higher ratios in the Inuvik Region for all fractions considered. Statistically, only organic layer and POM fraction show no significant difference between the two catenae, and the highest differences occur in the bulk samples and S+A fraction for the aliphatic/aromatic ratio; and in the bulk, S+A, s+c, and rSOC fractions for the cellulose/lignin ratio (represented with *). Generally, the lowest ratios are found in the S+A fraction, especially in the South Slave Lake Region.

The lack of any difference between some groups, despite the clearly different group medians in the plots, is attributable to the many outliers and the non-normal distribution. Finally, depth profiles for both ratios have been computed for bulk samples and individual fractions and can be found in the figures 29 and 30 in the appendix.

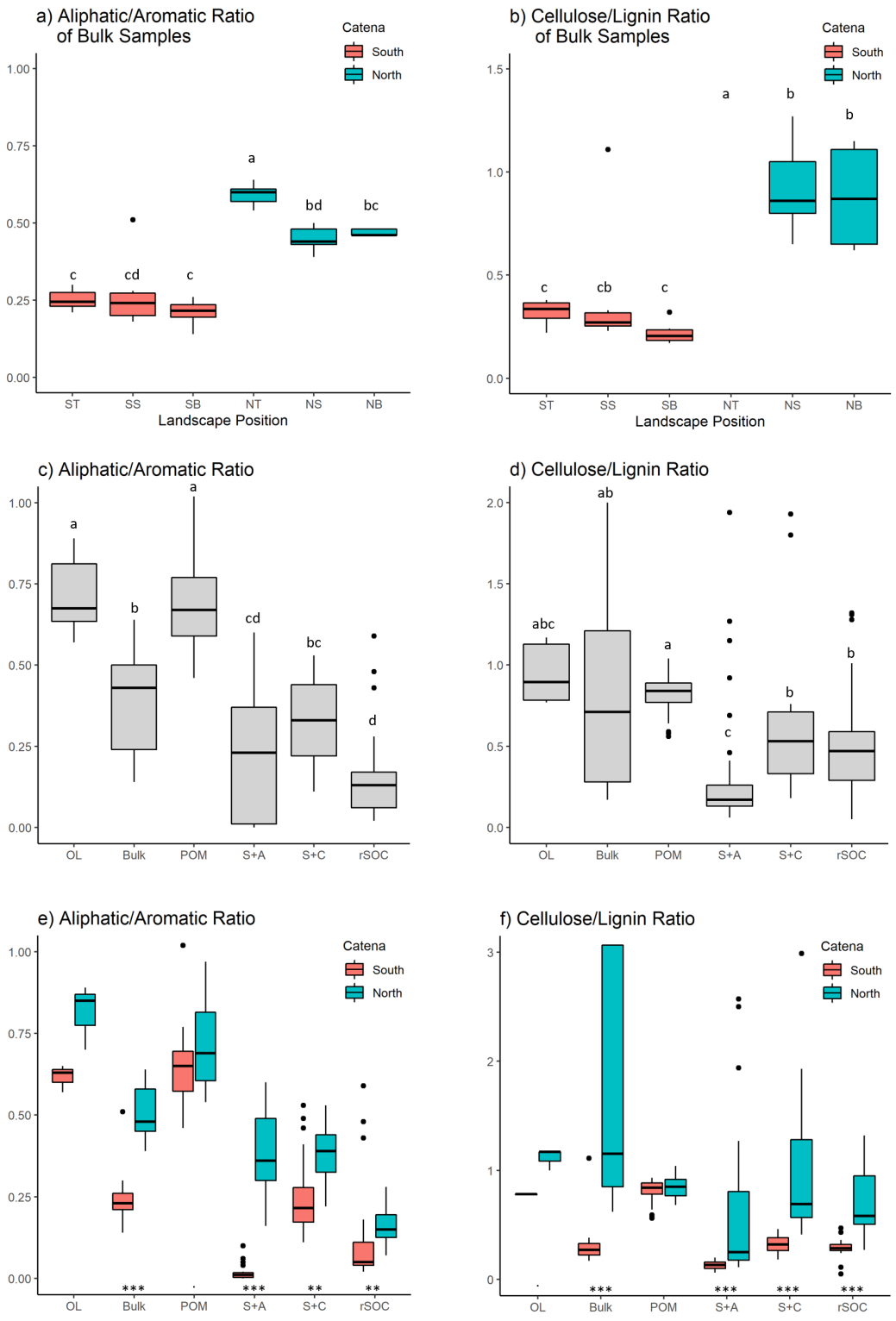

Figure 24: Aliphatic/aromatic (left) and cellulose/lignin (right) ratios along landscape gradients (a and b) an in bulk samples, SOC fractions and organic layers (c, d, e and f). In the two lower plots statistical significance between the catenae was calculated individually for each group.

Chapter 4

Discussion

4.1 Comparison of Results with Literature

The stocks of SOC in the first 30 cm depth in the South Slave Lake Region (Alberta) are around 40 tha^{-1} at all landscape positions. In comparison, Bhatti et al. (2002) estimated SOC stocks in central Canada (Alberta, Saskatchewan, and Manitoba) to be 1.4-7.7 $kg\ C\ m^{-2}$ in the first 30 cm depth, which corresponds to 14-77 tha^{-1} and correlates with the results found for the southern catena, which is located in Alberta, and thus in the same region of the compared literature.

On the other hand, stocks of SOC are much higher in the first 30 cm depth in the Inuvik Region, with 48, 86, and 116 tha^{-1} on top, slope, and bottom, respectively. SOC stocks were expected to be higher in the Inuvik Region than in the South Slave Lake Region since soils in northern permafrost regions and high latitudes are known to store large amounts of SOC due to lower decomposition rates and burial of SOC at greater depths due to cryoturbation (Hugelius et al., 2013, 2014).

Indeed, Tamocai et al. (2009) estimated the SOC stock of the northern permafrost region to be around 191 Pg C for the first 30 cm depth, making permafrost-affected mineral soils have the highest mean soil organic carbon content worldwide (32.2-69.6 $kg\ m^{-2}$). These are 322-696 tha^{-1}, thus the SOC stocks in the Inuvik Region are lower than estimated by Tamocai et al. (2009).

Further, SOC concentrations were estimated by Sothe et al. (2022) for each Canadian ecozone at several depths. In the Boreal Plains, home to the South Slave Lake Region, estimations of SOC concentrations are in the range 33.7 $\pm$ 28.5 $g\ kg^{-1}$ at 15 cm depth and 24.7 $\pm$ 26.4 $g\ kg^{-1}$ at 30 cm depth. The calculated SOC concentrations were illustrated in Fig. 16 and are in the range of 10-15 $g\ kg^{-1}$ and 5-10 $g\ kg^{-1}$ at 15 and 30 cm depth, respectively, in the three landscape positions in the South Slave Lake Region.

In the Taiga Plains, home to the Inuvik Region, estimations of the SOC concentration consists in 104.2 $\pm$ 52.4 $g\ kg^{-1}$ at 15 cm depth and 85 $\pm$ 50.1 $g\ kg^{-1}$ at 30 cm depth, but where found to be between 20-45 $g\ kg^{-1}$ and 10-35 $g\ kg^{-1}$ at 15 and 30 cm depth, respectively, in the landscape gradient in the Inuvik Region. Thus, the obtained results for the southern landscape gradient better correlate with estimations of SOC stocks and concentrations from the literature, while the results for the northern catena are slightly lower than found in other studies.

For what concerns the pyrogenic carbon, in the South Slave Lake Region there is 1 tha^{-1} of PyC_{CTO} in the first 30 cm depth in all three landscape positions, leading to an average of $PyC_{CTO}/SOC = 3$ %, whereas in the Inuvik Region there is 1-2 tha^{-1} but much more SOC, leading to an average of $PyC_{CTO}/SOC = 2.1$ %. Thus, it appears that in the northern boreal region the SOC has a low PyC content, the but SOC stocks are very important (Reisser et al., 2016).

Estimations of the proportion of PyC in SOC found by other studies are highly variable and

range between 0-35 % (Bird et al., 2015; Santín et al., 2016), with a recent analysis estimating PyC to represent around 13.7 % of the SOC worldwide (Reisser et al., 2016). However, the lowest concentrations of PyC are, above all, situated in boreal regions of the northern hemisphere.

According to Bird et al. (2015), in the same interval of 0-30 cm depth, PyC/SOC < 5 % for the boreal moist climate region. This considering, the proportion of PyC_{CTO}/SOC is as expected in comparison with the literature. However, PyC_{BPCA}/SOC is much higher (Fig. 23), exceeding 15 % in the South Slave Lake Region and 25 % in the Inuvik Region (after considering a correction factor of 2.27 as determined by Glaser et al. (1998)). Thus, the applied methods (CTO-375 and BPCA) highly affect the results.

Despite BPCA analysis method being proposed as robust against interfering materials and as not producing any PyC by itself (Wiedemeier et al., 2016), by comparing the PyC_{BPCA}/SOC with PyC_{CTO}/SOC and with literature results, it seems likely that BPCA analyses detected some non-PyC components as PyC and thus overestimated the actual PyC content. Overestimation of PyC by BPCA analysis is perhaps less common as by applying other methods, but can still happen (Hammes et al., 2007).

4.2 Distribution of SOC and PyC in Landscape Gradients

Results highlighted that soils from the Inuvik Region, which are affected by continuous permafrost conditions, higher soil moisture, pH-values lower than 5, and greater clay content, store more SOC and PyC than soils from the South Slave Lake Region, which are affected by sporadic permafrost conditions, lower soil moisture, pH-values near or greater than 6 due to carbonates, and higher relative sand and aggregate content.

Further, there is no trend of increase or decrease along the southern catena, not for SOC nor for PyC, whereas there is a trend of increasing SOC stock in the bottom direction along the northern catena. Still, the highest stock of PyC is not at the bottom, but rather along the slope of the northern catena, whereas the stocks at the top and bottom are almost the same.

The huge difference in stocks between the two Canadian regions is likely caused by differences in permafrost conditions and soil moisture content. Indeed, Cryosols, such as in the Inuvik Region, experience lower temperatures and seasonal freezing and thawing (Bockheim, 2007), which lead to strong heaving forces and soil movement (i.e., cryoturbation), while underlying permafrost impedes subsurface drainage, leading to wet and cold soils, ultimately reducing their decomposition rate (Bockheim, 2007; Ping et al., 2015).

Specifically, low soil temperatures and high soil moisture reduce SOC decomposition, while cryoturbation leads to the re-mobilization and consequent burial of SOC in greater soil depths (Ernakovich et al., 2015), significantly enhancing the total SOC mass stored in soils. After SOC entered greater soil depths, little to no decomposition occurs, thus also labile carbon compounds are protected against decomposition. This causes the accumulation of large stores of organic carbon in the active layer and underlying permafrost (Hugelius et al., 2010; Koven et al., 2009; Kuhry et al., 2010; Ping et al., 2015).

Furthermore, the lower decomposition rate and the cryoturbation processes in the Inuvik Region can affect the proportion of labile carbon in soil, since the cold and wed soil conditions limit microbial activity and also microbial access to SOC, stabilizing and protecting also more labile forms against decomposition (Ping et al., 2015). Indeed, organic matter in arctic soils can be relatively non-decomposed due to frozen and waterlogged conditions, and organic matter in permafrost can be more labile than organic matter found in the active layer (Ernakovich et al., 2015).

This correlates with the higher absolute content of SOC_{POM} in the Inuvik Region (Fig. 18)

than in the South Slave Lake Region (at equal soil depth). Indeed, carbon associated with POM is considered to be more labile than carbon associated with S+A and s+c (Abramoff et al., 2018; Zimmermann et al., 2007). Thus, the higher proportion of soil carbon associated with POM in the Inuvik Region is likely due to a lower decomposition rate in the northern catena, while a higher SOC cycling in the southern catena would explain lower contribution of labile SOC from the POM fraction in that region.

On the other hand, soils in the South Slave Lake Region experience only sporadic permafrost conditions and reduced soil moisture, which likely lead to a higher decomposition rate. These different conditions between the two catenae are likely to affect SOC quality, as visible in Fig. 24 e and f. Indeed, the quality of SOC differs between the two landscape gradients for almost all soil fractions (with the sole exception of organic layer and POM being similar), and lower ratios are found in the South Slave Lake Region. Therefore, permafrost is a main driver affecting differences in both stocks and quality of SOC, causing higher stocks and higher proportion of labile SOC in the Inuvik Region.

Other soil properties that differ between the two Canadian landscapes are the pH and the effective cation exchange capacity (eff. CEC), both available in Table 10 in the appendix. A high pH is usually associated to higher decomposition rates, while a high cation exchange capacity in soil was expected to correlate with higher levels of PyC (Liang et al., 2006). Indeed, soils from the Inuvik Region exhibit higher PyC stocks and concentrations, and as expected, higher effective CEC. Still, these two soil properties are likely less affecting SOC and PyC stocks and concentrations than the permafrost conditions and the soil moisture content.

Thus, greater stocks of SOC and PyC in the Inuvik Region than in the South Slave Lake Region are likely due to lower decomposition rates and higher uptake to soil organic matter caused by the continuous permafrost conditions and the higher soil moisture content in the northern landscape gradient (Kuhry et al., 2010; Reisser et al., 2016).

Concerning differences along the catenae, the initial hypothesis of an increase in the stocks of SOC and PyC in the bottom direction along the two landscape gradients relies on the assumption that soil carbon can be translocated to depositional landscape position due to soil steepness and surface water flow (Abney and Berhe, 2018).

However, in the South Slave Lake Region, the difference in height between the top and bottom of the catena is circa 10 m and the distance between the two external positions is circa 200 m, leading to an average steepness of 5 %, which is likely to be not enough for it to cause soil erosion and translocation in the bottom direction. Nevertheless, the difference in height between the top and bottom of the catena in the Inuvik Region is almost 50 m, and the distance between these two positions is 600 m, leading to an average steepness of ca. 8 %, which is might enough to cause erosion and consequent translocation of soil material (and thus, among other elements, also SOC and PyC).

Thus, the low difference in height in the South Slave Lake Region correlates with the homogeneous distribution of SOC and PyC stocks along that catena, whereas the considerable difference in height in the Inuvik Region relates to the increase in SOC stocks in the bottom direction and to the increase in stock of PyC from the top to the slope of the northern catena, but not with the reduction from the slope to the bottom. Thus, steepens cannot explain why the highest PyC stock is found along the slope and not at the bottom of the northern catena, while similar stocks of PyC are found at the top and the bottom. Indeed, Abney et al. (2019) found that burn severity can act as a primary control on PyC transport, while the slope angle likely plays a secondary role along a single hillslope after a fire.

4.3 Distribution of SOC and PyC in Soil Depths

Concerning the distribution of carbon along soil depths, the concentrations of SOC and PyC_{CTO} with respect to the total bulk mass usually decrease with depth (Fig. 16) in the South Slave Lake Region, except at the bottom of the catena, which is subject to an increase in PyC concentration from 0-15 cm to 15-30 cm depth. This reduction in the concentration of SOC and PyC_{CTO} in bulk soil with depth can be explained by the input direction, since PyC must enter deeper soils from the surface soil (Bird et al., 2015), and the sporadic permafrost conditions, which unlikely cause burial of soil carbon at greater depths. Further, the increase in the concentration of PyC_{CTO} with depth at the bottom of the catena is minimal in term of quantities (from 0.22 to 0.25 mg PyC per gram of bulk soil) and even negligible if also the standard error is considered (Fig. 20).

On the other hand, the Inuvik Region exhibits the same trend of decrease in SOC concentration with depth till 30 cm, confirming the assumption of higher SOC concentrations in soils near the surface (Bird et al., 2015), albeit the concentration stays stable (NT, NS) or even increases (NB) at greater depths (Fig. 16), likely due to burial of soil carbon throughout cryoturbation processes (Ping et al., 2015). Furthermore, the trend in the concentration of PyC_{CTO} in the north encompasses both decreases and increases with depth, suggesting that the vertical transport of PyC differs from that of SOC.

A possible explanation for both decreases and increases in SOC and especially PyC with depths along the catena in the Inuvik Region is given by the continuous permafrost conditions, which make the soil subject to cryoturbation and consequently to the re-distribution of soil organic matter into greater depths (Kuhry et al., 2010). Thus, permafrost could drive the vertical transport of SOC and, consequently, PyC due to cryoturbation (Bockheim, 2007; Kuhry et al., 2010).

This process is not visible in the South Slave Lake Region, where permafrost conditions are sporadic and SOC concentration decreases with depth, while PyC concentration shows almost no variations with depth. The sporadic permafrost conditions of the South Slave Lake Region are not sufficient to trap more carbon in soils, whereas the continuous permafrost conditions in the Inuvik Region likely influence the hold back of soil carbon, contributing to greater stocks of both SOC and PyC, and even increasing with increasing depth. Thus, generally, the extent to which soil organic and pyrogenic carbon contribute to the total soil mass decreases with increasing soil depth, except in case of re-distribution or burial of soil carbon in permafrost-affected soils.

Considering PyC not with respect to the total soil mass but with respect to total SOC, a total different picture appears, especially if PyC_{BPCA} is considered instead of PyC_{CTO}, (Fig. 23). Indeed, despite the concentration of SOC as part of the total soil mass generally decreases with depth in both landscape gradients, the concentration of PyC with respect to SOC in soils is more stable of even increases. Interestingly, while the percentage of PyC_{CTO}/SOC tend to increase with depth, that of PyC_{BPCA}/SOC tend to decreases. In both cases, this suggests that there is a preferential transfer of PyC to the subsoil compared to other SOC moieties (Soucémarianadin et al., 2019). Between both, PyC_{CTO}/SOC goes better with literature, as it was found that while the absolute PyC content decreases with depth, its proportion to the soil organic carbon remains constant or tends to increase (Soucémarianadin et al., 2019).

Thus, the content of PyC with respect to SOC (Fig. 23) is greatly affected by the quantification method (i.e., CTO-375 and BPCA). The increase with depth of PyC_{CTO}/SOC is caused by a decrease in SOC with no major changes in the PyC_{CTO} content, whereas the content of PyC_{BPCA} usually decreases with depth, except at 30-45 cm depth in the Inuvik Region. Another factor playing against the reliability of PyC_{BPCA}/SOC is the high relative proportion of PyC, which is 5-25 %, while, as previously discussed, PyC/SOC in boreal regions is usually lower than 5 % (Bird et al., 2015). On the other hand, PyC_{CTO}/SOC is between 1-5 %, and thus in the expected range.

4.4 Distribution of SOC and PyC in Soil Fractions

The proportion of SOC and PyC in the single fractions is consistently different among the two landscape gradients considered, with the majority of PyC associated with s+c in the Inuvik Region, and with S+A in the South Slave Lake Region, with no strong linear correlation between the concentrations of PyC and SOC in the bulk samples or in SOC fractions.

Up to 30-50 % of SOC can be found in the POM fraction of both catenae (Fig. 17). Despite these high amounts, less than 15 % of PyC_{CTO} is associated with this fraction in the first 15 cm of soil, and the content is even lower at greater depths, with 1-6 % of PyC originating from particulate organic matter at both catenae (Fig. 19). This phenomenon could be due to the aggressiveness of the CTO-375 method, which specifically detects the most condensed PyC compounds (Hammes et al., 2007), while carbon associated with POM is considered to be less protected against physical and chemical decomposition than carbon associated with other SOC fractions (Abramoff et al., 2018; Zimmermann et al., 2007).

Indeed, soils or fractions which are more enriched in labile compounds (POM) will have lower thermal stability as compared with soils or fractions that are more enriched in stable compounds (e.g. silt + clay fractions or a chemically resistant fraction), due to the lower activation energy needed to break the association bonds (Demyan et al., 2013). Further, the decrease of both SOC_{POM} and PyC_{POM} with depth can be explained by the lability of the POM fraction and the fact that POM is an input that enters the soil system from above (Bird et al., 2015).

Interestingly, in the Inuvik Region the concentrations of PyC and SOC in the POM fraction show a higher linear correlation than in the South Slave Lake Region (Fig. 21), maybe due to the permafrost conditions, which impede decomposition of labile SOC. In the southern catena, the concentration of PyC found in the POM fraction can be higher than in the northen catena, while that of SOC from the same fraction is lower, suggesting that the labile SOC associated with POM is subject to higher levels of decomposition in the South Slave Lake Region.

Differently, SOC associated with silt and clay is greater than 40 % at all landscape positions considered except for SB, and differently from SOC associated with POM, it usually increases with depth, except at NT from 15-30 cm to 30-45 cm depth. PyC contributions from the s+c fraction remain high (15.5-71.3 % in the south and 25.7-82.8 % in the north), with both increases (SB, NB) and decreases (ST, SS, NT, NS) with depth.

The applied SOC fractionation led to a silt and clay fraction containing all soil particles finer than 45μm (Zimmermann et al., 2007) and SOC associated with soil particles smaller than 20 μm is considered relatively stable and to account for a large proportion of total SOC (Feng et al., 2013). Indeed, interactions with mineral surfaces influence the thermal degradation of organic molecules and thus their stabilization in soils (Demyan et al., 2013), leading to accumulation of SOC due to association with clay minerals (Gentsch et al., 2015). Organic carbon retained in association with fine soil particles has relatively longer turnover times and accounts for a large proportion of total SOC (Feng et al., 2013). Indeed, SOC stocks at clay rich sites were found to be higher than at more sandy sites (Don et al., 2007).

This is also the case for the two landscape gradients considered, with higher SOC and PyC stocks in the Inuvik Region, where soil texture is mainly made of silt and clay, and lower stocks in the South Slave Lake Region, where sand and aggregate affect soil texture more than silt and clay. The concentration of PyC in the s+c fraction is not linearly correlated with that of SOC in the same fraction. Generally, the clay content is considered a driver of potential PyC decomposition, and is also used to model the turnover of carbon in soils (Coleman and Jenkinson, 2014).

Further, part of the silt and clay fraction is the residual SOC fraction (rSOC), which is highly aromatic and thus recalcitrant. SOC association with this fraction usually increases with depth,

except at NB, where it remains almost constant at all soil depths and at NS, where the highest relative abundance is found in the middle soil depth. Further, the contribution to SOC from this fraction is greater in the north than in the south.

Furthermore, sand and aggregates are not rich in SOC but exhibit a very high relative content of PyC, especially in the South Slave Lake Region. Indeed, SOC associated with this fraction usually increases with depth (except at NS and NB where it remains stable) and is in the range of 3-18 % in the south, where it increases along the catena from the top to the bottom, whereas it is in the range of 9-35 % in the north. In contrast, the relative PyC content in that fraction is in the range 45-80 % in the south (except at the first 15 cm at the slope), and between 13-70 % in the north. Lastly, the relative abundance of PyC is greater in the S+A fraction than in the s+c fraction at ST, SB and in 15-30 cm at SS, whereas there is more PyC in the s+c fraction at NS, NB and and the first 30 cm depth at NT.

However, it is logical that in the south, where sand and aggregates are relatively more abundant than silt and clay, the majority of PyC is found in association with that fraction, whereas in the north, where soil texture is mainly affected by the high abundance of silt and clay, the majority of PyC can be found in that fraction. Thus, in general, PyC is found in higher abundance in association with the SOC fraction that accounts for the higher relative prominence in the soil. However, no statistical difference was provided for this trend.

Generally, PyC association with a specific SOC fraction has a strong influence on its potential physical-chemical alteration. Indeed, a crucial factor for the decomposition of organic material is its accessibility to microbes, an plant debris not physically protected, such as POM, is attacked first. Physical protection can be achieved through aggregation and adsorption of SOM on mineral surfaces, which strongly reduces its decomposability (Zimmermann et al., 2007). Thus, both s+c and S+A are physically protected against fast decomposition. Indeed, association of PyC to POM resulted in lower stability against decomposition (since almost no PyC was found in that fraction despite high SOC content), whereas association to s+c enhances resistance against physical-chemical alteration, thus the higher the clay content in soils, the higher the quantity of PyC.

Finally, higher concentrations of SOC were hypothesized to linearly correlate with higher concentrations of SOC. However, no such trend was found, nor in the bulks nor in the SOC fractions (Fig. 21). Indeed, the only positive linear correlation between SOC and PyC concentrations is found in the POM fraction in the Inuvik Region, while especially the S+A fraction shows absolutely no correlation between the SOC and PyC concentrations. Thus, PyC is preferentially associated with some fractions in the soil and its content with respect to the SOC in soil is highly variable. Indeed, PyC concentrations in the S+A fraction are highly variable in the south, while SOC concentrations mainly remain near to 1 $mgC\ gsoil^{-1}$, with the exception of the three replicates at SB, which show higher values.

The highest PyC concentration in SOC fractions belongs to the s+c fraction, with more than 0.4 $mgC\ gsoil^{-1}$, which is almost twice the concentration of PyC in the S+A fraction and more than four times that in the POM fraction (Table 14). This relates to other studies, where soils with clay content higher than 50 % were found to contain significantly more PyC than soils with clay content lower than 5% (Reisser et al., 2016).

4.5 Differences in SOC Cycling

The results of DRIFT analysis can be used to make inferences about the lability and the relative degree of decomposition of SOC (Ernakovich et al., 2015), in the two Canadian region and in the SOC fractions. Indeed, according to De la Rosa et al. (2019), aromatic bands centered at 1620 (aromatic peak) and 1510 cm^{-1} (lignin peak) play a relevant role for the assessment of stable C in soils.

After DRIFT analysis, aliphatic/aromatic and cellulose/lignin ratios were found to be higher in the Inuvik Region, especially in the bulk samples, S+A, s+c, and rSOC fractions, whereas no differences between landscape gradients were found for organic layer and POM fraction (Fig. 24). Further, both ratios tend to decrease in the bulk samples along the catenae in the bottom direction, and Fig. 24 a and b highlight that the highest ratios are found at NT, albeit no significant difference occurring between NS and NB.

In the South Slave Lake Region, no significant difference between the three landscape positions was found, despite the lower ratios at the bottom. Precisely, both ratios in the Inuvik Region are twice as high as in the South Slave Lake Region. Further, Fig. 26 highlights that the trend along the two landscape gradients remains the same for all soil depths considered, with the exception of higher cellulose/lignin ratios at NT with increasing depth. This trend is likely caused by a reduction in the lignin peak, which enhances the ratio.

In the light of lower ratios correlating with higher relative abundance of stable, slow cycling, carbon in soils (De la Rosa et al., 2019; Laub et al., 2020), the results suggest a higher potential cycling in the southern catena, leading to a disproportion of stable carbon in soil, while a lower potential cycling in the northern catena is attributable to the protection of labile carbon from decomposition due to the permafrost conditions.

Considering differences in the ratios between SOC fractions, for what concerns POM and organic layer, these two groups share the highest aliphatic/aromatic ratios, both near to 0.75, highlighting their high aliphatic content. Further, both their cellulose/lignin ratios are near to one, suggesting no disproportionate relative abundance of one of both compounds in respect to the other. Indeed, the POM fraction is made of free fragments of plant detritus, dead insects, fungi, and detritus generated through fragmentation and decomposition of litter, and from the breakup of preexisting soil aggregates (Abramoff et al., 2018), and is thus, in terms of composition, the most similar carbon pool to the organic layer, which is entirely made of leaves in decomposition.

All other fractions exhibit lower mean aliphatic/aromatic ratios, with the lowest one belonging to rSOC, which exhibits a relatively higher abundance of aromatic compounds. Differences between fractions are less prominent in their mean cellulose/lignin ratios, with the lowest ratio exhibited by the S+A fraction, especially in samples from the South Slave Lake Region.

According to Laub et al. (2020), the aliphatic/aromatic ratio corresponds to the DRIFTS stability index (DSI) of bulk soil samples and was defined as the ratio of the area below the aliphatic absorption band (2930 cm^{-1}) to the area below the aromatic–carboxylate absorption band (1620 cm^{-1}). This ratio (2930 cm^{-1}/1620 cm^{-1}) was set equal to the ratio of fast-cycling/slow-cycling SOM (Laub et al., 2020), thus the lower the ratio the greater the relative abundance of slow-cycling SOM in respect to fast-cycling SOM. Further, Demyan et al. (2012) showed that the ratio of the 1620 to 2930 cm^{-1} band area had a significant positive correlation with the ratio of stable to labile SOM obtained by size and density fractionation. Thus, the low aliphatic/aromatic ratio of the rSOC fraction correlates with the definition of this fraction as a resistant soil organic carbon fraction.

Further, Fig. 27 highlights differences in the aliphatic/aromatic ratio between SOC fractions in all six landscape gradients. In the South Slave Lake Region (left), the S+A fraction exhibit

the lowest ratio at all landscape positions, followed by the rSOC and s+c fractions, which both increase at the bottom of the catena. This could indicate a higher relative abundance of aliphatic compounds in respect to aromatic compounds at the bottom of the southern catena. In the Inuvik Region (right), the ratio is higher at all landscape positions and fractions (including in the organic layer), suggesting a lower relative abundance of aromatic compounds. Considering that PyC is highly aromatic, despite DRIFT investigates SOC in general and do not focus on PyC, the lower relative proportion of aromatic compounds in the Inuvik Region correlates with the lower PyC/SOC proportion of that area.

Regarding the cellulose/lignin ratio in the soil fractions of all the six landscape gradients, Fig. 28 highlights huge variations in the ratio in the bulk samples, especially at the top of the northern catena, while the lowest ratios belong to the S+A fraction.

Considering the depth profiles of the individual fractions in Fig. 29 and 30, the cellulose/lignin ratios at NT are far higher than at all other landscape positions in the bulk samples, S+A and s+c fractions, with values increasing with depth, and also higher for the POM and rSOC fractions, albeit with less differences from the other landscape gradients. Further, both increases and decreases in the ratios are visible in all fractions with depth. This extreme high cellulose/lignin ratios suggest a minimal relative abundance of lignin, which is unexpected considering its chemical recalcitrance (Thevenot et al., 2010).

Indeed, due to its complex structure, only a few organisms, such as some bacteria and fungi, are able to degrade lignin. According to (Thevenot et al., 2010), degradation of lignin through mineralization and alteration of its initial structure results in a decrease in its concentration in soils, which is likely to reduce its cellulose/lignin ratio.

The DRIFT analysis highlights that each SOC fraction has a specific stability against potential carbon cycling, and that potential cycling is higher in the South Slave Lake Region than in the Northern Inuvik Region, for all fractions except for OL and POM. Differences in SOC cycling between the two catenae can be reconducted to differences in climatic conditions (e.g., low temperatures, high soil moisture class and continuous permafrost conditions in the Inuvik Region), and in the different soil texture. Indeed, clay binds to organic matter, protecting it from being broken down and limiting access to it by microbes and other organisms, while organic matter associated with sand, such as in the South Slave Lake Region, is less protected from microbial degradation, ultimately decomposing more rapidly. Hence, a faster cycling in the south leads to a more rapid decomposition of aliphatic compounds, and thus to lower ratios.

4.6 Quality of PyC

BPCA analysis provided information about the quality of PyC, at all six landscape positions for each depth, ad revealed that more condensed structures were found in greater soil depths at ST, SS, NS and NB, but not at SB, while both increases and decreases of the proportion of the individual BPCAs was detected at NT. High proportion of B5CA and B6CA are indicative of more condensed and aromatic material, while B3CA and B4CA are the product of small condensed units of three aromatic rings minimum (Soucémarianadin et al., 2019).

The proportion of B3CA and B4CA decreased with depth (except at SB, and from 15-30 to 30-45 cm at NS and NB), and together account for less than 40 %, while B5CA and B6CA account for 60-70 % of PyC. A study on French soils on which BPCA analysis was applied indicated that more condensed structures were found in the subsoil (Soucémarianadin et al., 2019). However, this is only partially the case for the two catenae investigated (Fig. 22). Thus, more altered PyC is not necessarily located in depositional landscape positions, nor at greater depths.

4.7 Uncertainties and Limitations

Soil organic carbon can be defined by measurable chemical and physical pools, such as mineral-associated carbon, carbon physically entrapped in aggregates, dissolved carbon, and fragments of plant detritus (Abramoff et al., 2018). These conceptual pools ideally correspond to measurable SOC fractions but differ from each other in decomposition rates and characteristic stabilization mechanisms (Zimmermann et al., 2007; Abramoff et al., 2018). However, the fractionation of bulk soil in individual SOC fractions can lead to greater or smaller fractions, depending on how fractionation was executed and how the fractions were initially defined. For example, the sole variation in ultrasonic power might lead to significantly different dispersion and thus a different breakdown of aggregates (Poeplau and Don, 2014).

Further, quantities of PyC in the 41 bulk samples were determined by using both CTO-375 (applied to bulk samples and fractions) and BPCA analysis (applied only to bulk samples), producing PyC_{CTO} and PyC_{BPCA}, respectively. Methods developed for the quantification of PyC in soils and sediments rely on its resistance to degradation, and in particular, oxidation (Hammes et al., 2007).

Hammes et al. (2007) compared the quantification of PyC through several methods and found that PyC concentrations determined using CTO-375 were generally at least an order of magnitude lower than those measured by other techniques, such as BPCA. This is because CTO-375 specifically detects the most condensed PyC, so if low-condensed char PyC is present, it will not be detected, whereas BPCA also detects small units of condensed aromatic systems, leading to higher quantification of PyC (Hammes et al., 2007).

However, both CTO-375 and BPCA might detected some non-PyC material as PyC. This is the case for the discussed results, since the high proportion of PyC_{BPCA} in SOC is reasonably attributable to detection of some non-PyC materials as PyC. Similarly, also PyC_{CTO} in the rSOC fraction led to unrealistic high amount of PyC in that fraction (especially at SB), leading to higher PyC quantities in the rSOC fraction (which is a sub-fraction of s+c) than in the whole s+c fraction. This is why PyC_{CTO} in the rSOC fraction was not considered at all, and the relative and absolute distributions of PyC in SOC fractions do not comprehend rSOC. Thus, it is reasonable that PyC might is produced during measurement, for both CTO-375 and BPCA analysis methods.

Furthermore, Table 5 highlights that $PyC_{BPCA} < PyC_{CTO}$ only at 15-30 cm at ST, while in all other cases $PyC_{BPCA} > PyC_{CTO}$, with 0.53-16.46 times more PyC detected with BPCA. It is thus possible that the higher quantity of PyC_{CTO} in the ST is due to other carbon compounds reacting to CTO-375 and leading to an overestimation of PyC_{CTO} in 15-30 cm depth at ST, while the variations in PyC_{BPCA} with respect to PyC_{CTO} could be understood in terms of the selectivity of the methods across the black carbon continuum (Hammes et al., 2007).

4.8 Outlook

Terrestrial ecosystems, and their soils, are key components in the global carbon cycle, with the world soils holding at least twice as much carbon as the atmosphere, and with 30 % of the global SOC stock held in the Northern Circumpolar Region, which is considered most sensitive to climate change (Batjes, 2016). As the more recalcitrant component of SOC, PyC stocked in soils is recognized as an important potential sink within the global C-cycle (Bird et al., 2015; De la Rosa et al., 2019). However, a more exact quantification of PyC stored in soils is mandatory for the proper estimation of its relevance.

Indeed, the impact of pyrogenic carbon on the global carbon cycle can only be reliably investigated if its detection and quantification in soils are accurate. However, all so-far available methods focus on a restricted proportion of the black carbon continuum and are subject to potential positive bias (De la Rosa et al., 2019; Hammes et al., 2007).

Regarding the vulnerability of SOC and PyC to climate change, permafrost affected soils such as those of the Inuvik Region are important but vulnerable carbon pools (Ernakovich et al., 2015). Indeed, the thawing of permafrost can result in large pools of both labile and stable, previously protected soil carbon, that potentially become available for biological decomposition, leading to increased greenhouse gas fluxes into the atmosphere from northern environments (Hugelius et al., 2013; Ping et al., 2015).

Finally, there is evidence that soils from the Inuvik Region store also more labile SOC and protect it against decomposition. According to Zimmermann et al. (2007), stabilized SOC is of special importance with respect to long-term CO_2 sequestration because it accounts for most of the SOC. The response of soil pyrigenic carbon to environmental factors and climate change is essential for the estimation of its potential as an atmospheric carbon sequestration tool.

Chapter 5

Conclusions

After the production of PyC during wildfires and its entrance in the terrestrial pyrogenic carbon pool, its fate in the landscape embraces a variety of options. Despite PyC being largely aromatic, inert, and recalcitrant, at least a component of PyC is involved in a range of physical and chemical processes that alter its form over time and lead to its decomposition or dispersal throughout the soil system.

Drivers controlling the translocation and physical-chemical altering of PyC in Canadian boreal soils mainly comprehend permafrost and related cryoturbation processes, soil texture and the consequent association with specific SOC fractions (all of which exhibit a different stabilization of carbon in soil), and, to minor extent, transposition due to steepness.

The permafrost conditions drive both translocation and physical-chemical altering of PyC in soils, especially in the Inuvik Region, as cryoturbation buries PyC at greater soil depths, protecting it from biotic and abiotic decomposition. Permafrost drives translocation of PyC through vertical re-distribution at greater depths, finally enhancing its stocks. Further, permafrost also affects the SOC quality, with a higher relative abundance of labile, fast cycling soil carbon in the Inuvik Region. Differences in PyC stocks and concentrations between and along the two locations considered are thus primarily attributable to differences in the permafrost conditions.

Concerning the soil texture, PyC was mainly found in association with the mineral fraction such as silt and clay in the Inuvik Region, whereas association with sand and aggregates was more prominent in the South Slave Lake Region. This correlates with the soil texture, since soils in the southern catena exhibit a higher sand content than those in the northern one, while the latter exhibit a higher content of clay. Contributions of PyC from particulate organic matter are generally lower in both landscape gradients, likely due to the lability of this SOC fraction. Fine soil particles further exhibited a higher potential stabilization of carbon in soils.

Differences in stocks along landscape gradients are scarcely attributable to the steepness. The homogeneous stocks of both SOC and PyC along the southern landscape gradient are likely due to a lack of altitude differences and permafrost, while increases in the stocks of SOC in the bottom direction in the northern catena is at least partially due to high differences in altitude.

From all available evidences, the initial hypotheses can be answered as follows:

There is a preferential way of PyC translocation in respect to translocation of SOC along landscape gradients and soil depths, as changes in the concentrations of both do not follow the same trend.

Soil erosion due to steepness was not ubiquitously found to cause a translocation of PyC to more depositional landscape positions in both catenae, as greater PyC stocks were not found at the bottom of the landscape gradients. Still, differences in steepness likely drive translocation of SOC,

especially in the Inuvik Region, but not in the South Slave Lake Region, due to a too low difference in height for it to cause soil surface erosion and consequent transport in the bottom direction.

Qualitative analysis of PyC revealed that more altered PyC is not necessarily located in depositional landscape positions. Results indicated an increase in the mean B5CA and B6CA along the catena in the South Slave Lake Region at the costs of the mean B3CA and B4CA content, together with a decrease in the aliphatic/aromatic ratio, suggesting a higher relative abundance of stable and aromatic carbon compounds at the bottom of the southern catena. However, this trend is not visible Inuvik Region. The the relative proportion of mean B3CA and B4CA slightly increased in the bottom direction, at the cost of B5- and B6CA, and DRIFT analysis highlighted no higher proportion of more stable and aromatic carbon compounds at the bottom of the catena with respect to the slope.

Soil texture drives the physical-chemical alteration of PyC, as the extent to which PyC was found in association with a specific soil fraction was found to correlate with the different soil texture of the two landscape gradients, with the majority of PyC found in both catenae associated with the SOC fraction mainly affecting the soil texture.

Permafrost affects vertical translocation of PyC by cryoturbation and reduces decomposition of SOC. Permafrost was found to be the most relevant driver affecting vertical translocation of PyC and burial in greater depths due to cryoturbation processes.

SOC cycling depends on both the permafrost conditions and the soil texture, with each soil fraction accounting for a specific aliphatic/aromatic ratio and a higher relative abundance of aliphatic, fast cycling compounds in the permafrost-affected soils of the Inuvik Region.

Bibliography

Aaltonen, H., Palviainen, M., Zhou, X., Köster, E., Berninger, F., Pumpanen, J., and Köster, K. (2019). Temperature sensitivity of soil organic matter decomposition after forest fire in canadian permafrost region. *Journal of Environmental Management*, 241:637–644.

Abiven, S. and Santín, C. (2019). Editorial: From fires to oceans: Dynamics of fire-derived organic matter in terrestrial and aquatic ecosystems. *Frontiers in Earth Science*, 7:1–4.

Abney, R. B. and Berhe, A. A. (2018). Pyrogenic carbon erosion: Implications for stock and persistence of pyrogenic carbon in soil. *Frontiers in Earth Science*, 6.

Abney, R. B., Kuhn, T. J., Chow, A., Hockaday, W., Fogel, M. L., and Berhe, A. A. (2019). Pyrogenic carbon erosion after the rim fire, yosemite national park: The role of burn severity and slope. *Journal of Geophysical Research: Biogeosciences*, 124:432–449.

Abramoff, R., Xu, X., Hartman, M., O'Brien, S., Feng, W., Davidson, E., Finzi, A., Moorhead, D., Schimel, J., Torn, M., and Mayes, M. A. (2018). The millennial model: in search of measurable pools and transformations for modeling soil carbon in the new century. *Biogeochemistry*, 137:51–71.

Agarwal, T. and Bucheli, T. D. (2011). Adaptation, validation and application of the chemo-thermal oxidation method to quantify black carbon in soils. *Environmental Pollution*, 159:532–538.

Batjes, N. H. (2016). Harmonized soil property values for broad-scale modelling (wise30sec) with estimates of global soil carbon stocks. *Geoderma*, 269:61–68.

Bhatti, J. S., Apps, M. J., and Tarnocai, C. (2002). Estimates of soil organic carbon stocks in central canada using three different approaches. *Canadian Journal of Forest Research*, 32:805–812.

Bird, M. I., Wynn, J. G., Saiz, G., Wurster, C. M., and McBeath, A. (2015). The pyrogenic carbon cycle. *Annual Review of Earth and Planetary Sciences*, 43:273–298.

Biskaborn, B. K., Smith, S. L., Noetzli, J., Matthes, H., Vieira, G., Streletskiy, D. A., Schoeneich, P., Romanovsky, V. E., Lewkowicz, A. G., Abramov, A., Allard, M., Boike, J., Cable, W. L., Christiansen, H. H., Delaloye, R., Diekmann, B., Drozdov, D., Etzelmüller, B., Grosse, G., Guglielmin, M., Ingeman-Nielsen, T., Isaksen, K., Ishikawa, M., Johansson, M., Johannsson, H., Joo, A., Kaverin, D., Kholodov, A., Konstantinov, P., Kröger, T., Lambiel, C., Lanckman, J. P., Luo, D., Malkova, G., Meiklejohn, I., Moskalenko, N., Oliva, M., Phillips, M., Ramos, M., Sannel, A. B. K., Sergeev, D., Seybold, C., Skryabin, P., Vasiliev, A., Wu, Q., Yoshikawa, K., Zheleznyak, M., and Lantuit, H. (2019). Permafrost is warming at a global scale. *Nature Communications*, 10.

Bockheim, J. G. (2007). Importance of cryoturbation in redistributing organic carbon in permafrost-affected soils. *Soil Science Society of America Journal*, 71:1335–1342.

Bockheim, J. G., Hinkel, K. M., and Nelson, F. E. (2003). Predicting carbon storage in tundra soils of arctic alaska. *Soil Science Society of America Journal*, 67:948–950.

Bond-Lamberty, B., Peckham, S. D., Ahl, D. E., and Gower, S. T. (2007). Fire as the dominant driver of central canadian boreal forest carbon balance. *Nature*, 450:89–92.

Braadbaart, F., Poole, I., and van Brussel, A. A. (2009). Preservation potential of charcoal in alkaline environments: an experimental approach and implications for the archaeological record.

Chatterjee, S., Santos, F., Abiven, S., Itin, B., Stark, R. E., and Bird, J. A. (2012). Elucidating the chemical structure of pyrogenic organic matter by combining magnetic resonance, mid-infrared spectroscopy and mass spectrometry. *Organic Geochemistry*, 51:35–44.

Coleman, K. and Jenkinson, D. S. (2014). Rothc-a model for the turnover of carbon in soil model description and users guide (windows version).

Conard, S. G. and Solomon, A. M. (2008). Chapter 5. Effects of Wildland Fire on Regional and Global Carbon Stocks in a Changing Environment. *Developments in Environmental Science*, 8:109–138.

Cotrufo, M. F., Boot, C., Abiven, S., Foster, E. J., Haddix, M., Reisser, M., Wurster, C. M., Bird, M. I., and Schmidt, M. W. (2016). Quantification of pyrogenic carbon in the environment: An integration of analytical approaches. *Organic Geochemistry*, 100:42–50.

De Groot, W. J., Cantin, A. S., Flannigan, M. D., Soja, A. J., Gowman, L. M., and Newbery, A. (2013). A comparison of canadian and russian boreal forest fire regimes. *Forest Ecology and Management*, 294:23–34.

De la Rosa, J. M., Jiménez-González, M. A., Jiménez-Morillo, N. T., Knicker, H., and Almendros, G. (2019). Quantitative forecasting black (pyrogenic) carbon in soils by chemometric analysis of infrared spectra. *Journal of Environmental Management*, 251.

Demyan, M. S., Rasche, F., Schulz, E., Breulmann, M., Müller, T., and Cadisch, G. (2012). Use of specific peaks obtained by diffuse reflectance fourier transform mid-infrared spectroscopy to study the composition of organic matter in a haplic chernozem. *European Journal of Soil Science*, 63:189–199.

Demyan, M. S., Rasche, F., Schütt, M., Smirnova, N., Schulz, E., and Cadisch, G. (2013). Combining a coupled FTIR-EGA system and in situ DRIFTS for studying soil organic matter in arable soils. *Biogeosciences*, 10:2897–2913.

Diochon, A., Gregorich, E. G., and Tarnocai, C. (2013). Evaluating the quantity and biodegradability of soil organic matter in some canadian turbic cryosols. *Geoderma*, 202-203:82–87.

Don, A., Schumacher, J., Scherer-Lorenzen, M., Scholten, T., and Schulze, E. D. (2007). Spatial and vertical variation of soil carbon at two grassland sites - implications for measuring soil carbon stocks. *Geoderma*, 141:272–282.

Ecological Stratification Working Group (1995). *A national ecological framework for Canada*. Centre for Land and Biological Resources Research, Research Branch, Agriculture and Agri-Food Canada.

Ernakovich, J. G., Wallenstein, M. D., and Calderón, F. (2015). Chemical indicators of cryoturbation and microbial processing throughout an alaskan permafrost soil depth profile. *Soil Science Society of America Journal*, 79:783–793.

FAO (2014). World reference base for soil resources 2014. international soil classification system for naming soils and creating legends for soil maps, world soil resources reports no. 106. food and agriculture organisation of the united nations, rome.

Feng, W., Plante, A. F., and Six, J. (2013). Improving estimates of maximal organic carbon stabilization by fine soil particles. *Biogeochemistry*, 112:81–93.

Flannigan, M., Stocks, B., Turetsky, M., and Wotton, M. (2009). Impacts of climate change on fire activity and fire management in the circumboreal forest. *Global Change Biology*, 15:549–560.

Gentsch, N., Mikutta, R., Alves, R. J., Barta, J., Čapek, P., Gittel, A., Hugelius, G., Kuhry, P., Lashchinskiy, N., Palmtag, J., Richter, A., Šantrůčková, H., Schnecker, J., Shibistova, O., Urich, T., Wild, B., and Guggenberger, G. (2015). Storage and transformation of organic matter fractions in cryoturbated permafrost soils across the siberian arctic. *Biogeosciences*, 12:4525–4542.

Glaser, B., Haumaier, L., Guggenberger, G., and Zech, W. (1998). Black carbon in soils: the use of benzenecarboxylic acids as specific markers.

Gustafsson, Ö., Bucheli, T. D., Kukulska, Z., Andersson, M., Largeau, C., Rouzaud, J. N., Reddy, C. M., and Eglinton, T. I. (2001). Evaluation of a protocol for the quantification of black carbon in sediments. *Global Biogeochemical Cycles*, 15:881–890.

Hammes, K., Schmidt, M. W., Smernik, R. J., Currie, L. A., Ball, W. P., Nguyen, T. H., Louchouarn, P., Houel, S., Örjan Gustafsson, Elmquist, M., Cornelissen, G., Skjemstad, J. O., Masiello, C. A., Song, J., Peng, P., Mitra, S., Dunn, J. C., Hatcher, P. G., Hockaday, W. C., Smith, D. M., Hartkopf-Fröder, C., Böhmer, A., Lüer, B., Huebert, B. J., Amelung, W., Brodowski, S., Huang, L., Zhang, W., Gschwend, P. M., Flores-Cervantes, D. X., Largeau, C., Rouzaud, J. N., Rumpel, C., Guggenberger, G., Kaiser, K., Rodionov, A., Gonzalez-Vila, F. J., Gonzalez-Perez, J. S., de la Rosa, J. M., Manning, D. A., López-Capél, E., and Ding, L. (2007). Comparison of quantification methods to measure fire-derived (black-elemental) carbon in soils and sediments using reference materials from soil, water, sediment and the atmosphere. *Global Biogeochemical Cycles*, 21.

Hugelius, G., Kuhry, P., Tarnocai, C., and Virtanen, T. (2010). Soil organic carbon pools in a periglacial landscape: A case study from the central canadian arctic. *Permafrost and Periglacial Processes*, 21:16–29.

Hugelius, G., Strauss, J., Zubrzycki, S., Harden, J. W., Schuur, E. A., Ping, C. L., Schirrmeister, L., Grosse, G., Michaelson, G. J., Koven, C. D., O'Donnell, J. A., Elberling, B., Mishra, U., Camill, P., Yu, Z., Palmtag, J., and Kuhry, P. (2014). Estimated stocks of circumpolar permafrost carbon with quantified uncertainty ranges and identified data gaps. *Biogeosciences*, 11:6573–6593.

Hugelius, G., Tarnocai, C., Broll, G., Canadell, J. G., Kuhry, P., and Swanson, D. K. (2013). The northern circumpolar soil carbon database: Spatially distributed datasets of soil coverage and soil carbon storage in the northern permafrost regions. *Earth System Science Data*, 5:3–13.

Johnstone, J. F., Hollingsworth, T. N., Stuart, F., and III, C. (2008). A key for predicting postfire successional trajectories in black spruce stands of interior alaska.

Jones, M. W., Coppola, A. I., Santín, C., Dittmar, T., Jaffé, R., Doerr, S. H., and Quine, T. A. (2020). Fires prime terrestrial organic carbon for riverine export to the global oceans. *Nature Communications*, 11.

Kaiser, C., Meyer, H., Biasi, C., Rusalimova, O., Barsukov, P., and Richter, A. (2007). Conservation of soil organic matter through cryoturbation in arctic soils in siberia. *Journal of Geophysical Research: Biogeosciences*, 112.

Koven, C., Friedlingstein, P., Ciais, P., Khvorostyanov, D., Krinner, G., and Tarnocai, C. (2009). On the formation of high-latitude soil carbon stocks: Effects of cryoturbation and insulation by organic matter in a land surface model. *Geophysical Research Letters*, 36.

Kuhry, P., Dorrepaal, E., Hugelius, G., Schuur, E. A., and Tarnocai, C. (2010). Short communication: Potential remobilization of belowground permafrost carbon under future global warming. *Permafrost and Periglacial Processes*, 21:208–214.

Lasslop, G., Coppola, A. I., Voulgarakis, A., Yue, C., and Veraverbeke, S. (2019). Influence of fire on the carbon cycle and climate. *Current Climate Change Reports*, 5:112–123.

Laub, M., Demyan, M. S., Nkwain, Y. F., Blagodatsky, S., Kätterer, T., Piepho, H. P., and Cadisch, G. (2020). Drifts band areas as measured pool size proxy to reduce parameter uncertainty in soil organic matter models. *Biogeosciences*, 17:1393–1413.

Leifeld, J., Alewell, C., Bader, C., Krüger, J. P., Mueller, C. W., Sommer, M., Steffens, M., and Szidat, S. (2018). Pyrogenic carbon contributes substantially to carbon storage in intact and degraded northern peatlands. *Land Degradation and Development*, 29:2082–2091.

Liang, B., Lehmann, J., Solomon, D., Kinyangi, J., Grossman, J., O'Neill, B., Skjemstad, J. O., Thies, J., Luizão, F. J., Petersen, J., and Neves, E. G. (2006). Black carbon increases cation exchange capacity in soils. *Soil Science Society of America Journal*, 70:1719–1730.

Masiello, C. A. (2004). New directions in black carbon organic geochemistry. *Marine Chemistry*, 92:201–213.

Ping, C. L., Jastrow, J. D., Jorgenson, M. T., Michaelson, G. J., and Shur, Y. L. (2015). Permafrost soils and carbon cycling. *SOIL*, 1:147–171.

Poeplau, C. and Don, A. (2014). Effect of ultrasonic power on soil organic carbon fractions. *Journal of Plant Nutrition and Soil Science*, 177:137–140.

Poeplau, C., Don, A., Dondini, M., Leifeld, J., Nemo, R., Schumacher, J., Senapati, N., and Wiesmeier, M. (2013). Reproducibility of a soil organic carbon fractionation method to derive rothc carbon pools. *European Journal of Soil Science*, 64:735–746.

Poeplau, C., Vos, C., and Don, A. (2017). Soil organic carbon stocks are systematically overestimated by misuse of the parameters bulk density and rock fragment content. *SOIL*, 3(1):61–66.

Reisser, M., Purves, R. S., Schmidt, M. W., and Abiven, S. (2016). Pyrogenic carbon in soils: A literature-based inventory and a global estimation of its content in soil organic carbon and stocks. *Frontiers in Earth Science*, 4.

Santín, C., Doerr, S. H., Kane, E. S., Masiello, C. A., Ohlson, M., de la Rosa, J. M., Preston, C. M., and Dittmar, T. (2016). Towards a global assessment of pyrogenic carbon from vegetation fires. *Global Change Biology*, 22:76–91.

Santín, C., Doerr, S. H., Preston, C. M., and González-Rodríguez, G. (2015). Pyrogenic organic matter production from wildfires: a missing sink in the global carbon cycle. *Global Change Biology*, 21:1621–1633.

Singh, N., Abiven, S., Torn, M. S., and Schmidt, M. W. (2012). Fire-derived organic carbon in soil turns over on a centennial scale. *Biogeosciences*, 9:2847–2857.

Sothe, C., Gonsamo, A., Arabian, J., and Snider, J. (2022). Large scale mapping of soil organic carbon concentration with 3d machine learning and satellite observations. *Geoderma*, 405.

Soucémarianadin, L., Reisser, M., Cécillon, L., Barré, P., Nicolas, M., and Abiven, S. (2019). Pyrogenic carbon content and dynamics in top and subsoil of french forests. *Soil Biology and Biochemistry*, 133:12–15.

Soucémarianadin, L. N., Quideau, S. A., and MacKenzie, M. D. (2014). Pyrogenic carbon stocks and storage mechanisms in podzolic soils of fire-affected quebec black spruce forests. *Geoderma*, 217-218:118–128.

Stumpe, B., Weihermüller, L., and Marschner, B. (2011). Sample preparation and selection for qualitative and quantitative analyses of soil organic carbon with mid-infrared reflectance spectroscopy. *European Journal of Soil Science*, 62:849–862.

Tamocai, C., Canadell, J. G., Schuur, E. A., Kuhry, P., Mazhitova, G., and Zimov, S. (2009). Soil organic carbon pools in the northern circumpolar permafrost region. *Global Biogeochemical Cycles*, 23.

Thevenot, M., Dignac, M. F., and Rumpel, C. (2010). Fate of lignins in soils: A review. *Soil Biology and Biochemistry*, 42:1200–1211.

Van Der Werf, G. R., Randerson, J. T., Giglio, L., Leeuwen, T. T. V., Chen, Y., Rogers, B. M., Mu, M., Marle, M. J. V., Morton, D. C., Collatz, G. J., Yokelson, R. J., and Kasibhatla, P. S. (2017). Global fire emissions estimates during 1997-2016. *Earth System Science Data*, 9:697–720.

Walter, K., Don, A., Tiemeyer, B., and Freibauer, A. (2016). Determining soil bulk density for carbon stock calculations: A systematic method comparison. *Soil Science Society of America Journal*, 80:579–591.

Walthert, L., Graf, U., Kammer, A., Luster, J., Pezzotta, D., Zimmermann, S., and Hagedorn, F. (2010). Determination of organic and inorganic carbon, δ13c, and nitrogen in soils containing carbonates after acid fumigation with hcl. *Journal of Plant Nutrition and Soil Science*, 173:207–216.

Wiedemeier, D. B., Lang, S. Q., Gierga, M., Abiven, S., Bernasconi, S. M., Früh-Green, G. L., Hajdas, I., Hanke, U. M., Hilf, M. D., McIntyre, C. P., Scheider, M. P., Smittenberg, R. H., Wacker, L., Wiesenberg, G. L., and Schmidt, M. W. (2016). Characterization, quantification and compound-specific isotopic analysis of pyrogenic carbon using benzene polycarboxylic acids (bpca). *Journal of Visualized Experiments*, 2016.

Yeasmin, S., Singh, B., Johnston, C. T., and Sparks, D. L. (2017). Evaluation of pre-treatment procedures for improved interpretation of mid infrared spectra of soil organic matter. *Geoderma*, 304:83–92.

Zimmermann, M., Leifeld, J., Schmidt, M. W., Smith, P., and Fuhrer, J. (2007). Measured soil organic matter fractions can be related to pools in the rothc model. *European Journal of Soil Science*, 58:658–667.

Zimov, S. A., Schuur, E. A. G., and III, F. S. C. (2006). Permafrost and the global carbon budget. *Science*, 312:1612–1613.

Appendix A

Appendix

Table 8: $\delta^{13}C$ values after fumigation (left) and chemothermal oxidation (right), for bulk samples and individual SOC fractions at each landscape position and soil depth.

EUP	Location	Depth	TOC δ^{13}C [‰]					PyC_{CTO} δ^{13}C [‰]				
		[cm]	**Bulk**	**POM**	**S+A**	**S+C**	**rSOC**	**Bulk**	**POM**	**S+A**	**S+C**	**rSOC**
3	ST	0-15	-29.78	-28.54	-31.13	-28.59	-34.97	-28.67	-34.70	-41.12	-31.78	-30.33
		15-30	-31.47	-28.78	-33.24	-28.77	-29.09	-28.72	-35.39	-35.72	-32.72	-23.51
2	SS	0-15	-29.74	-28.90	-32.28	-28.53	-35.34	-29.89	-28.36	-27.78	-30.31	-34.22
		15-30	-31.91	-28.30	-32.55	-28.37	-30.75	-26.11	-39.67	-35.97	-30.49	-34.01
1	SB	0-15	-29.62	-29.15	-32.97	-28.51	-22.70	-31.69	-29.84	-13.29	-15.01	-10.29
		15-30	-29.86	-29.06	-32.91	-28.41	-26.54	-30.57	-30.70	-17.76	-20.28	-14.80
8	NT	0-15	-30.14	-29.34	-30.08	-32.16	-35.28	-32.16	-33.73	-30.45	-30.43	-29.86
		15-30	-29.13	-29.25	-29.92	-31.28	-31.12	-31.28	-34.20	-29.01	-32.01	-30.96
		30-45	-30.29	-29.41	-30.75	-36.06	-26.82	-36.06	-39.14	-28.03	-33.28	-32.35
10	NS	0-15	-29.32	-29.68	-29.41	-30.79	-28.44	-30.79	-31.55	-26.18	-29.11	-33.06
		15-30	-29.16	-28.97	-29.62	-32.27	-28.76	-32.27	-37.48	-31.12	-29.44	-37.13
		30-45	-28.63	-29.23	-29.38	-30.80	-29.97	-30.80	-36.61	-29.85	-28.46	-36.48
9	NB	0-15	-29.37	-29.59	-29.08	-29.19	-28.90	-29.19	-41.80	-29.20	-30.93	-31.94
		15-30	-28.98	-28.74	-27.98	-31.25	-29.08	-31.25	-39.67	-23.68	-32.42	-33.01
		30-45	-29.13	-28.66	-28.33	-29.34	-30.21	-29.34	-39.62	-22.28	-34.65	-34.17

Table 9: List of 41 composite samples. Each composite originates from 1-3 sampling locations on the same landscape position (EUP) and depth.

EUP	Landscape Position	Depth [cm]	Replicate	Sample Locations	No
1	SB	0-15	A	1,2,3	1
			B	4,5,6	2
			C	7,8	3
		15-30	A	1,2,3	4
			B	4,5,6	5
			C	7,8	6
2	SS	0-15	A	1,2,3	7
			B	4,5,6	8
			C	7,8,9	9
		15-30	A	1,2,3	10
			B	4,5,6	11
			C	7,8,9	12
3	ST	0-15	A	1,2,3	13
			B	4,5,6	14
			C	7,8,9	15
		15-30	A	1,2,3	16
			B	4,5,6	17
			C	7,8,9	18
8	NT	0-15	A	1,2,3	19
			B	4,5,6	20
			C	7,8,9	21
		15-30	A	1,2,3	22
			B	4,5,6	23
			C	7,8,9	24
		30-45	A	1,2	25
			B	4,5,6	26
			C	9	27
9	NB	0-15	A	1,2,3	28
			B	4,5,6	29
			C	7,8,9	30
		15-30	A	4,5,6	31
		30-45	A	4,5,6	32
10	NS	0-15	A	1,2,3	33
			B	4,5,6	34
			C	7,8,9	35
		15-30	A	3	36
			B	4,5,6	37
			C	7,8,9	38
		30-45	A	3	39
			B	5,6	40
			C	7,9	41

Table 10: Characterization of soil sampling size with average pH-values and effective cation exchange capacity (CEC) for each landscape position and also for individual soil depths.

EUP	Landscape Position	Depths [cm]	Average pH	Eff CEC [meq/100g]
3	Sout Top (ST)	0-30	4.9	4.64
		0-15	4.8	4.8
		15-30	5.0	4.47
2	South Slope (SS)	0-30	4.8	4.55
		0-15	4.6	4.81
		15-30	5.1	4.29
1	South Bottom (SB)	0-30	6.0	5.53
		0-15	5.9	6.15
		15-30	6.1	4.91
8	North Top (NT)	0-45	3.7	11.66
		0-15	3.6	11.47
		15-30	3.7	11.43
		30-45	3.7	12.07
10	North Slope (NS)	0-45	4.6	18.95
		0-15	4.5	18.89
		15-30	4.5	18.34
		30-45	4.8	19.61
9	North Bottom (NB)	0-45	4.6	21.94
		0-15	4.4	22.29
		15-30	4.6	21.58
		30-45	4.7	-

Table 11: Stocks of SOC in bulks and SOC fractions.

Stock of SOC				Bulk		POM		S+A		S+C		rSOC	
EUP	Location	Depth	BD fine soil	stock	SE	stock	SE	stock	SE	stock	SE	stock	SE
		[cm]	[gcm^{-3}]	[tha^{-1}]		[tha^{-1}]		[tha^{-1}]		[tha^{-1}]		[tha^{-1}]	
3	ST	0-15	1.35	27.575	2.643	13.835	2.064	0.846	0.159	11.991	0.757	0.904	0.016
		0-30	1.42	40.042	2.996	17.224	2.168	1.823	0.275	18.927	1.277	2.068	0.337
2	SS	0-15	1.27	22.515	1.601	10.006	1.084	1.502	0.115	10.378	0.499	0.629	0.076
		0-30	1.41	34.113	2.993	13.424	1.856	2.651	0.166	16.342	0.996	1.696	0.159
1	SB	0-15	1.28	26.728	1.832	14.999	1.917	3.296	1.002	5.406	1.627	3.027	0.908
		0-30	1.37	45.008	4.714	20.671	2.295	7.293	2.594	11.617	1.930	5.427	1.454
8	NT	0-15	0.94	30.656	1.851	13.326	2.295	3.414	0.174	12.904	0.424	1.011	0.189
		0-30	1.26	48.695	4.610	17.127	2.328	6.736	0.660	22.437	2.981	2.394	0.433
		0-45	1.34	65.358	4.749	18.772	2.456	12.310	1.764	30.173	3.503	4.103	0.761
10	NS	0-15	1.13	53.273	1.976	19.934	2.253	5.357	0.284	22.276	0.605	5.706	0.324
		0-30	1.41	86.084	2.807	25.293	2.331	8.920	0.473	38.311	2.539	13.560	1.030
		0-45	1.44	118.226	4.011	28.844	2.366	12.329	0.486	57.594	3.927	19.459	1.102
9	NB	0-15	0.91	56.281	7.508	16.460	1.948	4.980	0.224	27.978	2.521	6.863	1.166
		0-30	1.24	116.095	-	29.544	-	10.748	-	61.321	-	14.482	-
		0-45	1.26	183.975	-	38.445	-	17.126	-	105.792	-	22.612	-

Table 12: Stocks of PyC in bulks and SOC fractions.

Stocks of PyC				Bulk		POM		S+A		S+C	
EUP	Location	Depth	BD fine soil	stock PyC	SE	stock PyC	SE	stock PyC	SE	stock PyC	SE
		[cm]	[gcm^{-3}]	[tha^{-1}]		[tha^{-1}]		[tha^{-1}]		[tha^{-1}]	
3	ST	0-15	1.35	0.531	0.076	0.082	0.020	0.312	0.044	0.136	0.020
		0-30	1.42	1.016	0.090	0.109	0.021	0.696	0.059	0.210	0.021
2	SS	0-15	1.27	0.516	0.021	0.017	0.003	0.131	0.018	0.368	0.025
		0-30	1.41	1.089	0.098	0.064	0.038	0.429	0.051	0.596	0.100
1	SB	0-15	1.28	0.435	0.065	0.024	0.011	0.259	0.068	0.152	0.094
		0-30	1.37	0.950	0.082	0.099	0.042	0.505	0.116	0.347	0.106
8	NT	0-15	0.94	0.565	0.072	0.045	0.008	0.148	0.021	0.372	0.057
		0-30	1.26	1.091	0.090	0.063	0.009	0.371	0.041	0.657	0.066
		0-45	1.34	1.731	0.115	0.077	0.013	0.816	0.072	0.838	0.264
10	NS	0-15	1.13	0.843	0.057	0.049	0.016	0.145	0.030	52.595	0.026
		0-30	1.41	1.703	0.153	0.061	0.016	0.426	0.106	53.160	0.087
		0-45	1.44	2.374	0.154	0.093	0.018	0.730	0.129	53.496	0.103
9	NB	0-15	0.91	0.517	0.073	0.063	0.015	0.137	0.040	0.317	0.048
		0-30	1.24	1.309	-	0.110	-	0.262	-	0.936	-
		0-45	1.26	1.747	-	0.125	-	0.323	-	1.299	-

Table 13: Relative (%) and absolute (mgC gsoil^{-1}) content of SOC in the soil fractions. Standard error is not available for 15-30 cm and 30-45 cm depth in NB location, since only one composite was available.

Soil Organic Carbon																	
			Relative Content								Absolute Content							
EUP	Location	Depth	SOC_{POM}	SE	SOC_{S+A}	SE	SOC_{S+C}	SE	SOC_{rSOC}	SE	SOC_{POM}	SE	SOC_{S+A}	SE	SOC_{S+C}	SE	SOC_{rSOC}	SE
		[cm]	[%]		[%]		[%]		[%]		[mg gsoil^{-1}]		[mg gsoil^{-1}]		[mg gsoil^{-1}]		[mg gsoil^{-1}]	
3	ST	0-15	49.6	3.0	3.2	1.0	43.8	1.7	3.4	0.4	6.77	0.78	0.42	0.10	5.91	0.13	0.45	0.03
		15-30	26.6	2.6	8.0	1.8	55.1	2.4	10.3	4.0	1.60	0.34	0.46	0.12	3.27	0.54	0.54	0.15
2	SS	0-15	44.2	1.6	6.7	0.5	46.2	1.1	2.8	0.5	5.26	0.53	0.79	0.04	5.46	0.20	0.33	0.05
		15-30	27.0	6.0	10.5	1.5	52.9	4.0	9.6	1.2	1.61	0.70	0.54	0.06	2.82	0.40	0.50	0.06
1	SB	0-15	55.7	3.9	11.9	3.1	21.3	8.1	11.1	2.9	7.76	0.62	1.67	0.46	2.93	1.04	1.56	0.44
		15-30	31.7	2.3	18.8	8.5	38.0	9.1	11.5	5.0	2.70	0.45	1.83	1.04	3.02	0.45	1.11	0.52
8	NT	0-15	42.9	4.8	11.3	1.2	42.5	3.4	3.3	0.7	9.40	1.31	2.44	0.19	9.20	0.52	0.72	0.14
		15-30	22.5	3.5	18.8	1.3	51.2	3.6	7.5	0.3	2.01	0.17	1.74	0.27	4.97	1.35	0.72	0.18
		30-45	9.9	5.1	34.7	11.6	45.5	7.5	9.9	3.0	0.81	0.38	2.78	0.85	3.82	0.85	0.85	0.30
10	NS	0-15	37.2	3.0	10.1	0.4	42.0	2.5	10.7	0.5	12.00	1.86	3.19	0.15	13.36	1.06	3.40	0.12
		15-30	16.3	1.4	10.9	1.2	48.6	5.6	24.1	3.2	2.53	0.26	1.68	0.16	7.59	1.24	3.70	0.42
		30-45	11.1	0.9	10.8	1.2	59.2	4.5	18.9	3.1	1.65	0.21	1.58	0.05	8.98	1.48	2.73	0.15
9	NB	0-15	29.2	2.2	8.9	0.6	49.6	0.8	12.3	2.0	12.45	2.38	3.72	0.45	21.00	3.09	5.04	0.82
		15-30	21.9	-	9.6	-	55.7	-	12.7	-	7.02	-	3.10	-	17.90	-	4.09	-
		30-45	13.1	-	9.4	-	65.5	-	12.0	-	4.71	-	3.37	-	23.51	-	4.30	-

Table 14: Relative (%) and absolute content (mgC gsoil^{-1}) of PyC in the soil fractions. Standard error is not available for 15-30 cm and 30-45 cm depth in NB location, since only one composite was available.

Pyrogenic Carbon																
			Relative Content						Absolute Content							
EUP	Location	Depth	PyC_{POM}	SE	PyC_{S+A}	SE	PyC_{S+C}	SE	PyC_{POM}	SE	PyC_{S+A}	SE	PyC_{S+C}	SE		
		[cm]	[%]		[%]		[%]		[mg gsoil^{-1}]		[mg gsoil^{-1}]		[mg gsoil^{-1}]			
3	ST	0-15	15.2	2.0	58.8	0.5	25.9	2.4	0.04	0.01	0.15	0.02	0.07	0.01		
		15-30	5.2	1.1	79.3	1.5	15.5	1.2	0.01	0.00	0.18	0.02	0.04	0.00		
2	SS	0-15	3.3	0.5	25.4	3.8	71.3	3.4	0.01	0.00	0.07	0.01	0.19	0.01		
		15-30	6.6	4.8	56.3	14.5	37.1	10.9	0.02	0.02	0.14	0.02	0.11	0.04		
1	SB	0-15	5.3	2.1	62.3	16.6	32.4	17.8	0.01	0.01	0.13	0.03	0.08	0.06		
		15-30	14.6	8.5	45.4	12.7	40.1	13.0	0.03	0.02	0.12	0.04	0.10	0.03		
8	NT	0-15	8.2	1.6	26.2	1.8	65.6	3.2	0.03	0.00	0.11	0.01	0.27	0.04		
		15-30	3.6	1.0	42.0	4.1	54.4	3.9	0.01	0.00	0.12	0.02	0.15	0.01		
		30-45	2.6	1.9	71.7	13.0	25.7	13.1	0.01	0.00	0.22	0.03	0.09	0.05		
10	NS	0-15	5.8	1.9	16.8	2.3	77.4	2.7	0.03	0.01	0.08	0.01	0.39	0.02		
		15-30	1.5	0.2	31.6	7.4	66.9	7.4	0.01	0.00	0.13	0.05	0.27	0.04		
		30-45	4.8	1.4	45.0	10.4	50.2	9.1	0.01	0.00	0.14	0.03	0.16	0.03		
9	NB	0-15	12.0	1.6	26.1	4.9	61.9	6.5	0.05	0.02	0.11	0.04	0.23	0.03		
		15-30	5.9	-	15.8	-	78.3	-	0.03	-	0.07	-	0.33	-		
		30-45	3.3	-	13.9	-	82.8	-	0.01	-	0.03	-	0.19	-		

Figure 25: Relation between SOC and PyC concentration in the bulk samples and soil fractions for each soil depth.

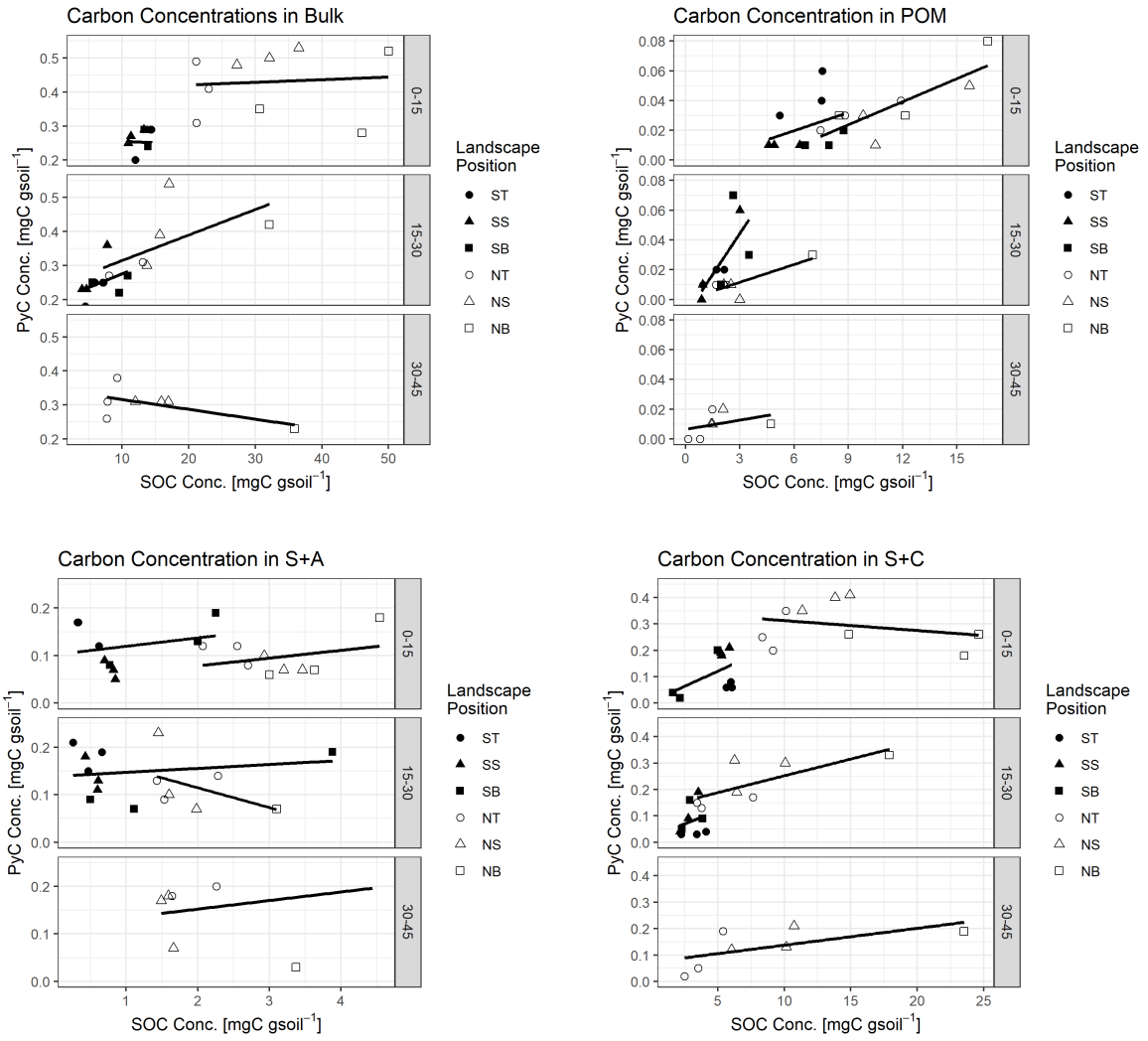

l

Table 15: Summary of mean ratio values and standard error (SE) for each landscape position and depth, including organic layer (at 0 cm depth). N refers to the number of counts.

EUP	Landscape Position	Depth [cm]	N	Mean Aliphatic/Aromatic Ratio	SE	Mean Cellulose/Lignin Ratio	SE
1	SB	0	1	0.57	-	0.77	-
		0-15	15	0.31	0.06	0.31	0.06
		15-30	15	0.27	0.06	0.33	0.05
2	SS	0	1	0.63	-	0.79	-
		0-15	15	0.24	0.06	0.45	0.09
		15-30	15	0.26	0.07	0.39	0.07
3	ST	0	1	0.65	-	0.78	-
		0-15	15	0.23	0.06	0.35	0.07
		15-30	15	0.26	0.08	0.39	0.06
8	NT	0	1	0.89	-	1.17	-
		0-15	15	0.48	0.06	1.31	0.20
		15-30	15	0.50	0.07	2.87	1.09
		30-45	15	0.54	0.06	6.30	2.04
9	NB	0	1	0.70	-	1.00	-
		0-15	15	0.41	0.03	0.68	0.07
		15-30	5	0.43	0.05	0.60	0.09
		30-45	5	0.41	0.06	0.55	0.12
10	NS	0	1	0.85	-	1.17	-
		0-15	15	0.38	0.05	0.56	0.06
		15-30	15	0.37	0.05	0.61	0.08
		30-45	15	0.37	0.06	0.64	0.08

Figure 26: Aliphatic/aromatic and cellulose/ligning ratios along the two catenae for each soil depth, with cellulose/lignin ratio to the right.

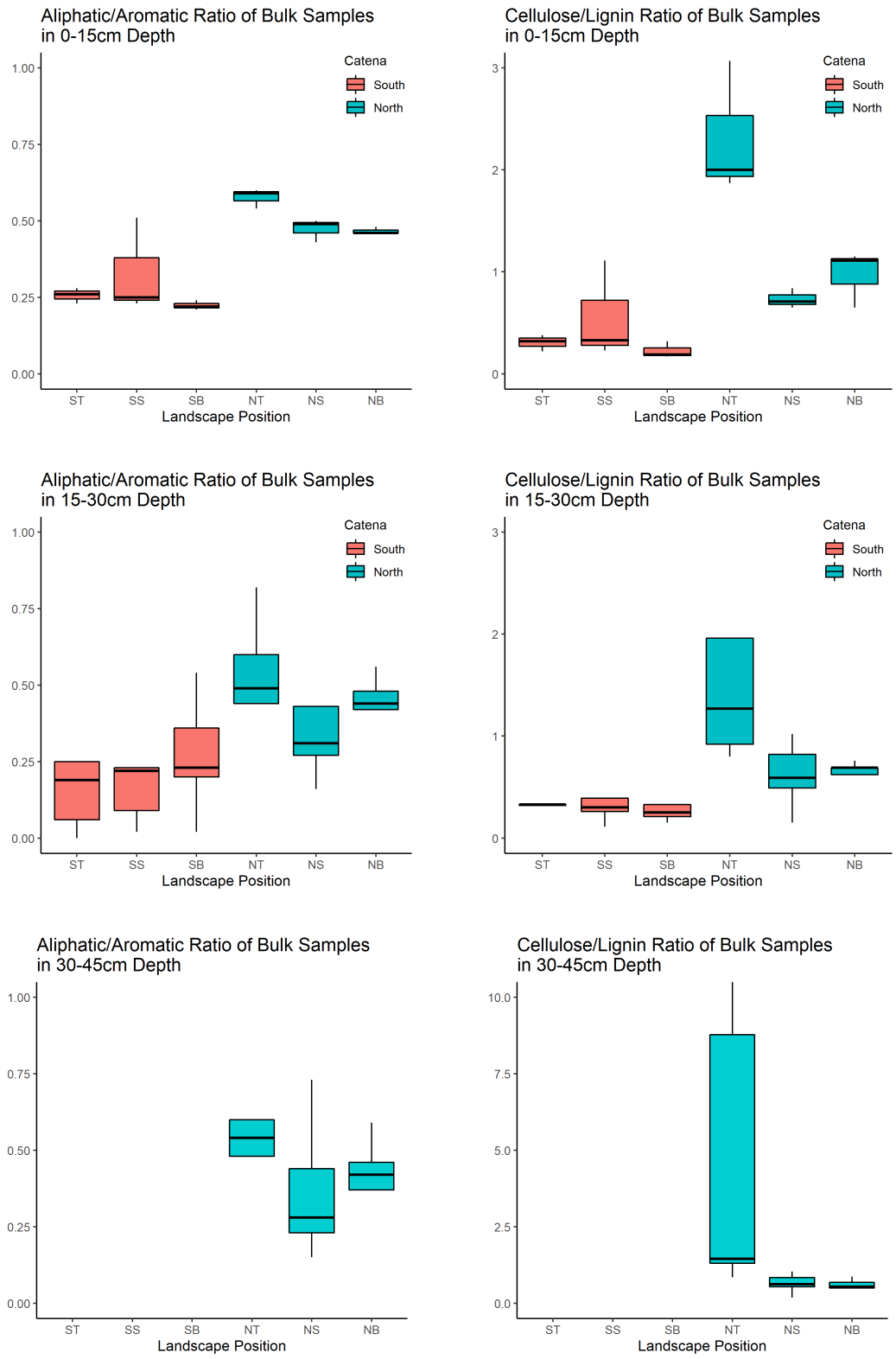

Figure 27: Aliphatic/Aromatic ratio in the individual fractions per each landscape position, with Northern catena to the right.

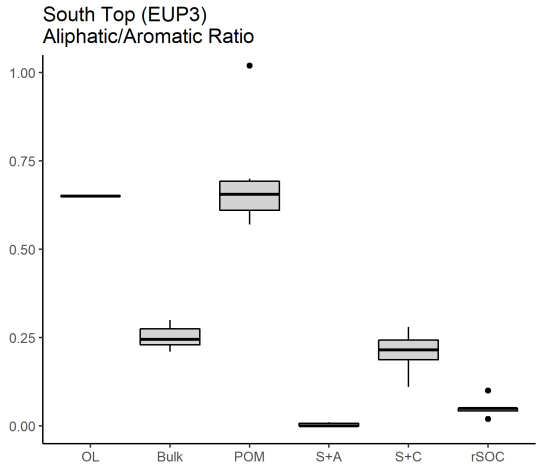

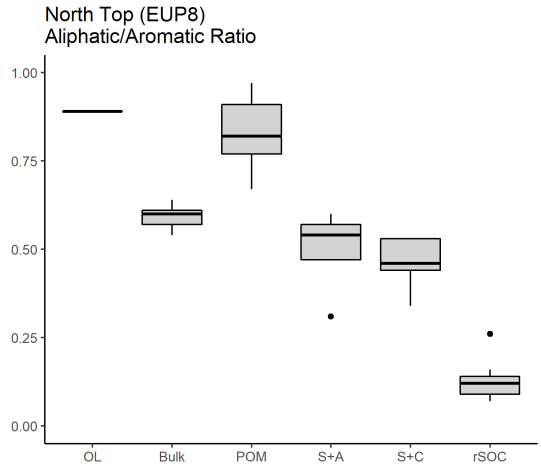

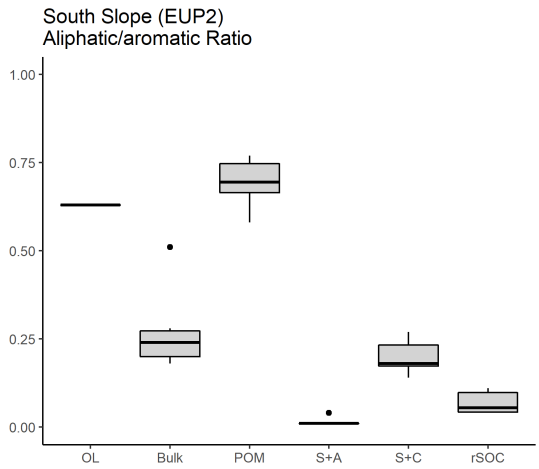

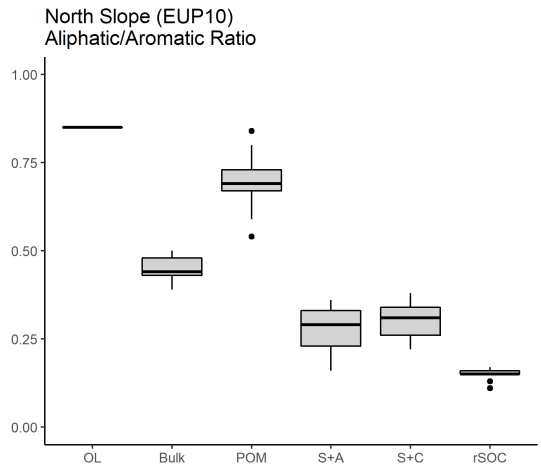

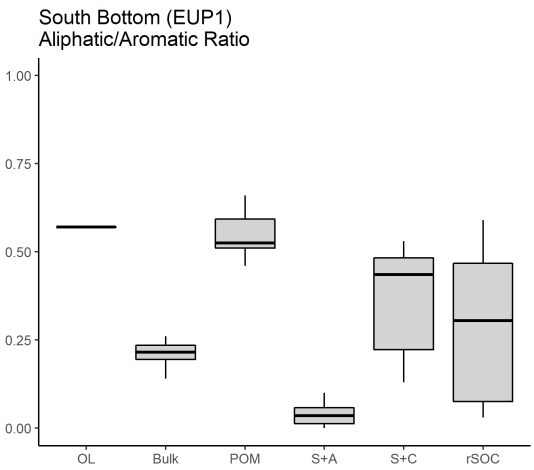

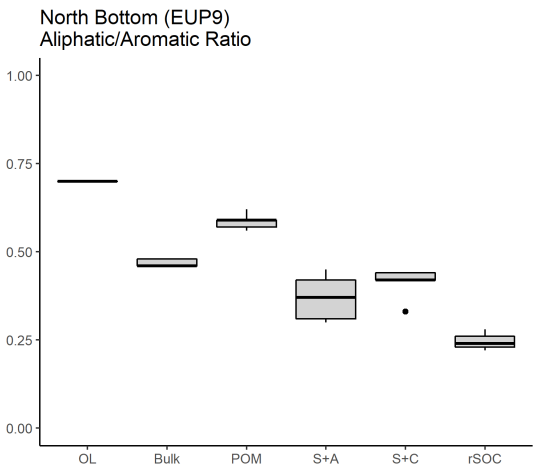

Figure 28: Cellulose/Lignin ratio in the individual fractions per each landscape position, with Northern catena to the right.

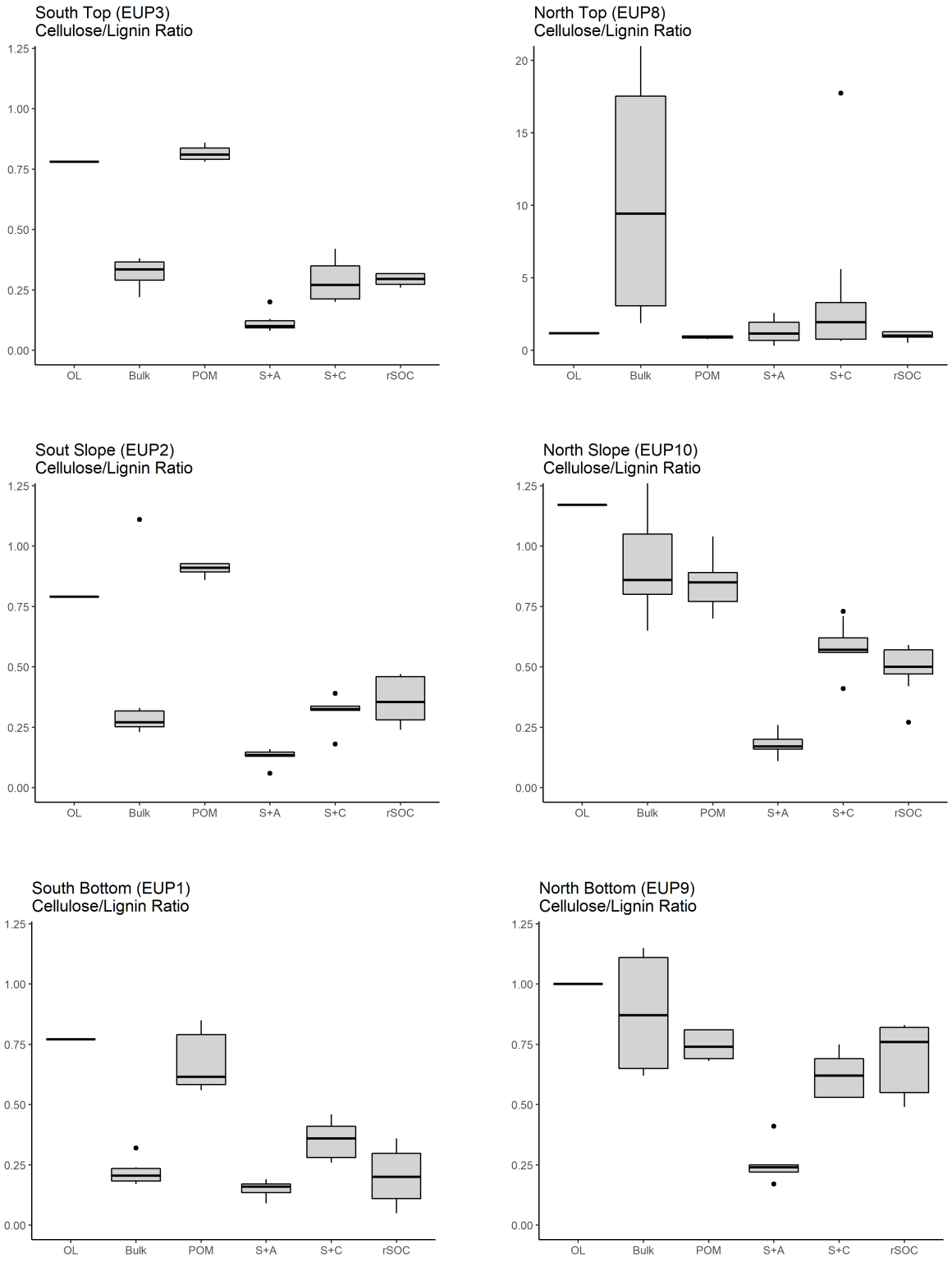

Figure 29: Depth profile of aliphatic/aromatic (left) and cellulose/lignin ratio along (right) of bulk, S+A and S+C fractions.

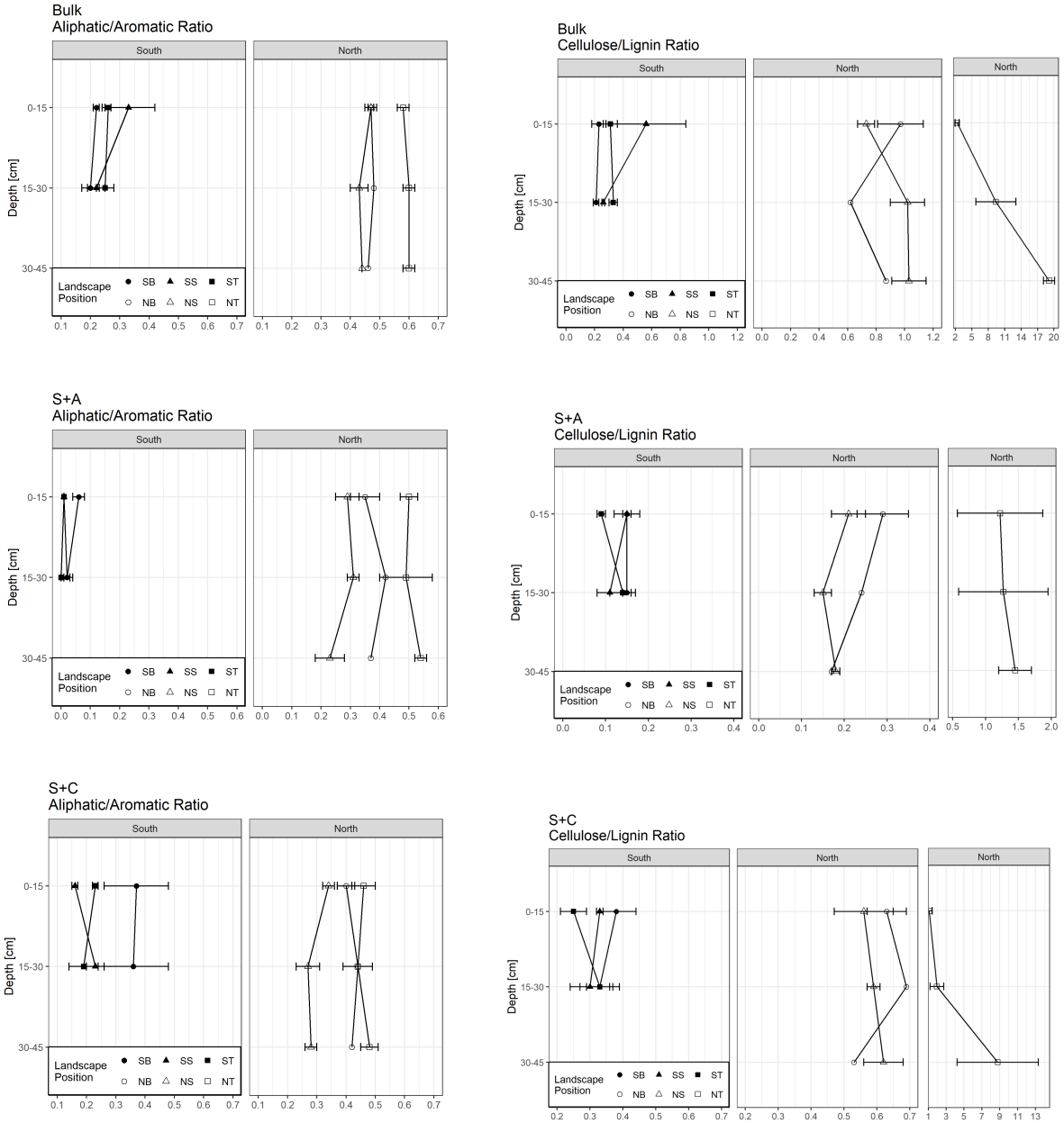

Figure 30: Depth profile of aliphatic/aromatic (left) and cellulose/lignin ratio along (right) of POM and rSOC fractions.

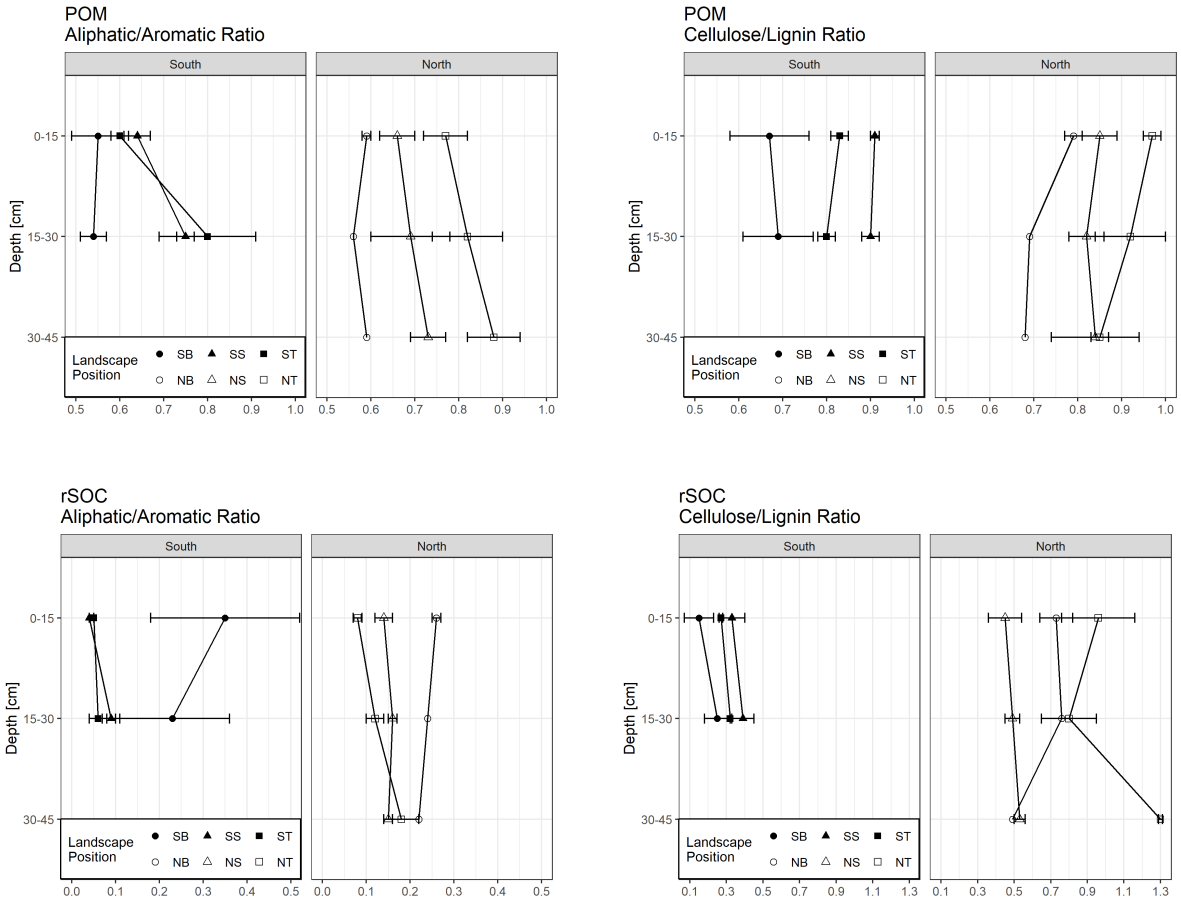

Personal Declaration

I hereby declare that the submitted Thesis is the result of my own, independent work. All external sources are explicitly acknowledged in the Thesis.